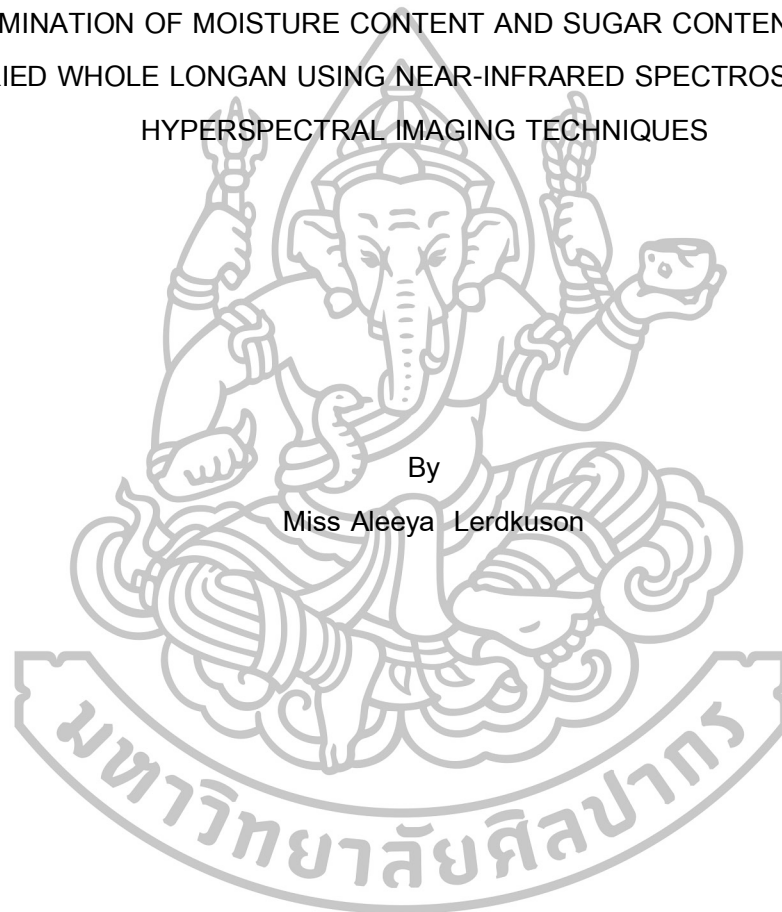




DETERMINATION OF MOISTURE CONTENT AND SUGAR CONTENT IN FLESH  
OF DRIED WHOLE LONGAN USING NEAR-INFRARED SPECTROSCOPY AND  
HYPER SPECTRAL IMAGING TECHNIQUES



By  
Miss Aleeya Lerdkuson

A Thesis Submitted in Partial Fulfillment of the Requirements for the Degree  
Master of Science Program in Food Technology  
Department of Food Technology  
Graduate School, Silpakorn University  
Academic Year 2015  
Copyright of Graduate School, Silpakorn University

DETERMINATION OF MOISTURE CONTENT AND SUGAR CONTENT IN FLESH OF  
DRIED WHOLE LONGAN USING NEAR-INFRARED SPECTROSCOPY AND  
HYPERSPETRAL IMAGING TECHNIQUES



A Thesis Submitted in Partial Fulfillment of the Requirements for the Degree  
Master of Science Program in Food Technology  
Department of Food Technology  
Graduate School, Silpakorn University  
Academic Year 2015  
Copyright of Graduate School, Silpakorn University

การใช้เทคนิคสเปกโทรสโกปีอินฟราเรดย่านใกล้และการถ่ายภาพสเปกตรัมในการติดตาม  
ปริมาณความชื้นและปริมาณน้ำตาลในเนื้อลำไยอบแห้งทั้งผล



วิทยานิพนธ์นี้เป็นส่วนหนึ่งของการศึกษาตามหลักสูตรปริญญาวิทยาศาสตรมหาบัณฑิต

สาขาวิชาเทคโนโลยีอาหาร

ภาควิชาเทคโนโลยีอาหาร

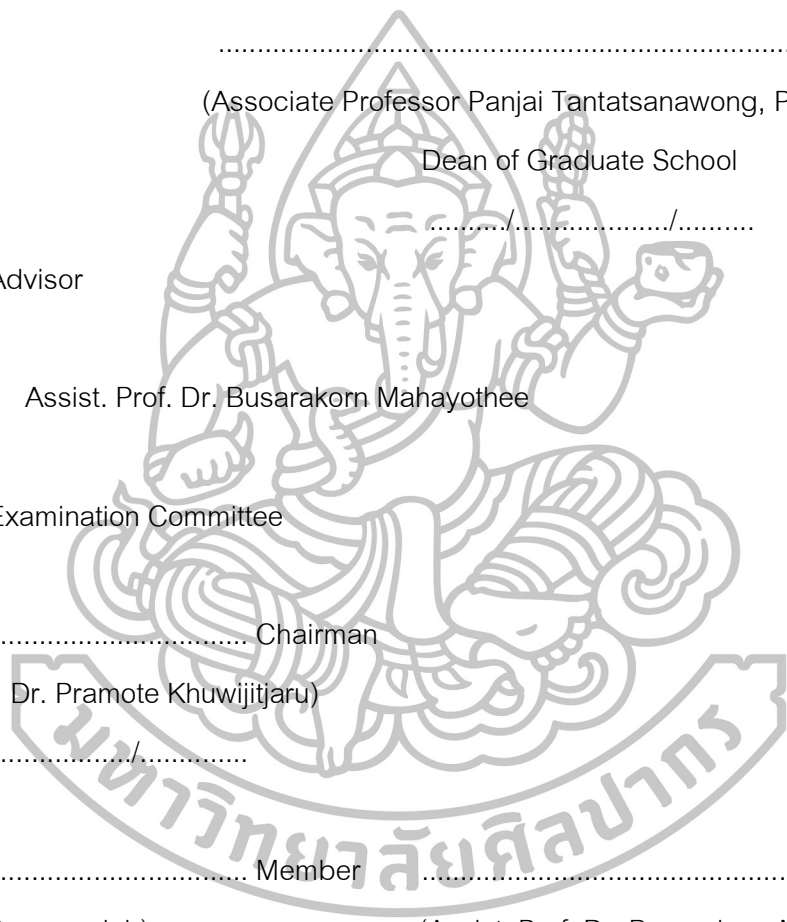
บัณฑิตวิทยาลัย มหาวิทยาลัยศิลปากร

ปีการศึกษา 2558

ลิขสิทธิ์ของบัณฑิตวิทยาลัย มหาวิทยาลัยศิลปากร

The Graduate School, Silpakorn University has approved and accredited the Thesis title of “Determination of moisture content and sugar content in flesh of dried whole longan using near-infrared spectroscopy and hyperspectral imaging techniques” submitted by Miss Aleeya Lerdkuson as a partial fulfillment of the requirements for the degree of Master of Science in Food Technology

.....  
(Associate Professor Panjai Tantatsanawong, Ph.D.)  
Dean of Graduate School  
...../.....  
The Thesis Advisor  
Assist. Prof. Dr. Busarakorn Mahayothee  
The Thesis Examination Committee  
..... Chairman  
(Assist. Prof. Dr. Pramote Khuwijitjaru)  
...../.....  
..... Member ..... Member  
(Dr. Rachit Suwapanich) (Assist. Prof. Dr. Busarakorn Mahayothee)  
...../...../..... ...../...../.....



56403225 : MAJOR : FOOD TECHNOLOGY

KEY WORD : MOISTURE CONTENT/SUGAR CONTENT/DRIED WHOLE LONGAN/  
NIRS/HSI

ALEEYA LERDKUSON : DETERMINATION OF MOISTURE CONTENT AND SUGAR CONTENT IN FLESH OF DRIED WHOLE LONGAN USING NEAR-INFRARED SPECTROSCOPY AND HYPERSPECTRAL IMAGING TECHNIQUES. THESIS ADVISOR: ASST. PROF. BUSARAKORN MAHAYOTHEE, Ph.D. 164 pp.

The objective of this study was to use near-infrared spectroscopy (NIRS) and hyperspectral imaging (HSI) as rapid and non-destructive techniques to analyze moisture and sugar contents in flesh of dried whole longan fruits. Total of 496 whole longans for moisture content analysis and the total of 186 samples for sugar content analysis with different moisture content of flesh ranged between 9.99-88.62% were taken for spectrum acquisition using an FT-NIR spectrometer (800 - 2500 nm) in reflectance mode with a nominal resolution of  $16 \text{ cm}^{-1}$  and scan time of 32 at four different positions (calyx, bottom and the both cheeks of fruit). After that, the samples were imaged by reflectance HSI at the wavelength of 400 - 1000 nm. The image was captured 1 position with the equator position facing toward the lens. Then sample was examined for moisture contents of peel, flesh, seed and whole fruit, total soluble solids (TSS) and sucrose, glucose, fructose and total sugar contents. Calibration and validation models of both techniques were built using a partial least square regression analysis. It was found that averaging spectra of all positions of dried whole longan by NIRS was suitable for determining the moisture content of flesh, TSS, sucrose, fructose and total sugar content that provided the coefficient of determination ( $R^2$ ) of 0.9513, 0.9219, 0.8343, 0.8158 and 0.9082, respectively and gave the root square error of prediction (RMSEP) of 5.53%, 6.52 °Brix, 53.8 mg/g fresh weight, 13.9 mg/g fresh weight and 51.9 mg/g fresh weight, respectively. While, the HSI could not be used for determining moisture content of flesh, TSS, sucrose, glucose, fructose and total sugar content due to low  $R^2$  of 0.7071, 0.6676, 0.5247, 0.2699, 0.4944 and 0.5333, respectively and high RMSEP of 13.60%, 13.36 °Brix, 90.93 mg/g fresh weight, 24.03 mg/g fresh weight, 23.86 mg/g fresh weight and 115.42 mg/g fresh weight, respectively.

---

Department of Food Technology

Graduate School, Silpakorn University

Student's signature .....

Academic Year 2015

Thesis Advisor's signature .....

56403225 : สาขาวิชาเทคโนโลยีอาหาร

คำสำคัญ : ปริมาณความชื้น/ปริมาณน้ำตาล/ลำไยอบแห้งทั้งผล/เทคนิคสเปกโทรสโกปีอินฟราเรดย่าน

ใกล้/เทคนิคการถ่ายภาพสเปกตรัม

เอเลียห์ เลิศกุล : การใช้เทคนิคสเปกโทรสโกปีอินฟราเรดย่านใกล้และการถ่ายภาพสเปกตรัมในการติดตามปริมาณความชื้นและปริมาณน้ำตาลในเนื้อลำไยอบแห้งทั้งผล.

อาจารย์ที่ปรึกษาวิทยานิพนธ์ : ผศ.ดร.บุศราภรณ์ มหาโยธี. 164 หน้า.

งานวิจัยนี้มีวัตถุประสงค์เพื่อนำเทคนิคสเปกโทรสโกปีอินฟราเรดย่านใกล้ (NIRS) และการถ่ายภาพสเปกตรัม (HSI) ซึ่งเป็นวิธีการที่รวดเร็ว และไม่ทำลายตัวอย่างมาประยุกต์ใช้ในการตรวจสอบปริมาณความชื้นและปริมาณน้ำตาลในเนื้อลำไยอบแห้งทั้งผล โดยจะทำการวัดสเปกตรัมของตัวอย่างลำไยสดและอบแห้งสำหรับการวิเคราะห์ปริมาณความชื้น 496 ผล และการวิเคราะห์ปริมาณน้ำตาล 186 ผล ในตำแหน่งที่ต่างกัน ได้แก่ ขั้ว ก้น และด้านข้างทั้งสองข้างของลำไย ด้วยเครื่อง FT-NIR (800-2500 นาโนเมตร) จากนั้นทำการถ่ายภาพสเปกตรัมด้วยกล้องถ่ายภาพสเปกตรัม (400-1000 นาโนเมตร) 1 ภาพต่อผล โดยให้ด้านกว้างของลำไยตรงกับเลนส์กล้อง สำหรับการสร้างสมการทำนายปริมาณความชื้นในส่วนเปลือก เนื้อ เมล็ด และทั้งผล ปริมาณของแข็งทั้งหมดที่ละลายได้ (TSS) และปริมาณซูโครส กลูโคส และฟรุกโตสของเนื้อลำไยอบแห้ง สร้างสมการทำนายโดยใช้วิธีการถดถอยกำลังสองน้อยที่สุดบางส่วน (partial least squares, PLS) จากการศึกษาพบว่า การเฉลี่ยเส้นสเปกตรัมที่วัดจากทุกตำแหน่งของลำไยอบแห้งทั้งผลด้วยเทคนิค NIRS มีความเหมาะสมในการนำมาตรวจสอบปริมาณความชื้น TSS ปริมาณซูโครส ฟรุกโตส และปริมาณน้ำตาลทั้งหมดได้ โดยให้ค่าสัมประสิทธิ์การตัดสินใจ (coefficient of determination,  $R^2$ ) เท่ากับ 0.9513, 0.9219, 0.8343, 0.8158 และ 0.9082 ตามลำดับ และมีค่าความคลาดเคลื่อนในการทำนาย (root square error of prediction, RMSEP) เท่ากับ 5.53% 6.52 องศาบริกซ์ 53.8 มิลลิกรัมต่อกรัม น้ำหนักสด 13.9 มิลลิกรัมต่อกรัม น้ำหนักสด และ 51.9 มิลลิกรัมต่อกรัม น้ำหนักสด ตามลำดับ และจากผลการศึกษาด้วยเทคนิค HSI พบว่าเทคนิค HSI ยังไม่สามารถใช้ในการตรวจสอบปริมาณความชื้นในเนื้อลำไย TSS ปริมาณซูโครส กลูโคส ฟรุกโตส และปริมาณน้ำตาลทั้งหมดลำไยอบแห้งทั้งผลได้ เนื่องจากให้ค่า  $R^2$  และ RMSEP ที่ต่ำ โดยให้ค่า  $R^2$  เท่ากับ 0.7071, 0.6676, 0.5247, 0.2699, 0.4944 และ 0.5333 ตามลำดับ และให้ค่า RMSEP ที่สูงเท่ากับ 13.60% 13.36 องศาบริกซ์ 90.93 มิลลิกรัมต่อกรัม น้ำหนักสด 24.03 มิลลิกรัมต่อกรัม น้ำหนักสด 23.86 มิลลิกรัมต่อกรัม น้ำหนักสด และ 115.42 มิลลิกรัมต่อกรัม น้ำหนักสด ตามลำดับ

ภาควิชาเทคโนโลยีอาหาร

บัณฑิตวิทยาลัย มหาวิทยาลัยศิลปากร

ลายมือชื่อนักศึกษา.....

ปีการศึกษา 2558

ลายมือชื่ออาจารย์ที่ปรึกษาวิทยานิพนธ์ .....

## Acknowledgements

Firstly, I would like to express my sincere gratitude to my advisor, Assist. Prof. Dr. Busarakorn Mahayothee, for the continuous support of this research for her patience, motivation, and extensive knowledge. Her guidance helped me in all the time of research and writing of this thesis. I could not have imagined having a better advisor and mentor for my master study.

Furthermore, I would like to thank Assist. Prof. Dr. Pramote Khuwijtjaru for his assistance to my research for hyperspectral imaging and HPLC analysis.

I would like to thank my thesis committee, Dr. Rachit Suwapanich for her insightful comments and encouragement.

I am also thankful to Dr. Marcus Nagle from the Institute of Agricultural Engineering, Hohenheim University, Stuttgart, Germany for his helpful suggestion about using a hyperspectral imaging.

My sincere thanks also goes to Ms. Parika Rungpichayapichet, Ph. D. student at the Institute of Agricultural Engineering, Hohenheim University, Germany for her suggestions, encouragement and all her kind supports.

Prof. Dr. Joachim Müller from the Institute of Agricultural Engineering, Hohenheim University, Stuttgart, Germany is also acknowledge for his kind support to allow me to use the HSI equipment.

I would also like to thank the bachelor's degree student Ms. Thiparat Thamsala, Ms. Chattha Tathong and Mr. Pasawee Auppathmkuldilok for their help, for the stimulating discussions and for the sleepless nights we were working together.

Finally, I would like to thank my family: my parents and to my sister for supporting me spiritually throughout writing this thesis. To my friends and everybody in iTAP office (Silpakorn University), thank you for listening and all their support throughout the period of this research.

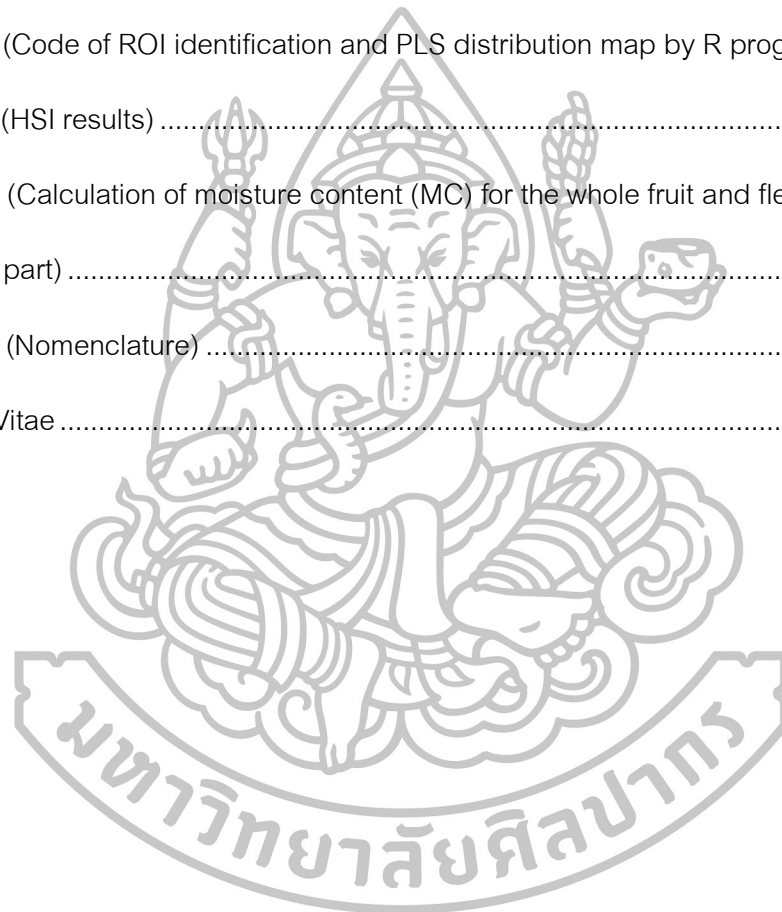
## Table of Contents

	Page
Abstract in English .....	d
Abstract in Thai.....	e
Acknowledgements.....	f
Table of Contents .....	g
List of Tables .....	j
List of Figures .....	m
Chapter	
1 INTRODUCTION.....	1
Background.....	1
Aim of the study.....	3
Hypothesis.....	3
Scope.....	3
2 LITERATURE REVIEWS.....	5
Longan .....	5
Drying whole longan.....	7
Standard for exporting dried whole longan fruit.....	8
Whole longan dryer.....	8
Method of processing of dried whole longan.....	9
Changes of longan after drying.....	10
Near- infrared spectroscopy (NIRS).....	13
Near- infrared spectroscopy for food analysis.....	15
Hyperspectral imaging (HSI).....	19



	Page
Hyperspectral imaging for food analysis .....	22
3 MATERIALS AND METHODS.....	29
Materials.....	29
Longan samples.....	29
Chemicals.....	29
Methods .....	30
Physical and chemical properties of fresh longan .....	30
Sample preparation.....	32
Nondestructive measurement for determination of moisture content and sugar content in dried whole longan .....	34
4 RESULTS AND DISCUSSION .....	40
Physical and chemical properties of fresh longan .....	40
Near-infrared spectroscopy for determination of moisture content and sugar content in dried whole longan .....	42
Diffuse reflectance spectra of fresh and dried whole longan by NIRS .....	42
Calibration models for moisture content by NIRS.....	45
Calibration models for TSS of flesh by NIRS .....	74
Calibration models for sugar content of flesh by NIRS .....	79
Hyperspectral imaging for determination of moisture content and sugar content in dried whole longan.....	95
HSI images and reflectance spectra of fresh and dried whole longans.....	95
Calibration models for moisture content by HSI .....	97
Calibration models for TSS of flesh by HSI.....	109
Calibration models for sugar content of flesh by HSI.....	111
5 CONCLUSION.....	119
References .....	120

	Page
Appendix A (Sugars standards) .....	127
Appendix B (NIRS) .....	130
Appendix C (Regression coefficient of NIRS).....	132
Appendix D (Verify accuracy of calibration models).....	135
Appendix E (Code of ROI identification and PLS distribution map by R program) .....	142
Appendix F (HSI results) .....	146
Appendix G (Calculation of moisture content (MC) for the whole fruit and flesh and seed part) .....	146
Appendix H (Nomenclature) .....	160
Curriculum Vitae .....	163



## List of Tables

Tables	Page
1 The nutritional composition of flesh longan .....	6
2 The capabilities of near- infrared spectroscopy for quantitative analysis of food. ....	16
3 Main differences among imaging, spectroscopy and hyperspectral imaging techniques. ....	22
4 The capabilities of HSI for quantitative analysis of food .....	23
5 Drying conditions and sampling of longan for the study. ....	33
6 Height, diameter, width and weight per fruit of fresh longan .....	40
7 Moisture content (MC) of peel, flesh and seed as well as the whole fruit, TSS, sucrose, glucose and fructose content of fresh flesh longan .....	41
8 Mean, standard deviation (SD), minimum and maximum of moisture content (%) for longan fruit samples from different fruit parts and the whole fruit. ....	45
9 Calibration and validation results for moisture content of peel by NIRS. ....	49
10 Calibration and validation results for moisture content of flesh by NIRS. ....	52
11 Calibration and validation results for moisture content of flesh (9-40%) by NIRS. ....	54
12 Calibration and validation results for moisture content of seed by NIRS. ....	56
13 Calibration and validation results for moisture content of flesh and seed by NIRS. ....	59
14 Calibration and validation results for moisture content of whole fruit by NIRS. ....	62
15 The absorption bands with high regression coefficients of model for moisture content of flesh of the longan fruits. ....	65
16 The absorption bands with high regression coefficients of the PLS model for moisture content of the whole longan fruits. ....	67
17 The comparison of measured and predicted moisture content of flesh of 120 dried whole longan fruits from this study by the best fit model. ....	69
18 The comparison of measured and predicted moisture content of flesh of 20 unknown samples by the best fit models. ....	72

Tables	Page
19	Verifying the accuracy by bias checking, SEP checking and slope checking method for NIRS moisture content models. ....73
20	Mean, standard deviation (SD), minimum and maximum of TSS of flesh in longan fruit samples. ....74
21	Calibration and validation results for TSS in flesh of dried whole longan by NIRS. ....76
22	Verifying the accuracy by bias checking, SEP checking and slope checking method for TSS model.....78
23	Mean, standard deviation (SD), minimum and maximum of sugar content of flesh in longan fruit samples. ....80
24	Calibration and validation results for sucrose content of flesh by NIRS. ....84
25	Calibration and validation results for glucose content of flesh by NIRS. ....87
26	Calibration and validation results for fructose of flesh by NIRS. ....89
27	Calibration and validation results for total sugar of flesh by NIRS. ....91
28	Verifying the accuracy by bias checking, SEP checking and slope checking method for sugar content models.....94
29	Mean, standard deviation (SD), minimum and maximum of moisture content (%) for longan fruit samples from different fruit parts and the whole fruit (HSI). ....98
30	Calibration and validation results for moisture content from different fruit parts and the whole longan fruit samples by HSI. ....100
31	Mean, standard deviation (SD), minimum and maximum of TSS of flesh in longan fruit samples for predicting TSS (HSI). ....109
32	Calibration and validation results for TSS in flesh of longan fruit samples by HSI ..110
33	Mean, standard deviation (SD), minimum and maximum of sugar content for longan fruit samples (HSI).....112
34	Calibration and validation results for sugar content in flesh of longan fruit samples by HSI .....114
35	Verifying the accuracy by bias checking, SEP checking and slope checking method.....138

Tables	Page
36 Bias checking .....	139
37 SEP checking .....	140
38 Slope checking.....	141
39 Calibration and validation results for moisture content of peel of whole longan fruit samples by HSI. ....	147
40 Calibration and validation results for moisture content of flesh of whole longan fruit samples by HSI. ....	148
41 Calibration and validation results for moisture content of seed of whole longan fruit samples by HSI. ....	149
42 Calibration and validation results for moisture content of whole longan fruit samples by HSI. ....	150
43 Calibration and validation results for moisture content of flesh and seed of whole longan fruit samples by HSI. ....	151
44 Calibration and validation results for TSS in flesh of dried whole longan fruit samples by HSI. ....	152
45 Calibration and validation results for sucrose in flesh of dried whole longan fruit samples by HSI. ....	153
46 Calibration and validation results for glucose in flesh of dried whole longan fruit samples by HSI. ....	154
47 Calibration and validation results for fructose in flesh of dried whole longan fruit samples by HSI. ....	155
48 Calibration and validation results for total sugars in flesh of dried whole longan fruit samples by HSI. ....	156

## List of Figures

Figures	Page
1	Export volume and value of dried whole longan fruit between 2006-2015. .... 7
2	Structure and operation process of a batch dryer cabinet. .... 9
3	Drying curve of longan fruit at relative humidity 8 %, temperature 50-90 °C and air velocity 0.2 m/s. .... 11
4	Drying curve of longan fruit at different size, relative humidity 8 %, temperature 80°C and air velocity 0.2 m/s. .... 11
5	Moisture content from experiment of seed, pericarp and aril during drying at 70°C. . 12
6	NIRS system ..... 13
7	NIRS measuring modes (A/B) transmittance, (C) diffuse reflectance and (D/E) transfectance. .... 14
8	Hyperspectral image cube (hypercube). .... 19
9	Components of a typical hyperspectral imaging system. .... 20
10	Acquisition of hyperspectral images and modes of measurement. .... 21
11	Moisture distribution maps in salmon fillets. The values in the bottom of figures showed the average concentration of moisture in the whole fillet. Fillets (a) and (b) had high moisture content (MC) while fillets (c) and (d) had low MC. .... 24
12	Visualization map of lychee with different browning levels. .... 26
13	Moisture content distributions on mango slices of different shape. .... 26
14	Averaged (a) uncorrected spectra of healthy zones of clemenules mandarin and (b) corrected spectra of healthy zones of clemenules mandarin of four different regions of the image. .... 27
15	Fresh longan fruits cultivar Edor grade AA. .... 29
16	Measuring size of longan by using vernier caliper. (a) height, (b) diameter and (c) width. .... 30
17	The placement of longans for drying. .... 32
18	Near-infrared spectroscopy system. .... 34

Figures	Page
19 The four measured positions for NIR spectrum acquisition. ....	35
20 Schematic diagram of hyperspectral image system. ....	37
21 Example of hyperspectral images of fresh and dried whole longan obtained from drying at 60°C for 15, 30 and 50 hr. ....	38
22 10 points selected of sample in R program. ....	38
23 Example of original spectra of fresh and dried whole longans dried at different temperatures for 40 hours at measurement position 1 (P1). ....	43
24 Example of original spectra of dried whole longans obtained from different positions and drying at 60°C for 40 hours. ....	43
25 Example of second derivative spectra of fresh and dried whole longan dried at different temperatures for 40 hours at measurement position 1 (P1). ....	44
26 Histogram of distribution of moisture content of peel, flesh, seed, flesh and seed and the whole fruit of samples in calibration set and validation set. ....	47
27 Scatter plot of moisture content of peel from the model built from averaging spectra. ....	50
28 Scatter plot of moisture content of flesh from the model built from averaging spectra. ....	53
29 Scatter plot of moisture content of seed of from the model built from averaging spectra. ....	57
30 Scatter plot of moisture content of flesh and seed from the model built from averaging spectra. ....	60
31 Scatter plot of moisture content of whole fruit from the model built from averaging spectra. ....	63
32 Regression coefficient plot of moisture content of flesh from the model built from averaging spectra. ....	64
33 Regression coefficient plot of of moisture content of the whole fruit from the model built from averaging spectra. ....	66

Figures	Page
34	Histogram of the distribution of TSS of flesh of samples in calibration and validation set. ....74
35	Scatter plot of TSS of flesh from the model built from averaging spectra.....77
36	Regression coefficient plot of TSS of flesh from the model built from averaging spectra.....78
37	Histogram of the distribution of sugar content of flesh of samples in calibration and validation set. ....82
38	Scatter plot of sucrose of flesh from the model built from averaging spectra. ....85
39	Scatter plot of glucose of flesh from the model built from averaging spectra. ....88
40	Scatter plot of fructose of flesh from the model built from averaging spectra. ....90
41	Scatter plot of total sugar of flesh from the model built from averaging spectra. ....92
42	Regression coefficient plot of PLS models validated for sugar content of flesh of the longan fruits: (a) sucrose; (b) glucose; (c) fructose and (d) total sugars. ....93
43	Example of HSI image and reflectance spectrum of whole longan (a) fresh and (b) dried at 60°C for 40 hours. ....95
44	Example of original spectra of fresh and dried whole longan dried at different temperatures for 40 hour.....96
45	Example of second derivative HSI spectrum of dried whole longan obtained from drying at 60°C for 40 hours. ....97
46	Scatter plot of moisture content of peel by HSI. ....101
47	Scatter plot of moisture content of flesh by HSI. ....102
48	Scatter plot of moisture content of seed by HSI. ....102
49	Scatter plot of moisture content of flesh and seed by HSI. ....103
50	Scatter plot of moisture content of whole fruit by HSI.....103
51	Regression coefficient plots of (a) moisture content of flesh and (b) moisture content of the whole fruit by HSI. ....104



Figures	Page
52	The example of moisture content distribution maps of whole longan generated by PLS model of moisture content for flesh and the whole fruit (a) and (b) fresh whole longan; (c) and (d) dried whole longan at 60°C for 12 hr; (e) and (f) dried whole longan at 60°C for 30 hr; (g) and (h) dried whole longan at 60°C for 36 hr and (i) and (j) dried whole longan at 60°C for 60 hr. .... 108
53	Scatter plot of TSS of flesh by HSI ..... 110
54	Regression coefficient plots of TSS of flesh by HSI..... 111
55	Scatter plot of sucrose of flesh by HSI..... 115
56	Scatter plot of glucose of flesh by HSI..... 116
57	Scatter plot of fructose of flesh by HSI..... 116
58	Scatter plot of total sugar of flesh by HSI. .... 117
59	Regression coefficient plot of PLS models validated for sugar content of flesh of the longan fruits by HSI: (a) sucrose; (b) glucose; (c) fructose and (d) total sugars ..... 118
60	Chromatogram of individual sugars..... 128
61	Standard curve for sucrose (a) glucose (b) and fructose (c)..... 129
62	Regression coefficient plot of a PLS model validated for moisture content of peel of the longan fruits..... 133
63	Regression coefficient plot of a PLS model validated for moisture content of seed of the longan fruits..... 133
64	Regression coefficient plot of a PLS model validated for moisture content of flesh and seed of the longan fruits. .... 134

## CHAPTER 1 INTRODUCTION

### 1.1 Background

Longan (*Dimocarpus longan* Lour.) is one of the economically important crops in Thailand especially in Lamphun and Chiang Mai provinces. In 2015, around 553 thousand tons of longan was exported as fresh, frozen, dried and canned longan that earned the income approximately 15.8 billion Baht (Office of Agricultural Economics, 2016). Twenty five percent of the total production volume was processed by drying. More than 80% of fruits for drying were dried as whole longan which was then exporting to China and Hong Kong. Dried whole longan fruit has a high export volume about 110,729 tons with value around 5.4 billion Baht (Office of Agricultural Economics, 2016).

According to the Thai Agricultural Standard for exporting dried whole longan, the qualities required are size (19-25 mm), peel color (brown or reddish dark brown color), moisture content for the whole fruit not exceeding 13.5% or not exceeding 17% for the flesh only, water activity of the flesh not exceeding 0.6, total soluble solids of the flesh not lower than 76 °Brix and pH of the flesh not lower than 5.0 (Thai Agricultural Standard, 2006).

Major of drying method is used a batch dryer cabinet which has LPG burner for heat providing and the drying temperature is almost unstable (Tippayawong et al., 2008). Normally, non-homogeneity of drying is obtained and leads to higher moisture content of flesh which risks for mold growth during storage (Nagle et al., 2010). Thus, the moisture content of product at the end of acceptance point is absolutely important in drying.

In addition, most of the carbohydrates in longan are in the form of sucrose, glucose and fructose which provide longan's characteristic taste that is directly related to flavor and acceptability of consumers (Rangkadilok et al., 2005). Recently, there has been the production of longan syrup and longan sugar, new and high commercial product market. These products are studied to have functional properties such as the ability to act as a sugar replacer and use for fructo-oligosaccharides production (Surin et al., 2012).

In general, internal quality of dried longan is determined by chemical composition such as moisture content which has commonly been used a conventional oven-drying method and the sweetness has generally been assessed in term of total soluble solids (TSS) with refractometer and individual sugars by HPLC (high performance liquid chromatography) which provide acceptable accuracy for industry. However, standard methods for determining these qualities are destructive, time consuming and not suitable for rapid monitoring or on-line sorting applications (Rady and Guyer, 2015). Hence, rapid and nondestructive method is needed.

Nowadays, several studies have been successfully used the near-infrared spectroscopy (NIRS), which is a method to predict the quality of food due to the speed of analysis, nondestructive and chemical-free technique. In 2013, this technique was applied to study about olive and the result found that NIRS had a possibility to assess moisture content of olive (Morales-Sillero et al., 2011). According to Rady and Guyer (2015), the use of NIR diffuse reflection for quantitative analysis was effectively evaluated glucose and sucrose content of potatoes. Moreover, Bai et al. (2014) found that the different positions of measurement of NIRS on the blueberry fruits (the calyx or a position not on the calyx) gave different characteristics of spectra which related to the various prediction results. Furthermore, there is another technique that is acceptable in many industries. Hyperspectral imaging (HSI) is a technique that integrates imaging and spectroscopy technologies for attaining spatial and spectral information of product. The main advantage of this technique is to select any region of interest (ROI) in the HSI image, although NIRS is only to collect an individual spectrum at one point on the

sample (Elmasry and Sun, 2010). Several researches have been using this technique for the quality assessment in agricultural products for example; Huang et al. (2014) had successfully applied HSI for determining moisture content of soybean and the prediction of TSS of table grapes using HSI was operated by Baiano et al. (2012). However, nobody has used this technique for determining quality of dried whole longan of Thailand. Thus, the goal of this study is to examine the feasibility of two nondestructive techniques (NIRS and HSI) to apply for determining moisture content and sugar content in flesh of dried whole longan fruit which can be further using in routine analysis in industry.

### 1.2 Aim of the study

To study the possibility of NIRS and HSI for determining moisture and sugar contents of dried whole longan.

### 1.3 Hypothesis

Different conditions of drying (temperature and time) affect the changing of moisture and sugar content in longan. NIRS and HSI techniques can vibrate the chemical bonds of molecules of water and sugar that includes C, H, O and N atoms. Thus, there may be possible for determining moisture and sugar content in dried whole longan.

### 1.4 Scope

1.4.1 Fresh longan fruits cultivar Edor (AA grade, diameter 24-27 mm) were dried at different condition (60, 70 and 80 °C) using a tray dryer with a through flow mode or until the dried flesh had moisture content less than 18%. Samples were taken for analyses at different times of drying.

1.4.2 Dried longans (at different condition) were measured NIRS (800-2500 nm) and imaged by HSI (400-1000 nm).

1.4.3 To analyze moisture content by using hot air oven 105 °C until the weight was constant (AOAC, 2000) and sugar content by HPLC (Liu et al., 2013).

1.4.4 To build suitable model for predicting quality values of dried longan (from NIRS and HSI) and validate the model.



## CHAPTER 2

### LITERATURE REVIEWS

#### 2.1 Longan

Longan (*Dimocarpus longan* Lour.) is a subtropical fruit widely grown in China and Asia, including Thailand, Vietnam, and the Philippines (Angkasith et al., 1999). Longan has many scientific names such as *Euphoria longana* Lam., *Euphoria longan* Strend., *Nephelium longana* Camb. and *Dimocarpus longan* Lour. (Pawin et al., 2000) and common names are longan, lungan, dragon's eye or eyeball. Longan is one of the economically important crops in the northern part of Thailand. Moreover, the cultivars planted longans in the varied regions in Thailand, they are cv. Eдор, Chompoo, Haew and Biew Khiew. Thus, the most popular cultivar is Eдор about 66 % of the total longan growing area in the country. Second, cv. Chompoo about 10% and then, cv. Haew about 8%, cv. Biew Khiew about 7% and other cultivars about 9% (Pawin et al., 2000).

Longan is a non-climacteric fruit and accordingly, they do not ripen until they are harvested. Consequently, the fruit must be picked at an optimal eating quality (Huang, 1995). Longan fruit consists of an almost large black or dark brown seed at maturity. The fruit is heart-shaped or round with a thin and leathery pericarp. The pericarp has yellowish to light brown color, and the skin is smooth. The tissue of flesh is fleshy, soft and has translucent white color. In addition, the longan tree has the height approximately 10-20 feet. The tree is similar to lychee tree. Normally, longan tree flowers at the end of winter and the mature longan fruit was harvested over July to September (Jiang et al., 2002).

Harvest indexes of longan are skin color, weight of fruits and total soluble solids of flesh. The concentration of total sugar increases in longan fruit during ripening with total sugar content varying with stage of maturity and cultivar (Menzel and Waite, 2005).

In addition, Longan is a fruit which gives high energy for costumer as a result of the presence of sugars. The major sugars are sucrose, fructose and glucose (Li et al., 2009). The fresh pulp of longan has several nutritional components, and investigated to have health benefits (Huang et al., 2012). The nutritional composition of fresh flesh and dried flesh of longan are shown in Table 1. Moreover, longan involves high amount of secondary metabolites such as phenolic acids, flavonoids and polysaccharide. The major phenolic compounds of longan are gallic acids, ellagic acid and coliragin. These compounds were found in all parts of the fruit such as peel, flesh and seed (Prasad et al., 2009).

**Table 1** The nutritional composition of flesh longan

Nutritional composition	Fresh flesh longan	Dried flesh longan
Moisture content (%)	81.10	7.80
Fat (%)	0.11	0.40
Fiber (%)	0.28	1.60
Protein (%)	0.97	4.60
Ash (%)	0.56	2.86
Total carbohydrate (%)	16.98	72.70
Energy (kcal/kg)	305.70	1,310.00
Calcium (mg. 100 <sup>-1</sup> g)	5.70	27.70
Iron (mg. 100 <sup>-1</sup> g)	0.35	2.39
Phosphorus (mg. 100 <sup>-1</sup> g)	35.30	59.50
Ascorbic acid (mg. 100 <sup>-1</sup> g)	69.20	137.80
Sodium (mg. 100 <sup>-1</sup> g)	-	4.50
Potassium (mg. 100 <sup>-1</sup> g)	-	2,012.00
Nicotinic acid (mg. 100 <sup>-1</sup> g)	-	3.03
Vitamin B2 (mg. 100 <sup>-1</sup> g)	-	0.37

Source: Tongdee (1997)

## 2.2 Drying whole longan

Dried whole longan fruit is an important processed agricultural product and a significant export item of Thailand. The volume of dried whole longan exports increased slightly around 10 times during 2006-2015. In 2011 had the highest volume of exporting as shown in Figure 1 (Office of Agricultural Economic, 2016). Longan drying process can extend a period of time for preservation and can reduce loss arising from seasonal glut (Thai Agricultural Standard, 2006). There are many longan cultivars for drying which includes Edor, Chompoo, Haew and Biew Khiew. However, longan cv. Edor is the most popular cultivar for drying, because of its large size and good color of peel. Longan cv. Edor which is sweet and has good flavor, is rather tough and not as crispy as compared to the flesh of cv. Biew Khiew. About cv. Haew, it gives dark peel color when it was dried (Maitree and Wijit, 2004).

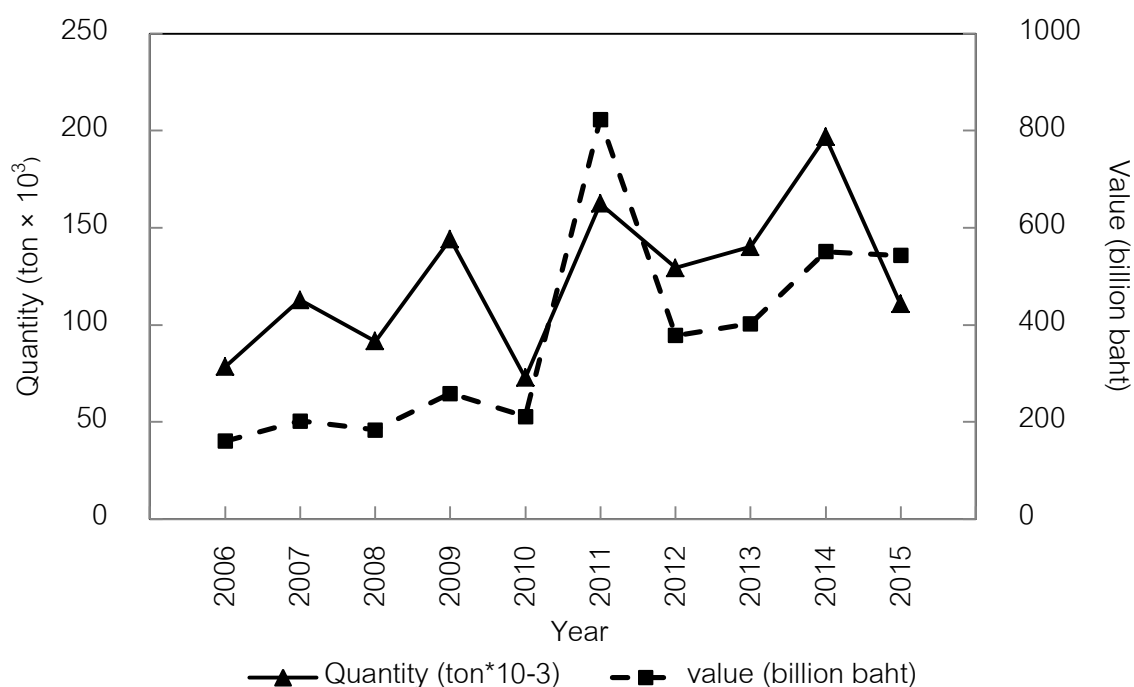


Figure 1 Export volume and value of dried whole longan fruit between 2006-2015.

Source: Office of Agricultural Economics (2016)



### 2.2.1 Standard for exporting dried whole longan fruit

According to the Thai Agricultural Standard for exporting dried whole longan, the fruit will have either brown or dark brown color. The skin will be free from burnt and mycelium. The flesh will be dry, non-sticky and its flavor will be sweet and free from sour or bitter taste (Thai Agricultural Standard, 2006).

Dried whole longan fruit according to this standard is classified into 4 sizes as follows: size code 1 (>2.5 cm diameter), 2 (>2.2-2.5 cm diameter), 3 (>1.9-2.2 cm diameter) and 4 (1.5-1.9 cm diameter)

For the chemical requirement, the moisture content for the whole fruit (including flesh, pit and skin) must not exceed 13.5% or not exceed 17% for the flesh only, water activity of the flesh must not exceed 0.6, total soluble solids of the flesh not lower than 76 °Brix and pH of the flesh must not be lower than 5.0 (Thai Agricultural Standard, 2006).

### 2.2.2 Whole longan dryer

There are many whole longan dryers in Thailand. Most dryers are manually used batch dryer cabinets. Generally, the drying cabinet has the dimensions of 2.35 m × 2.35 m × 1.0 m with a loading capacity of around 1,500- 2,000 kg of fresh longan per batch. The batch dryer consists of walls of galvanized steel sheet with a perforated metal tray which is higher from the floor of the bed for hot air transition as shown in Figure 2. Fresh unpeeled longan is laid on top of a stationary thick bed on one large tray. Heat is supplied to the fruit layer by a diesel or liquefied petroleum gas (LPG) burner. The hot air is induced by a fan, which is driven by a motor on the top. Hot air heats up the longans and also carries moisture out. The moist air leaves at the top of the bed to the ambient environment (Tippayawong et al., 2008). Normally, it uses time about 48 hr. for drying and the price of the dryer was about 30,000-40,000 Baht (Tippayawong et al., 2008).

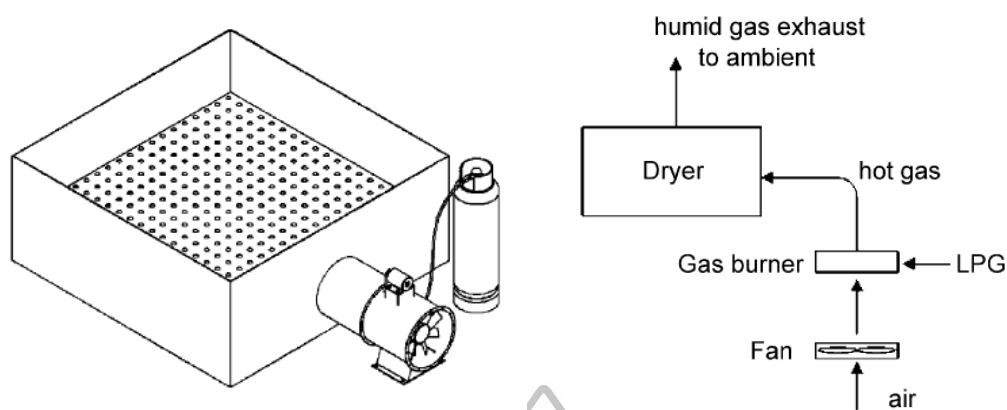


Figure 2 Structure and operation process of a batch dryer cabinet.

Source: Tippayawong et al. (2008)

### 2.2.3 Method of processing of dried whole longan

Presently, drying the whole longan in Thailand has many methods and processes. However, majority of drying methods is the same. Maitree and Wijit (2004) reported about the method of drying the whole longan as follows:

Firstly, fresh longan fruits cultivar Eador were graded into AA grade, A grade, B grade, C grade and broken longan. Due to the difference of sizes, the small fruit used at least 40 hr. for drying while the bigger one used at least 48 hr. After that, the fresh longan fruits were dried by batch dryer cabinet at temperature 70-80°C for 40-48 hr. The big fruits should be placed below the dryer for faster drying. The difference of fruit sizes were separated each other by perforated metal trays. During drying, operators usually turn the fruit layer upside down and inside out completely in 12-15 h intervals (Tippayawong et al., 2008). In drying process, the temperature should not be too high. It might lead to dark color or burn on longan peel. After finishing, dried longans were left for 1-2 hr. and then graded again by sorting machine. Finally, 10 kg plastic bags were packed inside the paper boxes for distributing (Maitree and Wijit, 2004).

According to drying the whole longan by batch dryer cabinet, non-uniform drying in term air flow and temperature is obtained. Drying operator usually solves this

problem by transposition layers of longans in the dryer. This method causes bruises and cracks of dried longans (Janjai et al., 2006). Thus, there were some researchers who studied about this problem for improving the drying.

Janjai et al. (2006) has studied on air velocity distribution in the plenum of the dryer for improving drying uniformity. It was found that the distribution of air temperature and air speed in the dryer were very non-regular that affected longans in the lower layer were dried faster than the fruits in other layers. This problem was solved by placing air guides and enlarging the space for mixing air under the perforated tray.

Nagle et al. (2010) has focused on improving quality and energy performance of a fixed-bed longan dryer by thermodynamic modification that included air deflector installations in the plenum and insulation. The study found that air velocity distribution was improved. Modifications decreased non-uniform drying and there were more homogenous product color. However, non-homogeneity of drying is still found.

#### 2.2.4 Changes of longan after drying

Phupaichitkun et al. (2005) reported that the moisture content of dried whole longan decreased when the drying time was increased. Air temperature and size of fruit affected the whole longan drying. Same as other agricultural products the drying time decreases when the air temperature is increased as shown in Figure 3. The larger fruit took longer time to dry whereas the increased diffusion path within the fruit (Figure 4). The result also found that the rate of water transfer from the surface of the fruit to the air was faster than the rate of water diffusion from the inside of the fruit to the surface of the fruit. However, the mass transfer from the inside to the surface was the main affecting factor during the drying process for the whole longan. About the water activity, often the water activity in the seed will be greater than 0.6 that still remains a storage risk. The higher water activity in comparison with the fruit flesh showed that the seed has a specific water sorption.

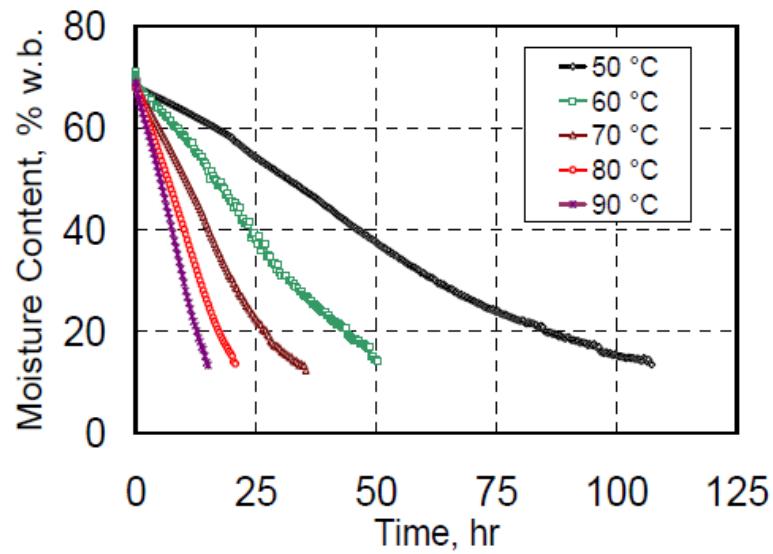


Figure 3 Drying curve of longan fruit at relative humidity 8 %, temperature 50-90 °C and air velocity 0.2 m/s.

Source: Phupaichitkun et al. (2005)

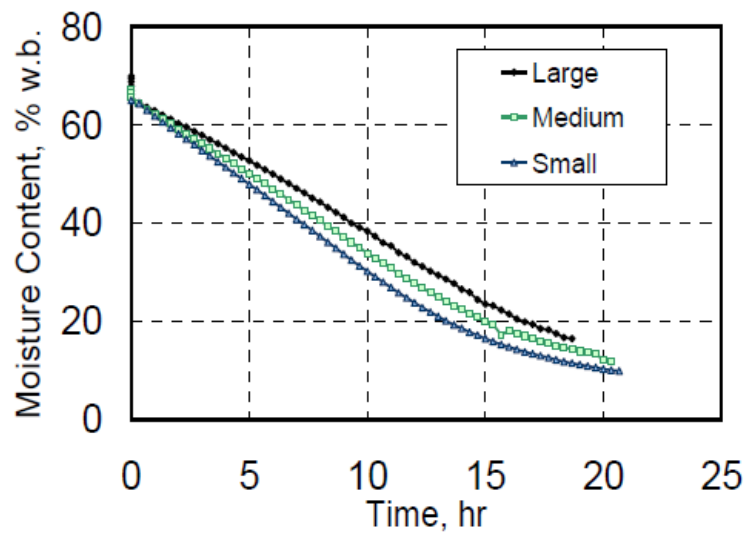
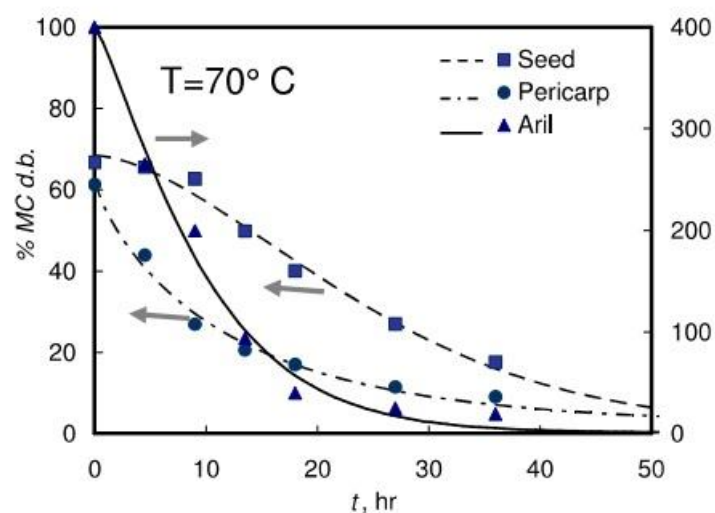


Figure 4 Drying curve of longan fruit at different size, relative humidity 8 %, temperature 80 °C and air velocity 0.2 m/s.

Source: Phupaichitkun et al. (2005)

Phupaichitkun et al. (2006) studied about the shrinkage inside Thai unpeeled longan fruit. Each part contains a different structure and substance. The shrinkage characteristic of longan depends on the structure of dried solid and interaction between liquid and solid in each part. According to the structure of peel, the external layer contains thick wall and high porosity cells that is why there are no shrinkage during drying. The aril comprises high concentration of sugar solution in soft tissue. Thus, the interaction between liquid and solid part is very high. Seed has white meat with black seed coat which is low water permeability and the shrinkage of seed has a specific characteristic because of non-deformation in seed coat during drying. The kinetic of seed, aril and pericarp are shown in Figure 5. It was found that the structure of fruit had an effect on water transportation. The water of the seed only diffused through the seed stalk to the drying air. Hence, the drying rate of the seed was very slow. About the aril, the moisture content can diffuse through the seed stalk and vaporize to air gap inside the fruit and also diffuse as vapor through the pericarp.



**Figure 5** Moisture content from experiment of seed, pericarp and aril during drying at 70°C.

**Source:** Phupaichitkun et al. (2006)

### 2.3 Near- infrared spectroscopy (NIRS)

Near- infrared spectroscopy (NIRS) has been used as a method to predict the quality of food due to the speed of analysis, nondestructive and chemical-free techniques. In addition this technique can determine both of quantity and quality of products. Thus, several studies have been successfully used the NIRS technology for determining total soluble solids, acidity, texture and moisture content (Nicolai et al., 2007). NIR radiation covers the range of the electromagnetic spectrum between 780-2500 nm or 12,500-4,000  $\text{cm}^{-1}$ . In NIRS spectroscopy, the product which has O-H, C-H, N-H and C=H bonds is irradiated with NIR radiation, and the reflected or transmitted radiation is measured. Although, the radiation passes through the sample, its spectral characteristics change by scattering and absorption processes. This change depends on the chemical composition of the product which is related to the microstructure in the sample. Moreover, advanced statistical techniques, such as partial least squares regression is then applied to extract the information from the spectra (Sun, 2009). An NIRS system consists of a light source (usually a tungsten halogen light), sample presentation (sample holder or sample cell), interferometer, detector, optical components, such as lenses, collimators, beam splitters, integrating spheres and optical fibers and computer. The example of NIRS system is shown in Figure 6.

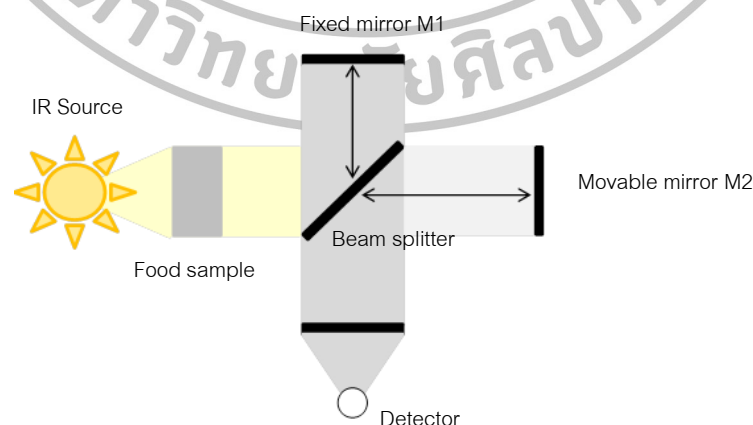


Figure 6 NIRS system

Source: Sun (2009).

NIR radiation has a penetration depth of up to 10 mm in the 800-1100 nm range and between 1 and 3mm in the 1100-2500 nm range (Nicolai et al., 2007). Furthermore, the appropriate mode of NIRS measurement will be controlled by the optical properties of the samples (Figure 7). Translucent materials are commonly measured in transmittance mode (Figure 7A). Impure liquids or semi-solids or solids may be measured in diffuse transmittance mode (Figure 7B), diffuse reflectance mode (Figure 7C) or transfectance mode (Figure 7D/E), depending on their absorption and scattering characteristics (Reich, 2005).

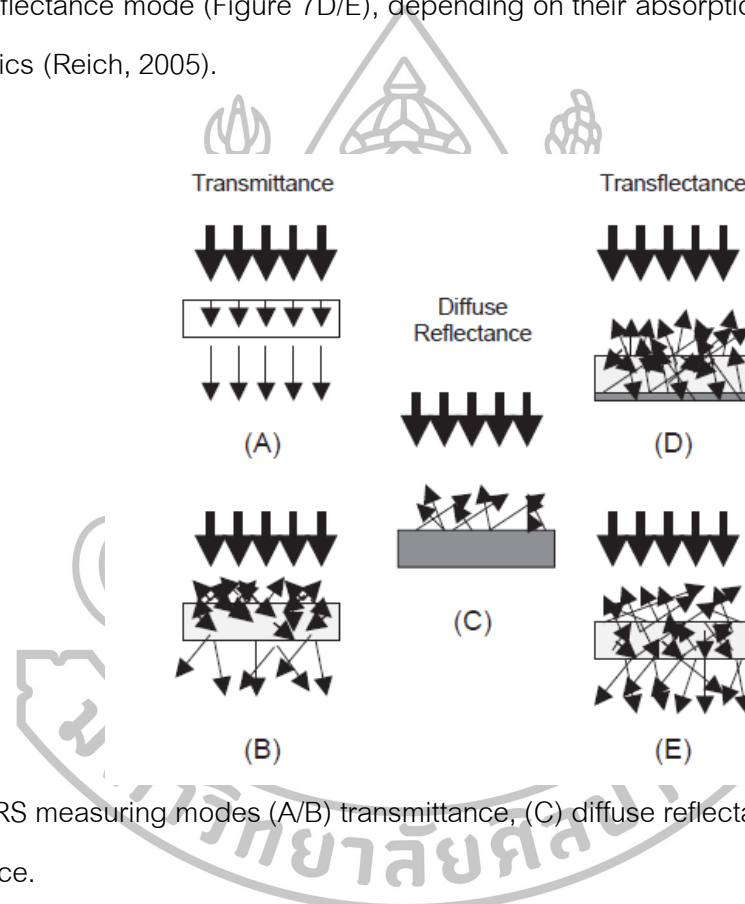


Figure 7 NIRS measuring modes (A/B) transmittance, (C) diffuse reflectance and (D/E) transfectance.

Source: Reich (2005)

NIRS technique can analyze both of quality and quantity information using relationship between spectral data and reference data. However, the spectra, received from this technique, were constructed from overtone and combination of function groups. Thus, NIRS spectra are often complex and normally acquire broad bands and overlapping peaks. Moreover, chemical, physical, and structural properties of sample

influence the measured spectra. Thus, there are some techniques for reducing this problem. Mathematical treatments used to develop NIRS spectra such as multiplicative scatter correction (MSC) and standard normal variate (SNV). Both methods have basically been used to process reflectance and transmittance spectra for reducing scatter-induced baseline offsets. Normalization algorithms used to reduce baseline shifts and intensity difference occurring from variable positioning or path length variations. Moreover, the resolution of overlapping bands and baseline offsets may be reduced by derivatives and smoothing algorithms (Reich, 2005).

After mathematical preprocessing, the multivariate regression methods most usually used in quantitative NIRS analysis are principal component regression (PCR) and partial least-squares (PLS) regression. Spectra acquisition and reference values are built the multivariate model to relate the spectral variations to the reference values of the analytical target. And then, cross validation or external validation performed to validate model (Reich, 2005).

### 2.3.1 Near- infrared spectroscopy for food analysis

NIRS technique is a promising technique for the non-destructive analysis and quality checks of many kinds of food. The capabilities of near- infrared spectroscopy for quantitative analysis of food (especially, moisture content and sugar) are shown in Table 2.



**Table 2** The capabilities of near- infrared spectroscopy for quantitative analysis of food.

Sample	Parameter	Range	No. of sample	Wavelength (nm)	Measurement mode	Data analysis	Accuracy	Reference
Ginseng powder	Moisture content	0-9%	92	1100-2500	Reflectance	PLS	R <sup>2</sup> = 0.998 RMSEP=0.140%	Ren and Chen (1996)
Potato chip	Moisture content	1.2-4.0%	15	1000-2500	Reflectance	PLS	R <sup>2</sup> = 0.990 RMSECV=1.93%	Shiroma and Rodriguez-Saona (2009)
Olive	Moisture content	54.7-75.9%	698	400-2498	Reflectance	PLS	R <sup>2</sup> = 0.880 RMSECV=1.35%	Morales-Sillero et al. (2011)
Cabbage	Moisture content	93.54-95.82%	120	500-1100	Reflectance	PLS	R <sup>2</sup> = 0.740 RMSEP=2.50%	Kramchote et al. (2014)
Potato	Sugar content	Glucose: 0.0028-1.1355% Sucrose: 0.0045-2.1842%	540	900-1685	Reflectance	PLS	R <sup>2</sup> = 0.77 RMSEP=0.0665% R <sup>2</sup> = 0.75 RMSEP=0.1324%	Rady and Guyer (2015)
Mango	TSS	7.7-26.3%	592	700-1100	Reflectance	PLS	R <sup>2</sup> = 0.9 SEP= 1.2%	Rungpichayapichet et al. (2016)
Curry soup	TSS	16.75-35.02%	113	800-2500	Reflectance	PLS	R <sup>2</sup> = 0.92 RMSEP= 0.95%	Sirisomboon and Nawayon (2016)

Ren and Chen (1996) used NIRS to measure the moisture content in the ginseng powder in the segment 1100-2500 nm. The spectra were treated by first derivative and scatter correction. A high correlation of determination was found to be 0.998, with a standard error of prediction (SEP) of 0.14%. Bias was only 0.12%. The results indicated that the equation obtained from this study would be used for the moisture content monitoring of the processed ginseng roots.

Shiroma and Rodriguez-Saona (2009) applied NIRS (1000-2500 nm) for rapid monitoring of potato chip quality including moisture content and fat content. The spectral data were analyzed by partial least squares regression (PLSR). Fat content ranged from 18 to 45% and moisture content ranged from 1.2 to 4%. Correlation coefficient (R) for moisture was  $>0.97$  with standard error of cross validation (SECV)  $< 0.3\%$  and the prediction models for fat had  $r > 0.96$  and  $SECV < 1.60$ .

Morales-Sillero et al. (2011) adopted NIRS in the range of 400-2498 nm to assess the properties of intact olives. Chemical parameters, such as oil and moisture contents were investigated. Coefficient of determination ( $R^2$ ) was 0.880 for moisture, with RMSECV of 1.35%. The results show that NIRS is a useful, rapid and non-destructive technique for determining moisture content of table olive industry.

de Oliveira et al. (2014) investigated the potential of NIRS to predict passion fruit ripening parameters as sugars, organic acids and carotenoids. Spectra of 56 samples of the lyophilized passion fruit were collected using in NIR range (800-2500 nm). Partial least square regression (PLSR) was used to build calibration models.  $R^2$  were found 0.862 for glucose, 0.756 for fructose, 0.691 for sucrose and 0.833 for total sugars. For glucose and fructose contents both methods were unsatisfactory due to low concentrations of these components in the passion fruits.

Kramchote et al. (2014) applied NIRS (500-1100 nm) to determine the quality of cabbage (moisture, SSC and ascorbic acid contents) and compare the prediction ability of interactance and reflectance measurements. The calibration model were built by partial least squares (PLS) regression. In case of moisture content, coefficient of determination ( $R^2$ ) of 0.67 and root mean square error of prediction (RMSEP) of 2.34

g/kg for interactance, with  $R^2$  of 0.74 and RMSEP of 2.50 g/kg for reflectance. Finally, there was possible to use the Vis/NIR spectroscopy as a rapid tool.

Rady and Guyer (2015) has been extensively and successfully applied NIRS (900-1685 nm) on sugar content in potatoes. This study aimed to study the prediction of glucose and sucrose for potato tubers that were important to the frying industry. Partial least squares regression (PLSR) was applied for building prediction models. Prediction models for glucose showed  $R^2$  was 0.77 with RMSEP of 0.0665% and for sucrose, the  $R^2$  was found 0.75 with RMSEP of 0.1324%. This study presented NIR reflectance spectroscopy to effectively evaluate the sugar content of potatoes.

Rungpichayapichet et al. (2016) used NIRS (700-1100 nm) to determine postharvest quality of mango such as firmness, total soluble solids (TSS), titratable acidity (TA) and ripening index (RPI) using partial least squares (PLS) regression analysis. For TSS, the results showed  $R^2$  of 0.9 and SEP of 1.2%. The results indicated that NIRS can be used as a good non-destructive technique for mango quality assessment.

Sirisomboon and Nawayon (2016) studied about the potential of NIRS (12,500-3600  $\text{cm}^{-1}$ ) to assess the total solids content of instant curry soups containing coconut milk.  $R^2$ , RMSEP, bias and RPD of 0.92, 0.95%, -0.20% and 3.71, respectively. The results showed that NIRS could be applied in an instant curry soup production line for production control and quality assurance.

From the results, it can be seen that NIRS gave high accuracy of moisture content and sugar content prediction. Thus, this technique might be used for determining moisture content and sugar content in flesh of dried whole longan in my study.

## 2.4 Hyperspectral imaging (HSI)

Hyperspectral imaging is a technique that integrates spectroscopy and imaging techniques to permit identification of different components and their spatial distribution in sample. This technique contributes a two-dimensional spatial array of vectors which represents the spectrum at each pixel location. The resulting three-dimensional dataset involving the two spatial dimensions and one spectral dimension is known as the datacube or hypercube (ElMasry and Sun, 2010) as illustrated in Figure 8. Every pixel in HSI image has an individual spectrum that containing information about chemical composition. Thus, the spectra can be collected at any points or areas of sample.

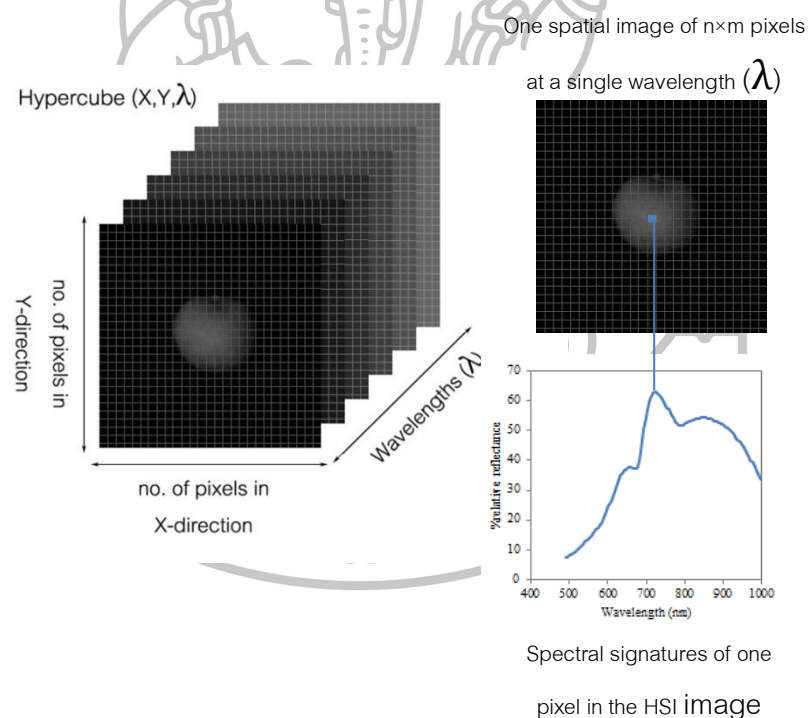


Figure 8 Hyperspectral image cube (hypercube).

The basic components of the system consist of illumination units (in the region 400-1000 nm), HSI camera with a CCD detector (charge-coupled device), spectrograph, translation stage and a computer system as shown in Figure 9.

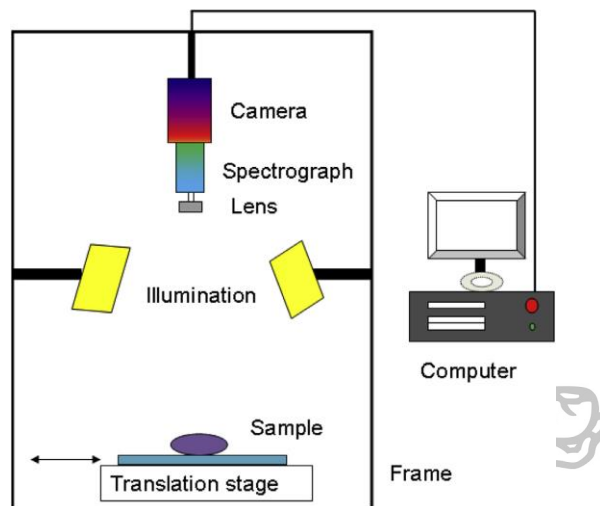


Figure 9 Components of a typical hyperspectral imaging system.

Source: Iqbal et al. (2014)

The theory of this technique is similar to NIRS, the light from light source (radiation in the wavelength range of 400-1000 nm) strikes the sample and then the reflected light beam from sample will enter the lens and passes into the spectrograph that has grating which can disperse the light into single wavelength. And then each wavelength will be captured by CCD detector. Hence, it can conduct the data in form 3 dimension of hypercube which  $x$  and  $y$  are rows and column of two dimensional spatial information and  $\lambda$  is spectral information.

There are four applications to acquire 3-D hypercube ( $x$ ,  $y$ ,  $\lambda$ ), which are point scanning, line scanning, area scanning, and single shot method as shown in Figure 10. First, point scanning method as the whiskbroom method (Figure 10a) a single point is scanned at one pixel to contribute the spectrum of this point. However, other points are scanned by moving sample or detector along spatial dimension. The weaknesses of

this application are time-delayed for positioning the object and need advanced hardware to support. Second method is line scanning or pushbroom method (Figure 10b), a hypercube can be obtained as the line is scanned along x dimension. Line scanning is especially suitable in conveyor belt systems that are commonly used in food process lines. Thus, this method is the most popular method for food quality and safety inspection. While the area or plane scanning (Figure 10c) is a method which obtains with full spatial information at a single wavelength at a time. Lastly, the single shot method archives both of spatial and spectral information in one exposure to capture the images (Figure 10d). This method is very suitable when fast imaging is required (Wu and Sun, 2013).

Moreover, there are three common modes of measurement for hyperspectral imaging i.e. reflectance, transmittance and interactance (ElMasry and Sun, 2010) as shown in Figure 10e-g.

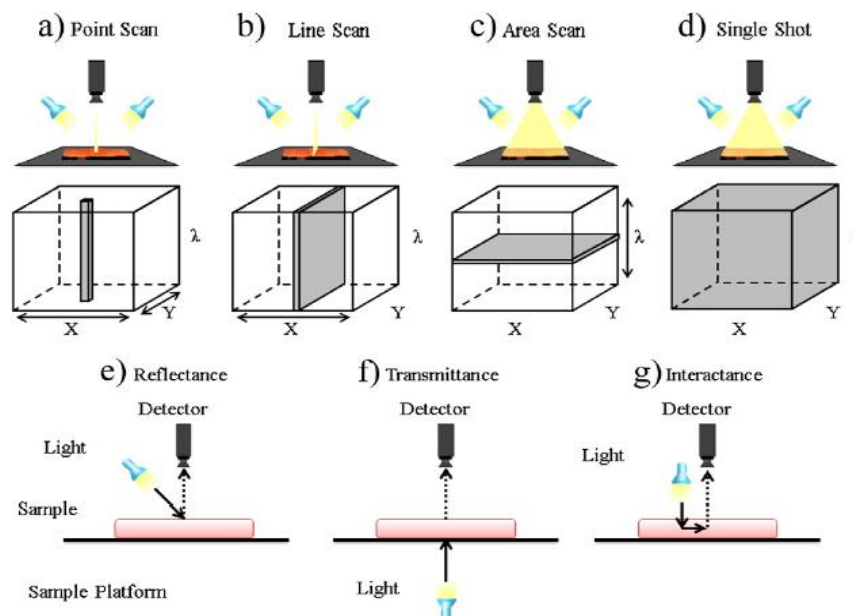


Figure 10 Acquisition of hyperspectral images and modes of measurement.

Source: Wu and Sun. (2013)

The advantages of hyperspectral imaging over the traditional methods include less sample preparation, nondestructive, fast acquisition times and visualizing whole spatial distribution of chemical compositions concurrently. The difference of HSI comparison between imaging and spectroscopy is shown in Table 3.

**Table 3** Main differences among imaging, spectroscopy and hyperspectral imaging techniques.

Features	Imaging	Spectroscopy	Hyperspectral imaging
Spatial information	✓	✗	✓
Spectral information	✗	✓	✓
Muti-constituent information	✗	✓	✓
Building chemical images	✗	✗	✓
Flexibility of spectral Information extraction	✗	✗	✓

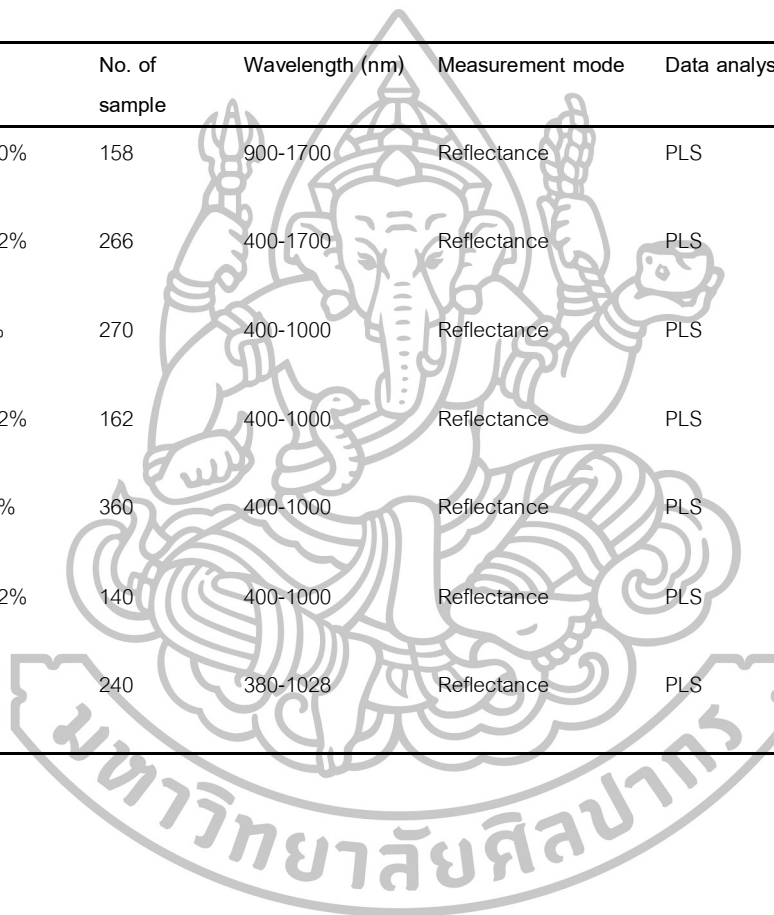
Source: ElMasry and Sun. (2010)

### 2.3.2 Hyperspectral imaging for food analysis

There are many researches that determine the potential of HSI in the application to assess of quantitative food. The capabilities of HSI for quantitative analysis of food (especially, moisture content and sugar) are shown in Table 4.

**Table 4** The capabilities of HSI for quantitative analysis of food

Sample	Parameter	Range (%)	No. of sample	Wavelength (nm)	Measurement mode	Data analysis	Accuracy	Reference
Pre-sliced turkey ham	Moisture content	43.03-80.40%	158	900-1700	Reflectance	PLS	R <sup>2</sup> = 0.88 RMSEP= 2.51%	Iqbal et al. (2013)
Atlantic salmon	Moisture content	54.19-76.52%	266	400-1700	Reflectance	PLS	R <sup>2</sup> = 0.85 RMSEP= 1.80%	He et al. (2013)
Soybean	Moisture content	49.0-67.7%	270	400-1000	Reflectance	PLS	R = 0.971 RMSEP= 9.2%	Huang et al. (2014)
Mango slices	Moisture content	10.35-90.12%	162	400-1000	Reflectance	PLS	R <sup>2</sup> = 0.972 RMSEP= 4.61%	Pu and Son (2016)
Lychee	Moisture content	8.36-70.26%	360	400-1000	Reflectance	PLS	R <sup>2</sup> = 0.948 RMSEP= 0.83%	Yang et al. (2015)
Table grape	TSS	11.92-21.12%	140	400-1000	Reflectance	PLS	R <sup>2</sup> = 0.94 RMSEP= 0.06%	Baiano et al. (2012)
Whole Port wine grape berry	TSS	9.1-25.0%	240	380-1028	Reflectance	PLS	R <sup>2</sup> = 0.89 RMSEP= 1.1%	Fernandes et al. (2015)





Baiano et al. (2012) applied the HSI technique (400-1000 nm) for prediction of some physico-chemical and sensory indices of table grapes. A partial least squares regression (PLSR) model was applied. In case of soluble solid contents, the result was found  $R^2 = 0.94$  with RMSEP 0.06%. However, the model of sensory gave a bad prediction because the spectra information did not correspond to the sensory data.

He et al. (2013) studied about the potential of HSI technique (400-1700 nm) for determining the distribution map of moisture content in farmed Atlantic salmon. The relationship between spectral data and the moisture content values was effectively conducted by partial least squares regression (PLSR). Three spectral ranges of 400–1000 nm, 900–1700 nm and 400–1700 nm were analyzed for selection of the best spectral range. The  $R^2$  of 0.893, 0.902 and 0.849, and RMSEP of 1.513%, 1.450% and 1.800% for three spectral ranges, respectively. The best model was built the image for visualizing moisture content of salmon fillets. The results showed that hyperspectral imaging technique has a great potential to predict the moisture content distribution of salmon fillets (Figure 11)

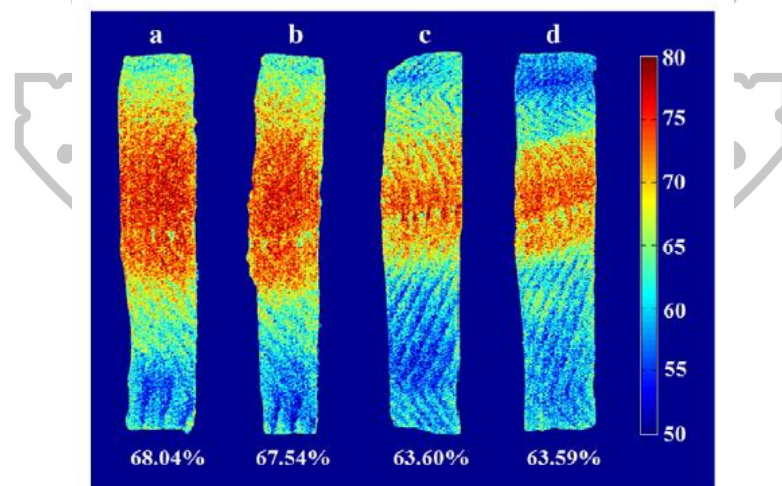


**Figure 11** Moisture distribution maps in salmon fillets. The values in the bottom of figures showed the average concentration of moisture in the whole fillet. Fillets (a) and (b) had high moisture content (MC) while fillets (c) and (d) had low MC.

**Source:** He et al. (2013)

Iqbal et al. (2013) developed a HSI system in the NIR region (900–1700 nm) to predict the moisture content, pH and color in cooked, pre-sliced turkey hams. Spectral data were extracted and analyzed by using partial least-squares (PLS) regression. Nine important wavelengths for moisture prediction were selected (927, 944, 1004, 1058, 1108, 1212, 1259, 1362 and 1406 nm). With the identified reduced number wavelengths, good coefficient of determination ( $R^2$ ) of 0.88 with RMSECV of 2.51% for moisture content.

Huang et al. (2014) developed regression models for predicting the color and moisture content of soybeans concurrently during the drying process using a HSI technique in the range of 400–1000 nm. Predicting models were built using the partial least squares regression method. The prediction results of moisture content were found correlation coefficient ( $R$ ) = 0.971 and root-mean-square errors of prediction or RMSEP = 9.2. The results showed significant potential in measuring moisture content of soybeans simultaneously during the drying process.

Fernandes et al. (2015) measured pH, sugars, and anthocyanin content of whole grape berries using HSI technique (380–1028 nm). The  $R^2$  of sugar content was found 0.89 with RMSEP of 1.1%. The results presented HSI had a potential to predict sugar content of whole grape berries.

Yang et al. (2015) focused on analyzing the relationship between browning levels of lychee and moisture contents of pericarp, and establishing calibration models for determining browning degree of lychee based on the MC prediction of pericarp using HSI technique (400–1000 nm). The results indicated that coefficients of determination ( $R^2$ ) of 0.948, and root mean square error (RMSEP) of 0.83% for moisture content. At last, the visualization map of lychee with different browning levels was build and distribution of browning degree in a pericarp was detected by considering color variation of pixels in the map as shown in Figure 12. According to the results, browning level 1 (no browning) had 55–70% moisture content, level 2 (slight browning) had 35–55% moisture content, level 3 (moderate browning) had 15–35% moisture content and level 4 (serious browning) had 0–15% moisture content.

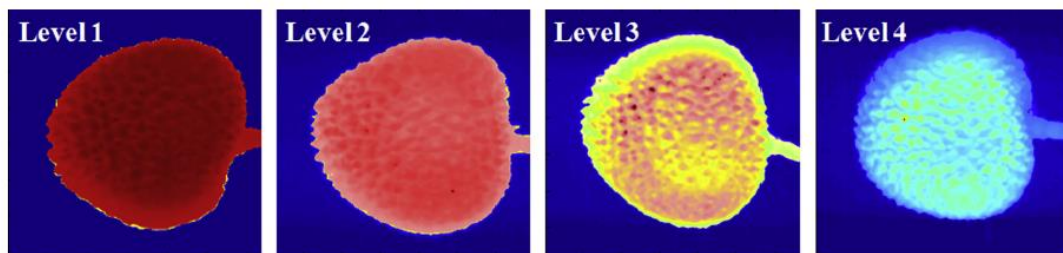


Figure 12 Visualization map of lychee with different browning levels.

Source: Yang et al. (2015)

Pu and Sun. (2016) used HSI system (400-1000 nm) for moisture prediction of mango slices. Partial least square (PLS) was applied to build calibration and validation models. The best model was found  $R^2 = 0.972$  and  $RMSEP = 4.611\%$ . The model was adapted into the moisture visualization. Moisture distribution map showed that the moisture content of the center of the mango slices was lower than the other parts (Figure 13). From this study indicated that hyperspectral imaging had a potential for measuring and visualizing the moisture content during drying process.

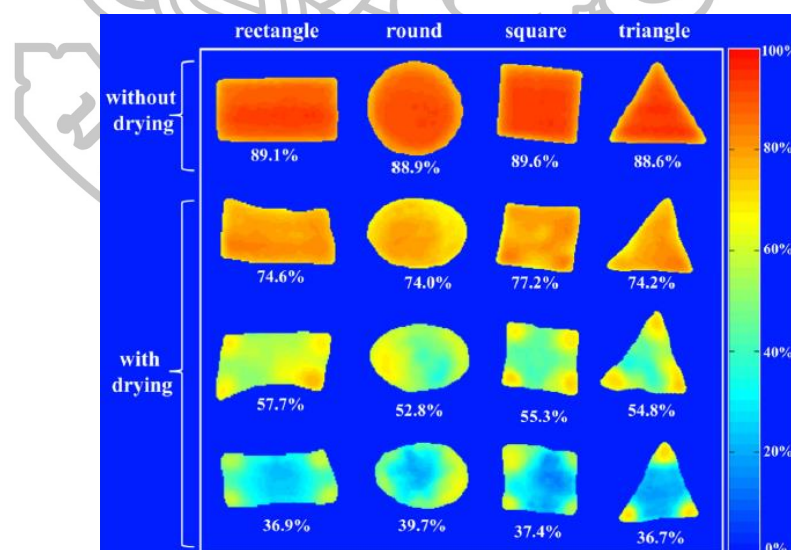
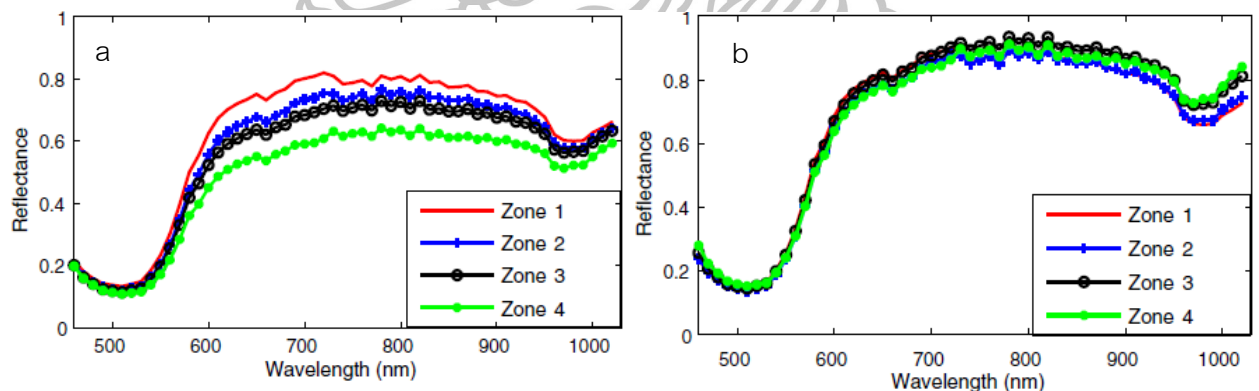


Figure 13 Moisture content distributions on mango slices of different shape.

Source: Pu and Sun. (2016)

Moreover, there was a research that studied the effects of the light source of HSI system on spherical objects. Gómez-Sanchis et al. (2008) said that the curvature of spherical objects as citrus fruits in acquiring HSI images affected some problems. The images of the fruits which were near the edge were darker than in the center. This problem made the images more difficult to analyze as the calibration which were achieved to correct the spatial and spectral inhomogeneity would have mistaken. A Lambertian ellipsoidal surface was applied to build 3D model of the fruit for calculating the part of the radiation that can reach the camera and to make the intensity of the radiation homogeneous over the whole of the fruit surface captured by the camera. The proposed correction methodology has demonstrated to be effective for minimizing the difference from the central area to edge areas. Figure 14 shows that this method can solve the problem. Four regions obtained from the hyperspectral image after being corrected with the proposed model become more uniform, to the point where they actually overlap.



**Figure 14** Averaged (a) uncorrected spectra of healthy zones of clemenules mandarin and (b) corrected spectra of healthy zones of clemenules mandarin of four different regions of the image.

**Source:** Gómez-Sanchis et al. (2008)

Obviously, the result of HSI technique found that the model gave high accuracy of moisture content and sugar content prediction. Thus, this technique also might be applied in moisture content and sugar content prediction in flesh of dried whole longan.



## CHAPTER 3

### MATERIALS AND METHODS

#### 3.1 Materials

##### 3.1.1 Longan samples

Fresh longan fruits cultivar Edor grade AA (Figure 15) with a diameter of 24-27 mm at a physiological maturity stage were purchased from the wholesale fruit market in Nakhon Pathom, Thailand. Fruits were transported from the orchards in Chiang Mai province. They were sorted for a uniform in size and shape with no visual damages (Figure 15). Then, they were trimmed to remove stalk and kept in a refrigerator ( $5.1\pm 0.8^{\circ}\text{C}$ ,  $79.9\pm 8.7\%\text{RH}$ ) until drying experiments. For this study, three batches of longan were purchased during August and September, 2014.



Figure 15 Fresh longan fruits cultivar Edor grade AA.

##### 3.1.2 Chemicals

Standard sucrose, glucose and fructose were purchased from the Sigma-Aldrich (USA). Distilled water (HPLC-grade) was obtained from the Vunique (Thailand).

## 3.2 Methods

### 3.2.1 Physical and chemical properties of fresh longan

#### 3.2.1.1 Physical properties

##### - Size and weight

Every longan fruit was measured for height, diameter and width (Thai Agricultural Standard, 2006) with vernier caliper (11205-200, INSIZE 1205 series, England) as shown in Figure 16. In addition weight per fruit was also measured using a digital scale (BP 211S, Sartorius AG, Germany).

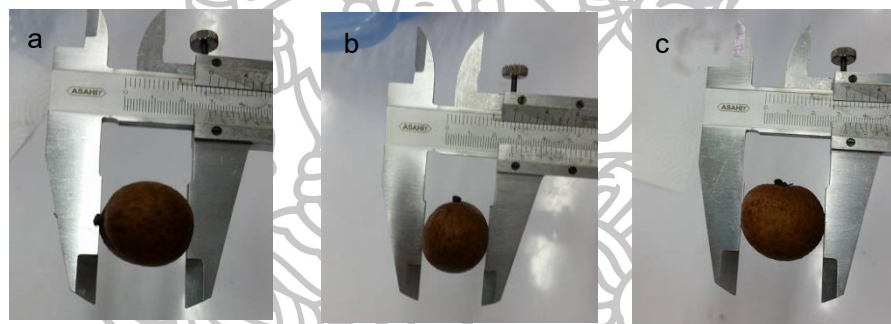


Figure 16 Measuring size of longan by using vernier caliper. (a) height, (b) diameter and (c) width.

#### 3.2.1.2 Chemical properties

##### - Total soluble solids

For each batch, ten fruits were peeled. Total soluble solids (TSS) of flesh longan from each fruit was examined in duplicate by dropping the juice through a muslin cloth onto the digital refractometer (Pal-1, Atago, Japan) with a scale 0-53 °Brix (AOAC, 2000).

- **Moisture content**

Sixteen fruits of each batch were separated into peel, flesh and seed and then they were blended by using a blender (A 11 Basic, IKA, Germany). Samples were weighted and put into a moisture can. The weight was recorded. The moisture content (MC) was measured using hot air oven at 105 °C until the weight was constant (AOAC, 2000). MC (wet basis) was calculated corresponding by Eq. 1.

$$\text{MC (\%)} = \frac{\text{weight of wet sample (g)} - \text{weight of dry sample (g)}}{\text{weight of wet sample (g)}} \times 100 \quad (1)$$

Moreover, the moisture contents of the whole fruit and flesh+seed were obtained by calculated from %weight of each fruit part (Appendix G).

- **Sugar content**

For each batch, six longans were peeled and the flesh was extracted for analysis of individual sugars using the method from Liu et al. (2013). The sample was homogenized. And then, 1 g of sample was mixed with 9 ml distilled water and then centrifuged at 8000 rpm for 10 min at 4 °C. The supernatant was filtrated by 0.45 nylon syringe filter. The filtered supernatant was kept at -18° C for HPLC analysis. Individual sugars were separated using Rezex RCM-Monosaccharide Ca<sup>+2</sup> column (300 × 7.8 mm i.d., 5 µm particle size) and the column was kept in a column heating box at 80 °C. Deionized water was used as a mobile phase at a flow rate of 0.6 ml/min. Individual sugar was detected by using a refractive index detector (RID-10A, Shimadzu, Japan). For quantification and calibration, a standard solution mixture was prepared by dissolving sucrose, glucose and fructose in distilled water (HPLC grade). Final values were expressed in mg/g fresh weight. Standard curves are shown in Appendix A.



### 3.2.2 Sample preparation

The total of 616 whole fresh longans were dried in a single layer by using a through flow mode laboratory tray dryer (the stem part was turned down). The placement of longans in the tray is shown in Figure 17.

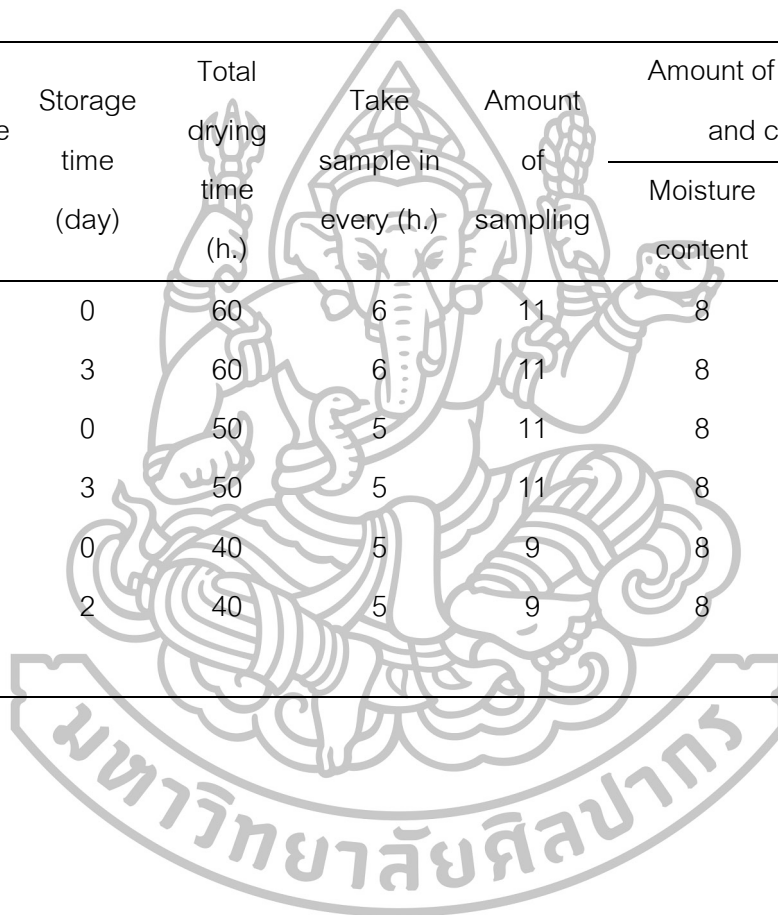


Figure 17 The placement of longans for drying.

The samples were dried at temperature of 60, 70, and 80 °C with an air velocity of 0.2 m/s. Drying had been done until the dried flesh of longan has water activity about 0.55-0.60. Samples were taken in every 6 h. for 60°C and 5 h for 70°C and 80°C. The samples were separated into 2 groups for analysis moisture content and individual sugars. Moreover, drying was repeated in duplicate of each temperature. Drying condition and sampling are shown in Table 5.

**Table 5** Drying conditions and sampling of longan for the study.

Drying batch	Replication	Temperature (°C)	Storage time (day)	Total drying time (h.)	Take sample in every (h.)	Amount of sampling	Amount of taken at each time and condition (fruit)		Amount of samples for the study (fruit)	
							Moisture content	Sugar content	Moisture content	Sugar content
Batch 1	1	60	0	60	6	11	8	3	88	33
	2	60	3	60	6	11	8	3	88	33
Batch 2	1	70	0	50	5	11	8	3	88	33
	2	70	3	50	5	11	8	3	88	33
Batch 3	1	80	0	40	5	9	8	3	72	27
	2	80	2	40	5	9	8	3	72	27
Total									496	186



### 3.2.3 Nondestructive measurement for determination of moisture content and sugar content in dried whole longan

#### 3.2.3.1 Near-infrared spectroscopy (NIRS) measurement

##### - Spectra Acquisition

Whole fresh and dried longans were measured spectra by NIRS measurement. The reflectance spectra of a total of 682 samples were measured using a FT-NIR spectrometer model MPA with OPUS software (Bruker optics, Ettlingen, Germany), as shown in Figure 18, in the wavenumber ranging from  $12,500\text{ cm}^{-1}$  to  $4,000\text{ cm}^{-1}$  (800-2500 nm) at a resolution of  $16\text{ cm}^{-1}$  and scan time of 32 scans. The sample temperature was controlled at  $25\text{ }^{\circ}\text{C}$  by keeping in cooled incubator (KB, Binder.Ltd., Germany) for 1 hr. before spectra measurement. The spectrum of each sample was collected at four positions; calyx (P1), bottom (P2) and the both cheeks of fruit (P3 and P4). The measured positions are shown in Figure 19.



Figure 18 Near-infrared spectroscopy system.

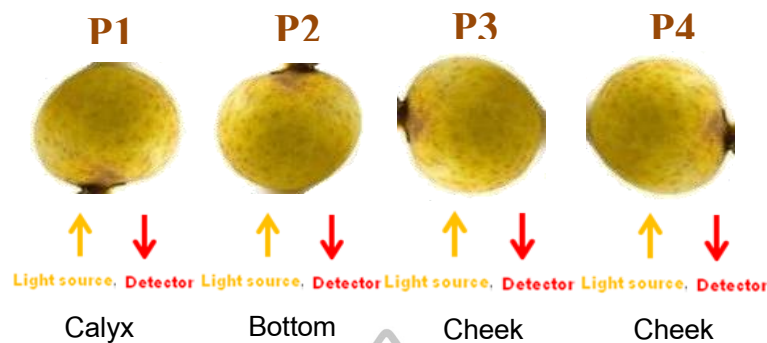


Figure 19 The four measured positions for NIR spectrum acquisition.

#### - Reference analysis for NIRS

The moisture content of peel flesh and seed as well as the whole fruit, TSS and sugar content of flesh were analyzed after spectra measurement. The samples were separated into peel, flesh and seed then measured moisture content of each part as well as the whole fruit by using a hot air oven at 105°C (AOAC, 2000), TSS (AOAC, 2000) and sugar content of flesh (Liu et al., 2013) were analyzed as described in 3.2.1.2.

#### - Spectral data analysis for NIRS

The calibration models were developed by partial least squares analysis (PLS) with an external validations (calibration: validation; 60:40) for considering observed spectra and results of chemical analyses. The OPUS chemometric software (Bruker optics, Ettlingen, Germany) version 7.2.139.1294 was applied. To improve calibration accuracy by reducing noises and scattering effects, spectral data were conducted to a variety of preprocessing such as first derivative, second derivative, min-max normalization, vector normalization or standard normal variate correction (SNV) and multiplicative scattering correction (MSC) together with a wavelength region selection were performed according to the optimization function of the OPUS software. The

performance of developed models was presented in terms of  $R^2$  (the coefficient of determination), RMSEP (root mean square error of prediction), PLS factor (or number of latent variables), bias and RPD (the ratio of the standard deviation of validation set to SEP). The RPD was calculated using Eq.2

$$RPD = \frac{SD_{val}}{SEP} \quad (2)$$

#### - Accuracy of calibration models for NIRS

The accuracy of prediction models which had RPD value more than 2.0 were tested by using bias checking (paired *t*-test) method, SEP checking (F-test, ratio of 2 variances) method and slope checking method from International standard ISO 12099 (2010). All statistic formulas are shown in Appendix D.

#### 3.2.3.2 Hyperspectral imaging (HSI) measurement

##### - Image acquisition for HSI

The laboratory hyperspectral imaging system was used to acquire hyperspectral images of longans in a reflectance mode. The main components of system are displayed in Figure 20. HSI system is mainly consisted of a hyperspectral frame camera with a spectrograph and CCD detector (Cubert GmbH, Germany) covering the spectral range of 400-1000 nm, a light source; 50 W tungsten halogen lamp (Pro Lamp, ASD, USA), two mirrors positioned at an angle of 120° and a computer with Cubert\_Gui software (Cubert GmbH, Germany). The distance between the lens and longan was fixed at 40 cm. Longan sample was placed on the sample holding. A total of 682 samples were measured. Each fruit was imaged for 1 position with the equator position facing vertically toward the imaging system. The hyperspectral images were recorded as spatial dimension of 910×900 pixels for every 4 nm and resulted in a total of 128 spectral bands.

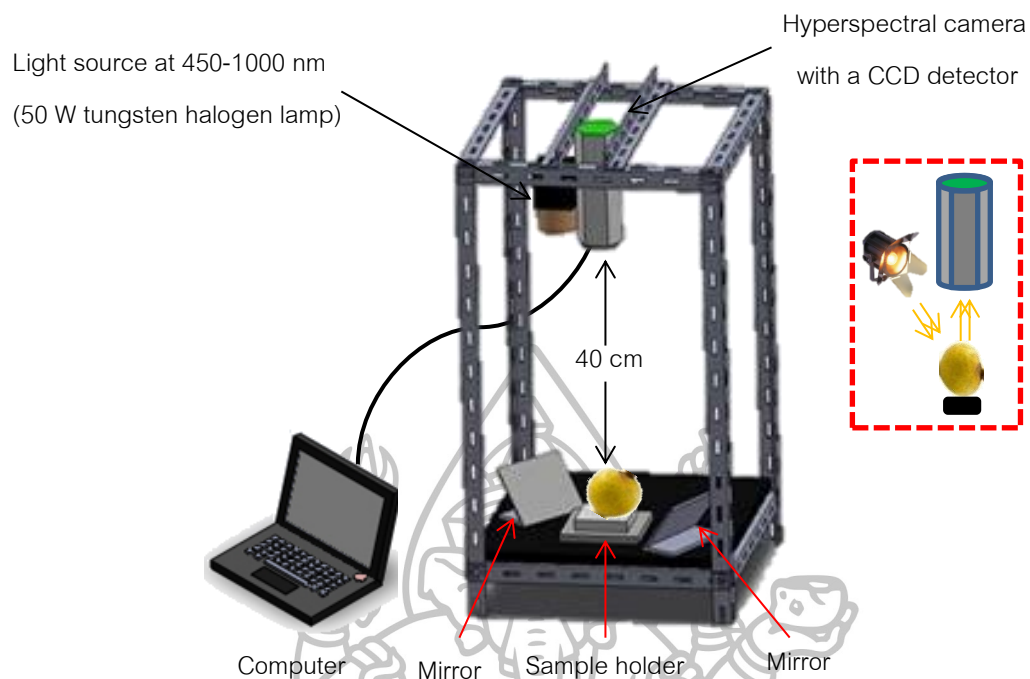


Figure 20 Schematic diagram of hyperspectral image system.

To improve the raw acquired hyperspectral images ( $I$ ), two images for black ( $B$ ) and white ( $W$ ) references were applied to reduce the effects of illumination and detector sensitivity. The light source was turned on for 15 min before hyperspectral image acquisition. And then the black image ( $\sim 0\%$  reflectance) was acquired by recording a spectral image after closed the camera lens completely with a black board. The white reference image was acquired by taking a spectral image from a white canvas ( $\sim 99\%$  reflectance). The corrected hyperspectral image in a unit of %relative reflectance ( $R$ ) was calculated using the following equations:

$$R_i = \frac{I_i - B_i}{W_i - B_i} \times 100 \quad (3)$$

Where  $I$  was the raw image,  $W$  was the white reference image,  $B$  was the dark reference image. The  $i$  is the pixel index, i.e.  $i = 1, 2, 3, \dots, n$  and  $n$  is the total number of pixels. The final improved spectral images were applied as the basis for spectral

extraction and data analysis (Iqbal et al., 2014). The final hyperspectral images are shown in Figure 21.

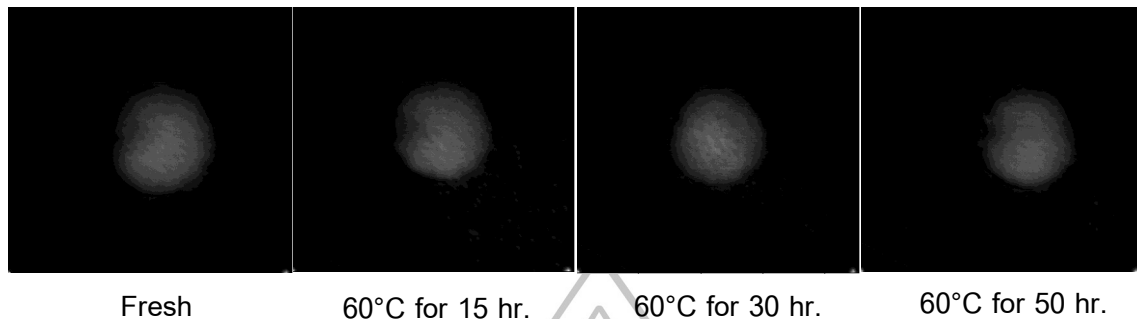


**Figure 21** Example of hyperspectral images of fresh and dried whole longan obtained from drying at 60°C for 15, 30 and 50 hr.

#### - ROI identification and spectra extraction for HSI

After image acquisition, the images were exported from Cubert\_Gui software (Cubert GmbH, Germany) in term .hdr and .cue. Ten regions of interests (ROIs) with circle shape (10\*10 pixels) within hyperspectral images were collected as displayed in Figure 22. The ROI identification process was developed and the spectral data within ROIs for the fruit were extracted and averaged by using R version 3.1.1 (R Foundation for Statistical Computing, Vienna, Austria) (Appendix E). The reflectance spectrum was obtained by averaging spectral data from 1000 pixels.

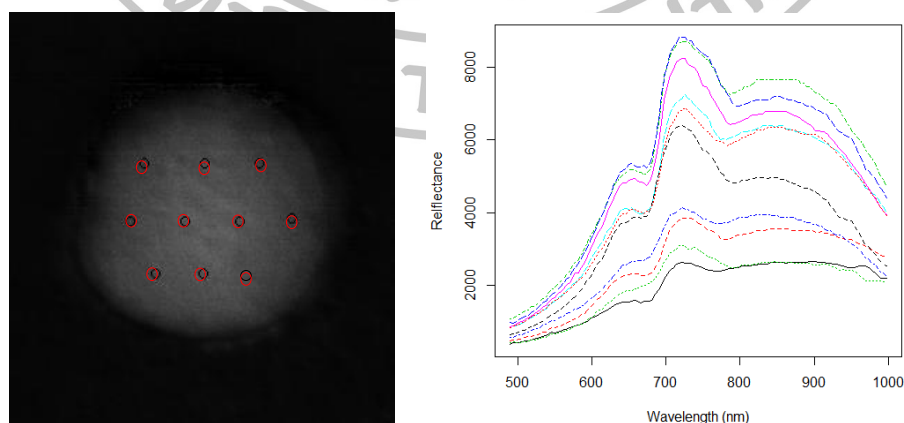


**Figure 22** 10 points selected of sample in R program.

#### - Reference analysis for HSI

The moisture content of peel flesh and seed as well as the whole fruit, TSS and sugar content of flesh were analyzed after image acquisition. The samples were separated into peel, flesh and seed then measured moisture content of each part as well as the whole fruit by using a hot air oven at 105°C (AOAC, 2000), TSS (AOAC, 2000) and sugar content of flesh (Liu et al., 2013) were analyzed as described in 3.2.1.2.

#### - Spectral data analysis for HSI

The Unscrambler software (CAMO Software AS, Oslo, Norway) was used to pretreat the spectral data such as first derivative, second derivative, standard normal variate correction (SNV) and multiplicative scattering correction (MSC), as well as produce calibration and validation model using partial least squares analysis (PLS). The data about 52.5% was set for calibration set and 47.5% was set for validation set. The predictive ability and accuracy of the models were presented in terms of  $R^2$  (the coefficient of determination), RMSEP (root mean square error of prediction), PLS factor (or number of latent variables), bias and RPD (the ratio of the standard deviation of validation set to SEP). The optimum model was selected if the model provided best prediction performance on a validation set which showed high  $R^2$  and RPD while low RMSEP (Kaewsorn and Sirisomboon, 2014).

Moreover, the distribution maps were carried out by using R version 3.1.1 (R Foundation for Statistical Computing, Vienna, Austria) (Appendix E). The result distribution map was presented in different colors, where each color shows specific concentration of the predicted chemical value in whole fruit.

#### - Accuracy of calibration models for HSI

The methods were the same as the verification of calibration models for NIRS.



CHAPTER 4  
RESULTS AND DISCUSSION

4.1 Physical and chemical properties of fresh longan

The physical properties of fresh longan are shown in Table 6. The width of fruits was not significantly different between each batch. It revealed that all sample had similar size which is important for NIRS measurement. Because of the size of object affect to the scattering and of light inside (Nicolai et al., 2007). According to Thai agricultural standard. (2004), the diameter of fruits in this research are classified into AA grade (>2.5 cm) which is suitable for dried whole longan production.

**Table 6** Height, diameter, width and weight per fruit of fresh longan

Batch	N	Height (mm)	Diameter (mm)	Width (mm) <sup>ns</sup>	Weight/fruit (g)
1	242	27.53±0.89 <sup>a</sup>	26.88±1.05 <sup>a</sup>	31.37±1.93	14.35±0.72 <sup>a</sup>
2	242	26.54±0.94 <sup>b</sup>	26.16±1.05 <sup>b</sup>	30.78±1.21	13.48 ±0.96 <sup>b</sup>
3	198	27.27±0.62 <sup>a</sup>	26.85±1.14 <sup>a</sup>	30.93±1.23	13.58 ±1.31 <sup>b</sup>
Average		27.11±0.93	26.63±1.12	31.03±1.50	13.80±1.09

<sup>a-b</sup> Mean values in the same column with different letters are significantly different ( $P \leq 0.05$ ).

<sup>ns</sup> Non-significant different ( $P > 0.05$ ).

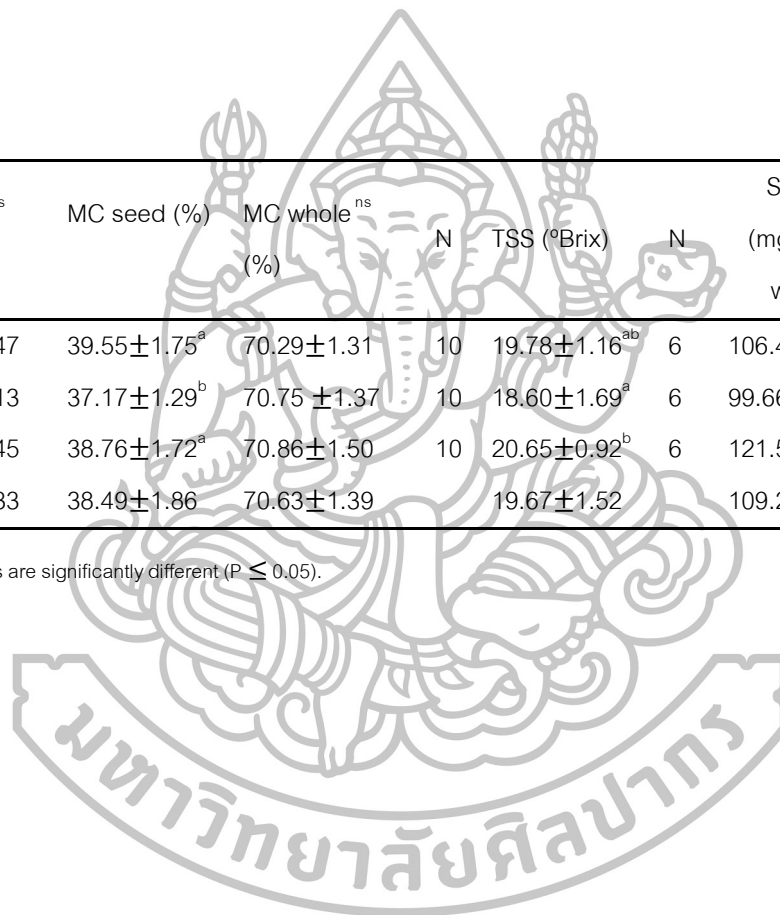
The chemical quality of the fresh longan can be seen from Table 7. The quality of the fruit in term moisture content (peel, flesh and seed as well as the whole fruit of fresh longan) for all the samples was the same. With regard to Phupaichitkun et al. (2005), initial moisture content of fruits was similar to the results of this study.

**Table 7** Moisture content (MC) of peel, flesh and seed as well as the whole fruit, TSS, sucrose, glucose and fructose content of fresh flesh longan

Batch	N	MC peel (%)	MC flesh <sup>ns</sup> (%)	MC seed (%)	MC whole <sup>ns</sup> (%)	N	TSS (°Brix)	N	Sucrose (mg/g fresh weight)	Glucose (mg/g fresh weight)	Fructose (mg/g fresh weight)
1	16	28.91±4.86 <sup>a</sup>	80.91±1.47	39.55±1.75 <sup>a</sup>	70.29±1.31	10	19.78±1.16 <sup>ab</sup>	6	106.44±17.25 <sup>a</sup>	25.64±4.68 <sup>ab</sup>	24.50±4.29 <sup>ab</sup>
2	16	33.37±7.15 <sup>ab</sup>	81.05±1.13	37.17±1.29 <sup>b</sup>	70.75±1.37	10	18.60±1.69 <sup>a</sup>	6	99.66±11.32 <sup>a</sup>	29.11±6.12 <sup>a</sup>	27.04±6.87 <sup>a</sup>
3	16	36.29±9.65 <sup>b</sup>	80.83±1.45	38.76±1.72 <sup>a</sup>	70.86±1.50	10	20.65±0.92 <sup>b</sup>	6	121.51±3.10 <sup>b</sup>	20.36±2.26 <sup>b</sup>	20.08±1.68 <sup>b</sup>
Average		32.86±7.94	80.93±1.33	38.49±1.86	70.63±1.39		19.67±1.52		109.20±14.71	25.04±5.71	23.88±5.37

<sup>a-b</sup> Mean values in the same column with different letters are significantly different ( $P \leq 0.05$ ).

<sup>ns</sup> Non-significant different ( $P > 0.05$ ).



## 4.2 Near-infrared spectroscopy for determination of moisture content and sugar content in dried whole longan

### 4.2.1 Diffuse reflectance spectra of fresh and dried whole longan by NIRS

Figure 23 shows the example of original spectra of fresh and dried whole longans obtained from different temperatures for 40 h at the measurement position 1 (P1) in the spectral region of 800-2500 nm. All temperatures of drying showed similar spectrum that has baseline shift from scattering effect due to water and fiber in fruits (Bai et al., 2014). These characteristic bands also found in blueberry fruit (Bai et al., 2014) and apple (Fan et al., 2016). Moreover, there were absorption peaks around 1100-1200 nm which related to C-H stretching of second overtone. These peaks are associated with carbohydrate (e.g. sucrose) or lipids and amino acids (proteins) (Kaewsorn and Sirisomboon, 2014). The region near 1400-1500 nm contains the first overtones O-H stretching that could be refer to water of the fruit (Osborne et al., 1993; Magwaza et al., 2012; Fan et al., 2016). The bands situated between 1700-1800 nm occur to due to the first overtone associated with C-H stretching that represent the structure of  $\text{CH}_2$ ,  $\text{CH}_3$  and cellulose (Osborne et al., 1993). And in the region 1900–2100 nm important bands related to water (Rungpichayapichet et al., 2016),

The example of original spectra of dried whole longans obtained from different positions and drying at 60°C for 40 hours and the average spectrum from all positions are shown in Figure 24. For the spectra observed at the calyx (P1) were different from those observed at other positions. These differences were caused by surface feature at the calyx which was different from the other positions and directly affect its diffuse reflectance (Bai et al., 2014). In addition, it was also due to amount of moisture content at the calyx that has higher moisture content than other positions. The higher moisture content at the calyx might be due to the sample which was turned down to the tray affected the moisture content was released from this part.

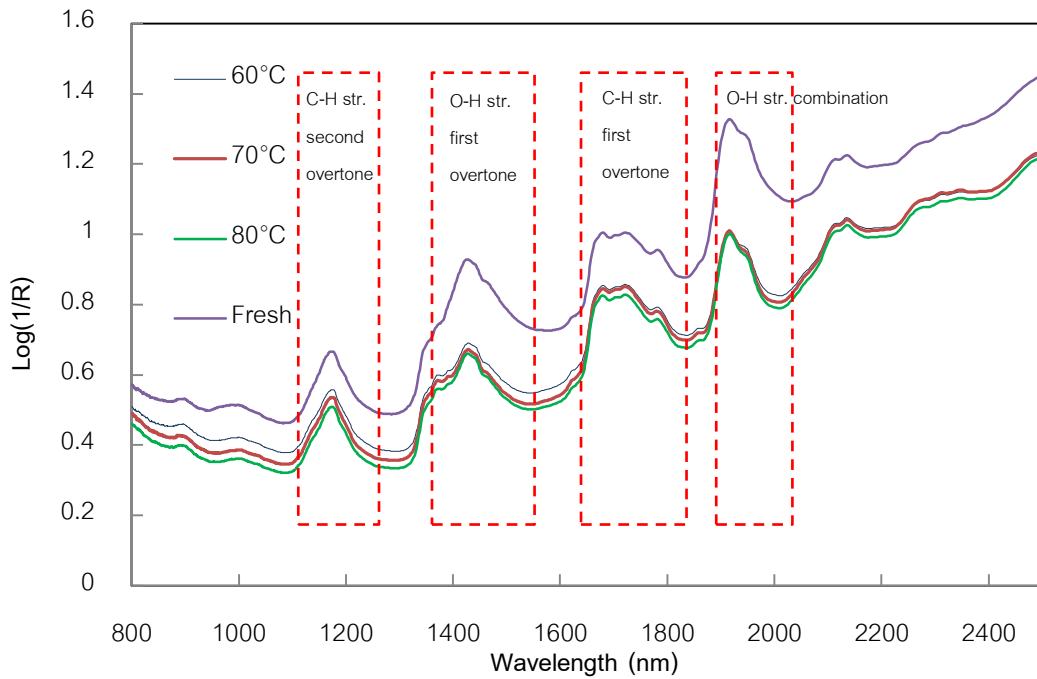


Figure 23 Example of original spectra of fresh and dried whole longans dried at different temperatures for 40 hours at measurement position 1 (P1).

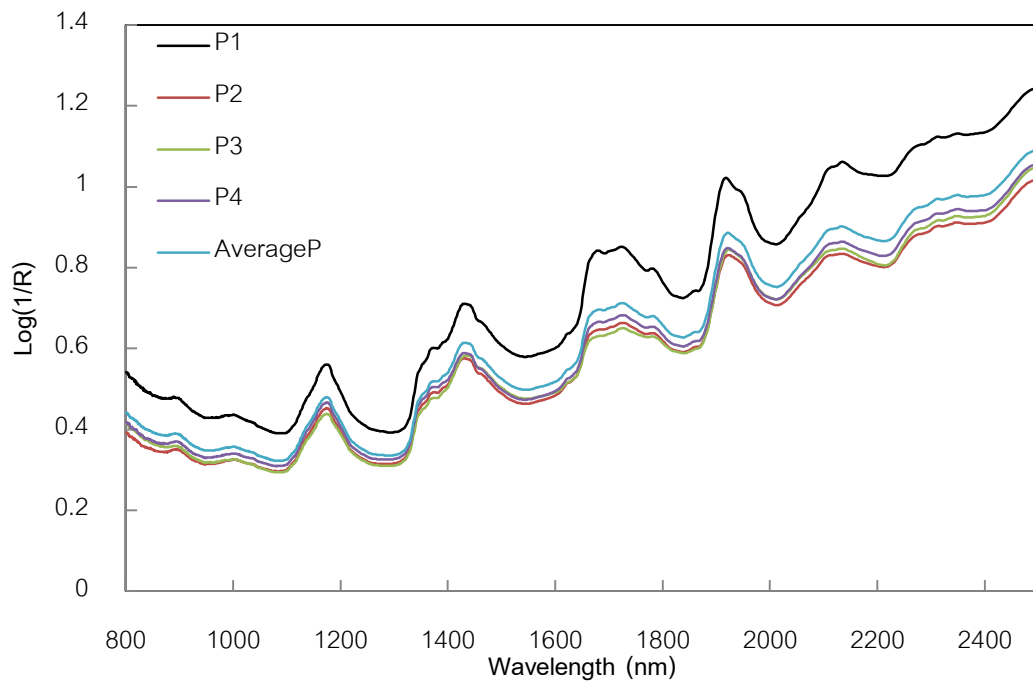
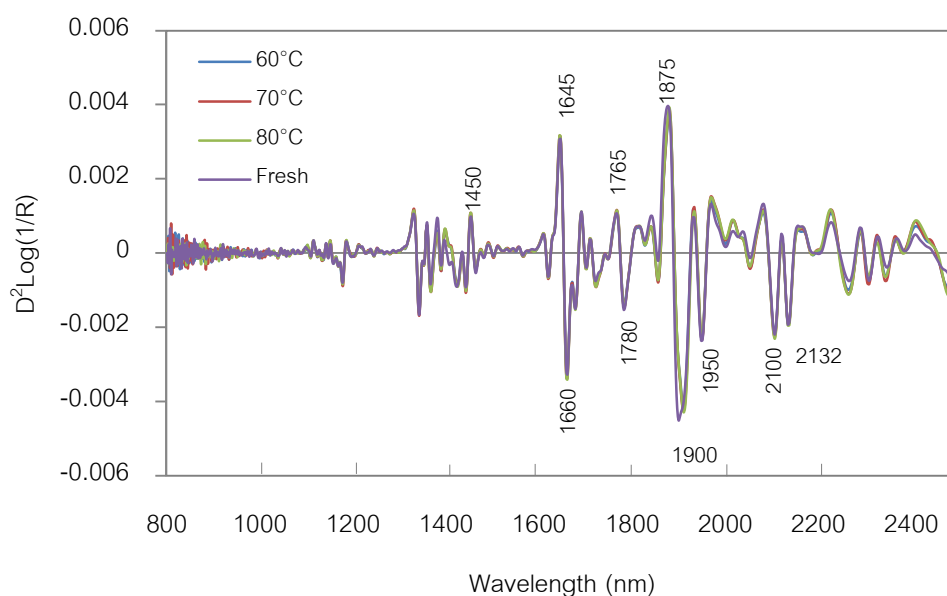


Figure 24 Example of original spectra of dried whole longans obtained from different positions and drying at 60°C for 40 hours.

However, many overlaps in the vibrations of chemical bonds result in large bands and poor peak resolution in original NIR spectra. Thus, using the second derivative techniques, which is one of spectral preprocessing, solved these problems and created a spectrum with specified peaks (Bai et al., 2014). The Savitzky–Golay second derivative spectra obtained from fresh and dried whole longans dried at different temperatures for 40 hours at measurement position 1 (P1) are shown in Figure 25. The figure shows eight similar peaks at 1450 nm, 1645 nm, 1660 nm, 1765 nm, 1780 nm, 1875 nm, 1900 nm and 2100 nm. The peak at 1450 nm occurs to be due to the first overtone associated with O-H stretching that represents the structure of water (Osborne et al., 1993; Magwaza et al., 2012; Rungpichayapichet et al., 2016). And the peaks at 1645 nm, 1660 nm, 1765 nm and 1780 nm occur to be due to the first overtone associated with C-H stretching that represent the structure of  $\text{CH}_2$ ,  $\text{CH}_3$  and cellulose (Osborne, 1993). The peaks at 1875 nm and 1900 nm occur to be due to the second overtone associated with C=O stretching and the peak at 2100 nm corresponds to the combination of O-H stretching and  $2\times\text{C-O}$  stretching that represent the structure of starch (Osborne et al., 1993; Kaewsorn and Sirisomboon, 2014).



**Figure 25** Example of second derivative spectra of fresh and dried whole longan dried at different temperatures for 40 hours at measurement position 1 (P1).

#### 4.2.2 Calibration models for moisture content by NIRS

A total of 496 spectra were divided into calibration set (60% of all samples) and validation set (40% of all samples) for building the models. Mean, standard deviation (SD), minimum and maximum of moisture content (%) of longan fruit samples from different fruit parts and the whole fruit showed in Table 8. The range in moisture content of peel was between 3.35-51.74%, the range in flesh was between 9.99-88.62%, the range in seed was between 7.61-49.90%. The range of moisture content in whole fruit was between 8.15-73.36%. The result showed that the flesh part had the widest range of moisture content. During drying, the moisture content of each part was changed. For example, fresh longan had the moisture content of 51.73%, 76.66%, 37.16% and 69.44% for MC peel, MC flesh, MC seed and MC whole, respectively. At the end point of drying, the moisture content of each part were found 3.35%, 13.17%, 8.95% and 9.40% for MC peel, MC flesh, MC seed and MC whole, respectively. Obviously, flesh had the highest moisture content in dried longan while, peel had the lowest value.

**Table 8** Mean, standard deviation (SD), minimum and maximum of moisture content (%) for longan fruit samples from different fruit parts and the whole fruit.

Fruit part	N	Calibration set (60%)				N	Validation set (40%)			
		Min	Max	Mean	SD		Min	Max	Mean	SD
Peel	298	3.35	51.74	15.81	9.51	198	3.73	46.51	15.75	9.34
Flesh	298	9.99	88.62	45.05	25.35	198	11.04	83.21	45.03	25.29
Seed	298	7.61	49.90	26.60	11.53	198	7.98	47.23	26.58	11.49
Flesh+seed	298	7.27	71.26	35.06	21.14	198	7.92	70.48	35.07	21.11
Whole fruit	298	8.15	73.36	37.34	21.87	198	8.77	73.03	37.32	21.85

N = number of samples

Figure 26(a) and (b) show the distribution of moisture content of peel in longan samples in calibration set and validation set, respectively. It can be seen that there were more samples at low moisture content (10%) than other values because of decreasing of water content in peel during drying. Figure 26(c) and (d) show the distribution of moisture content of flesh in longan samples in calibration set and validation set, respectively. The results also found that there were more samples at low moisture content (20%) than other values because most of fresh flesh of longans became to dried flesh. Figure 26(e) and (f) show the distribution of moisture content of seed in longan samples in calibration set and validation set, respectively. Obviously, most of samples had high moisture content of seed (40%) because the water in seed can only diffuse through the seed stalk that affect the drying rate of this part is very slow (Phupaichitkun et al., 2006). Thus, more samples still had high moisture content. Figure 26 (g) and (h) show the distribution of moisture content of flesh and seed in calibration set and validation set, respectively. And Figure 26 (i) and (j) show the distribution of moisture content of the whole fruit in calibration set and validation set, respectively. The results of these 2 part found that there were more sample at low moisture content (20%) because of decreasing of water content in sample during drying.



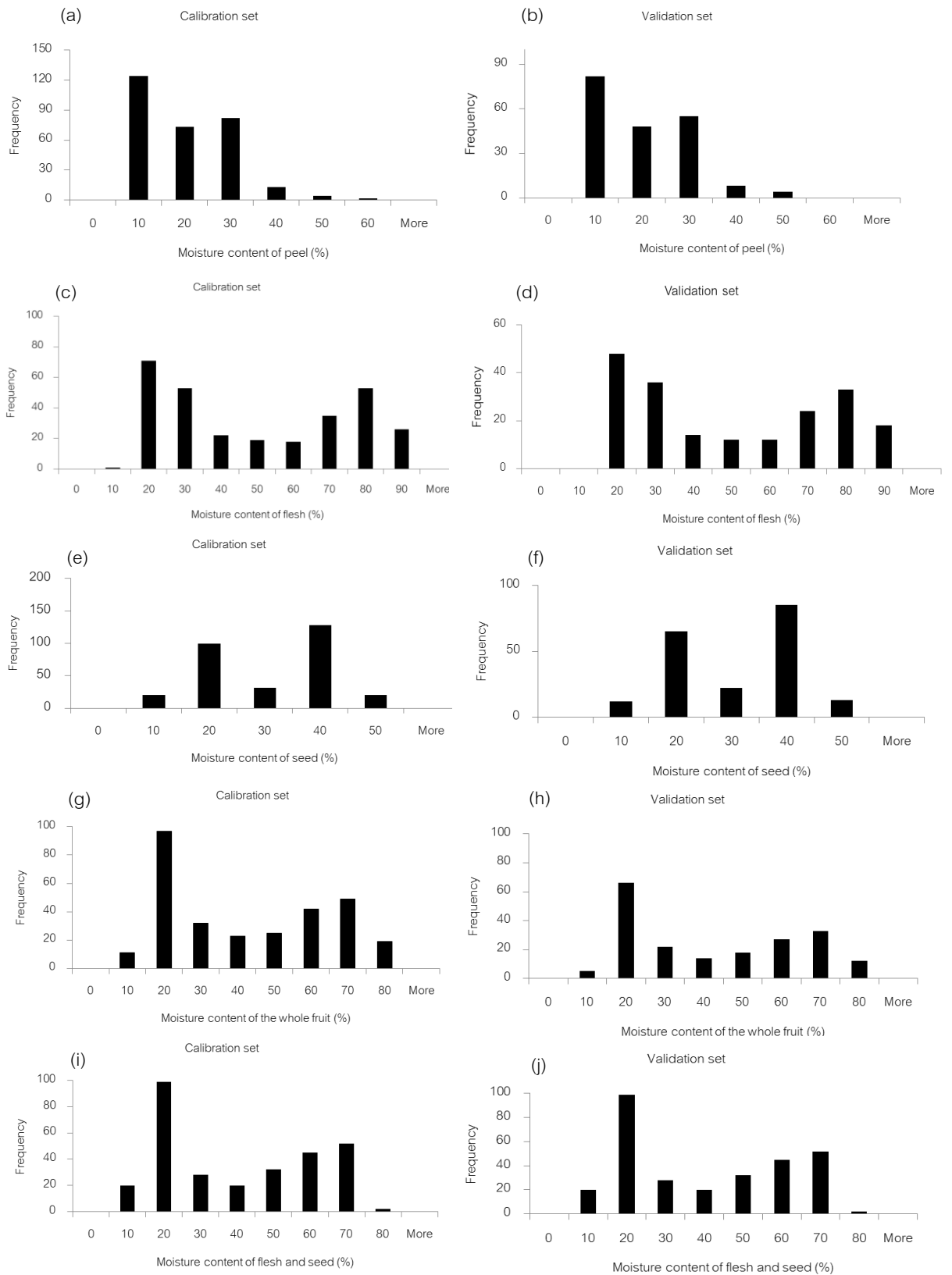


Figure 26 Histogram of distribution of moisture content of peel, flesh, seed, flesh and seed and the whole fruit of samples in calibration set and validation set.



The calibration and validation results associated with the PLS models for moisture content of peel by NIRS are shown in Table 9. The optimum model was selected if the model provided best prediction performance on a validation set which showed high  $R^2$  and RPD. In addition, Williams (2007) has indicated that an  $R^2$  of 0.98+ showed that a model is excellent and usable in any application and  $R^2$  between 0.92 and 0.96 showed that a model is usable in most applications, including that of quality assurance. Furthermore, RPD, which is the ratio of the standard error of performance to the standard deviation of the reference data (Huang and Lu, 2010), is a necessary parameter in assessing the performance of prediction models. An RPD between 1.5 and 2 demonstrates that the model can separate low from high values of the response variable. A value between 2 and 2.5 demonstrates that coarse quantitative predictions are possible, whereas a value between 2.5 and 3 or above corresponds to good and excellent prediction accuracy, respectively (Nicolai et al., 2007).

In this study, the result showed that the optimum models for moisture content of peel generated from averaging spectra at all positions of measurement by using 5 PLS factors in the range of 1182.7-1333.6 nm 1638.8-2175.0 nm that were pre-treated by the first derivative+SNV methods. This model showed a coefficient of determination ( $R^2$ ), root mean squared error of prediction (RMSEP), ratio of standard error of validation to the standard deviation (RPD) and a bias of 0.9850, 1.06%, 8.22 and -0.128% , respectively. Bias is the average difference between actual and NIRS predicted values. According to the best model of peel, It can be seen that the bias value had minus (-0.128%) which means the average actual value from reference method had higher value than the average NIRS predicted value (Nicolai et al., 2007). Moreover,  $R^2$  showed that a model is excellent and usable in any application. And RPD values was larger than 3 corresponds to excellent prediction accuracy. Therefore,  $R^2$  and RPD of these models can be used. The reason might be due to the peel which is external part was able to absorb the NIRS radiation directly. Good prediction results of moisture content of fruit peel also found in Ahmad et al. (2014) that used NIRS for predicting moisture content of mangosteen peel during storage ( $R = 0.882$ ).

**Table 9** Calibration and validation results for moisture content of peel by NIRS.

Fruit part	Position	Pre processing	Wavelength (nm)	PLS factor	Calibration set (60%)		Validation set (40%)			RPD
					R <sup>2</sup>	RMSEC(%)	R <sup>2</sup>	RMSEP(%)	Bias(%)	
Peel	P1	MSC	1063.4-1836.1 2171.3-2356.9	8	0.9232	2.67	0.9601	1.76	-0.1	5.01
	P2	First derivative (17pts.)	1063.4-1640.9 2171.3-2262.3	10	0.9364	2.44	0.9502	2.04	-0.301	4.53
	P3	First derivative+MSC (17pts.)	1063.4-2175.0	6	0.9272	2.59	0.9560	1.84	-0.0519	4.77
	P4	First derivative+SNV (17pts.)	1063.4-1836.1 1833.5-2356.9	6	0.9414	2.33	0.9680	1.60	-0.209	5.64
	P1P2P3P4	First derivative+MSC (17pts.)	1063.4-1333.6 2171.3-2356.9	10	0.9202	2.69	0.9548	1.94	-0.192	4.73
	Average P	First derivative+SNV (17pts.)	1182.7-1333.6 1638.8-2175.0	5	0.9636	1.83	0.9850	1.06	-0.128	8.22

Abbreviations: R<sup>2</sup>: coefficients of determination, RMSEC: root mean square error of calibration, RMSEP: root mean square error of prediction, RPD: ratio of standard deviation of reference data in validation set to SEP, MSC: multiplicative scatter correction, SNV: standard normal variate, 17 pts: 17 smoothing points, P1: calyx, P2: bottom, P3 and P4: 2 side of cheek, P1P2P3P4: all positions and Average P: average all positions.

The scatter plot demonstrating the measured value of moisture content and the prediction value for the peel model is shown in Figure 27. It can be seen that the points close to target line that mean the NIRS predicted values were similar to the measured values. However, most points were quite under the target line that affected to this result had negative bias value (Nicolai et al., 2007).

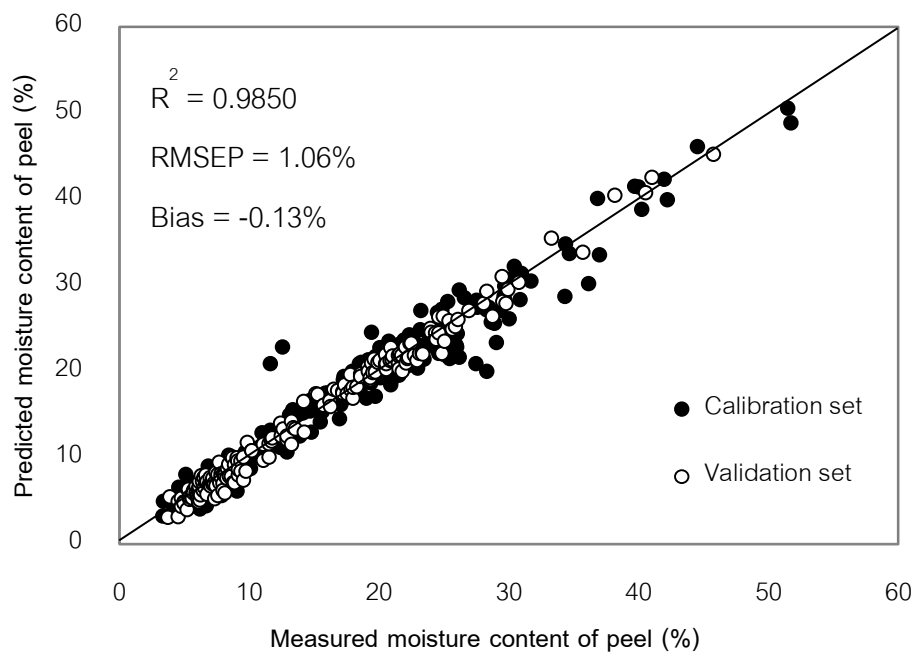
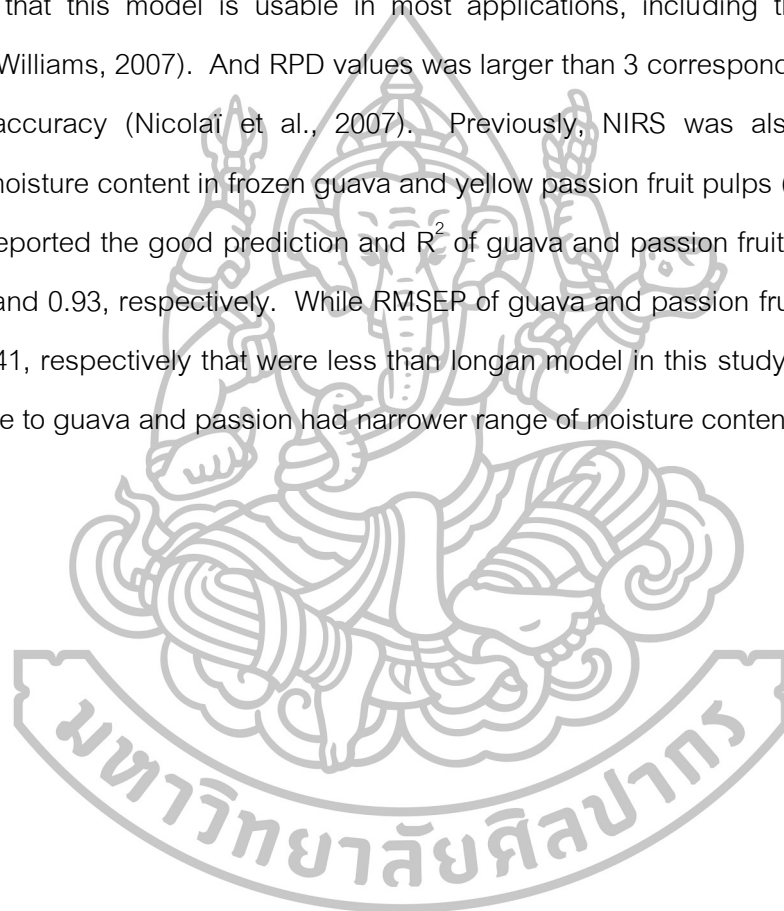


Figure 27 Scatter plot of moisture content of peel from the model built from averaging spectra.

The calibration and validation results associated with the PLS models for moisture content of flesh by NIRS are shown in Table 10. The result showed that the optimum models generated from averaging spectra at all positions of measurement were by using 10 PLS factors in the range of 1063.4-1640.9 nm and 2171.3-2356.9 nm that were pre-treated by the first derivative+SNV methods. This model shows  $R^2$ , RMSEP, RPD and a bias of 0.9513%, 5.53, 4.53 and 0.085%, respectively. The result of  $R^2$  showed that this model is usable in most applications, including that of quality assurance (Williams, 2007). And RPD values was larger than 3 corresponds to excellent prediction accuracy (Nicolai et al., 2007). Previously, NIRS was also applied to determine moisture content in frozen guava and yellow passion fruit pulps (Alamar et al., 2016) that reported the good prediction and  $R^2$  of guava and passion fruit models were found 0.94 and 0.93, respectively. While RMSEP of guava and passion fruit were found 0.24 and 0.41, respectively that were less than longan model in this study. The reason might be due to guava and passion had narrower range of moisture content.



**Table 10** Calibration and validation results for moisture content of flesh by NIRS.

Fruit part	Position	Pre processing	Wavelength (nm)	PLS factor	Calibration set (60%)		Validation set (40%)			RPD
					R <sup>2</sup>	RMSEC(%)	R <sup>2</sup>	RMSEP(%)	Bias(%)	
Flesh	P1	First derivative+MSC (17pts.)	1063.4-1640.9	8	0.9169	7.41	0.9277	6.76	0.401	3.73
			1833.5-2175.0							
	P2	SNV	1063.4-1183.8	10	0.9355	6.55	0.9341	6.43	0.232	3.90
			1638.8-1733.0							
			2171.3-2356.9							
	P3	First derivative+SNV (17pts.)	1063.4-2175.0	6	0.9278	6.88	0.9163	7.25	0.162	3.46
	P4	First derivative+MSC (17pts.)	1332.2-1640.9	10	0.9423	6.2	0.9407	6.09	0.57	4.13
P1P2P3P4	First derivative+MSC (17pts.)	1063.4-1640.9	10	0.9137	7.45	0.9367	6.37	-0.195	3.98	
Average P	First derivative+SNV (17pts.)	1063.4-1640.9	10	0.9596	5.18	0.9513	5.53	0.085	4.53	
			2171.3-2356.9							

Abbreviations: R<sup>2</sup>: coefficients of determination, RMSEC: root mean square error of calibration, RMSEP: root mean square error of prediction, RPD: ratio of standard deviation of reference data in validation set to SEP, MSC: multiplicative scatter correction, SNV: standard normal variate, 17 pts: 17 smoothing points, P1: calyx, P2: bottom, P3 and P4: 2 side of cheek, P1P2P3P4: all positions and Average P: average all positions

The scatter plot for the moisture content of flesh model is shown in Figure 28. The result found that most points close to the target line that means the NIRS predicted values were similar to the measured values (Nicolai et al., 2007). While, some points were spread out from the target line which related to rather high error from this model.

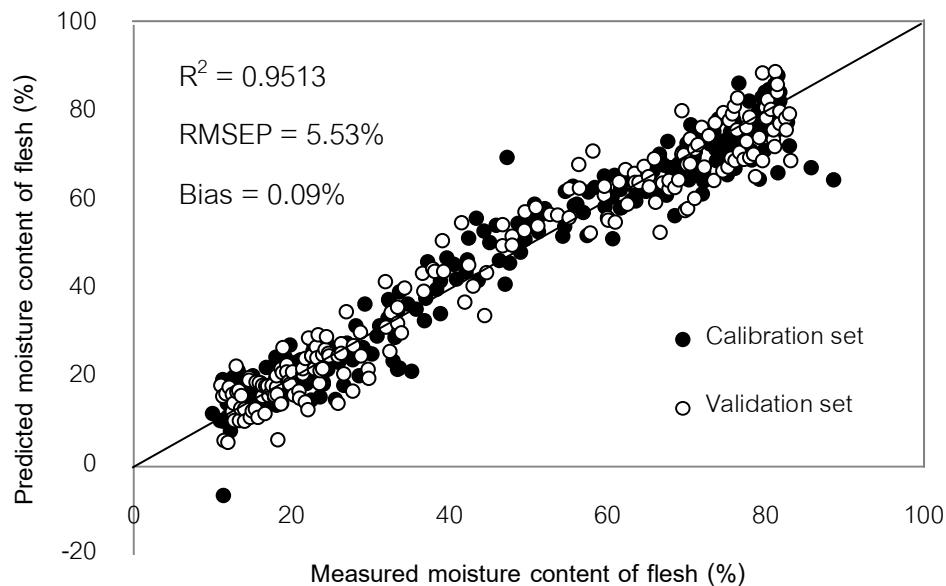


**Figure 28** Scatter plot of moisture content of flesh from the model built from averaging spectra.

However, RMSEP as an error of this model was rather high when applied for determining moisture content of flesh of dried whole longan fruit in exporting routines (<18%). The reason might be due to the wide range of the moisture content of flesh in fresh to dried longan (9.99-88.62%) and the penetration of light which had to pass through the peel and air gap between peel and dried flesh of longan affected to some errors of prediction model. To reduce the errors, the lower moisture content (such as 9-40% moisture content of flesh) could be used for developing new model. Table 11 showed that the errors were reduced but the performance of the model was also reduced. Thus, the old model was chosen for predicting the unknown samples.

**Table 11** Calibration and validation results for moisture content of flesh (9-40%) by NIRS.

Fruit part	position	Pre processing	Wavelength (nm)	PLS factor	Calibration set (60%)		Validation set (40%)			RPD
					R <sup>2</sup>	RMSEC(%)	R <sup>2</sup>	RMSEP(%)	Bias(%)	
Flesh (9-40%)	Average	SNV	1063.4-1333.6 2171.3-2356.9	10	0.8934	2.15	0.799	2.47	-0.403	2.26

Abbreviations: R<sup>2</sup>: coefficients of determination, RMSEC: root mean square error of calibration, RMSEP: root mean square error of prediction, RPD: ratio of standard deviation of reference data in validation set to SEP, SNV: standard normal variate, P1: calyx, P2: bottom, P3 and P4: 2 side of cheek, P1P2P3P4: all positions and Average P: average all positions



The calibration and validation results associated with the PLS models for moisture content of seed by NIRS are shown in Table 12. The result showed that the optimum models generated from averaging spectra at all positions of measurement were by using 7 PLS factors in the range of 1332.3-1640.9 nm that were pre-treated by the first derivative+SNV methods. This model showed  $R^2$ , RMSEP, RPD and a bias of 0.9577, 2.32%, 4.93 and -0.37%, respectively. The result of  $R^2$  showed that this model is usable in most applications, including that of quality assurance (Williams, 2007). And RPD values was larger than 3 corresponds to excellent prediction accuracy (Nicolai et al., 2007). Moreover, the negative bias was found in this result which means the average actual value from reference method had higher value than the average NIRS predicted value (Nicolai et al., 2007).

Good prediction result was found in Posom et al. (2016) that used NIRS for determining moisture content of *Leucaena leucocephala* pellets ( $R^2 = 0.995$  and RPD = 13.9). Nevertheless, the error of longan seed model might be occurred by the penetration of light from peel to the seed of longan and the characteristic of seed which has glossy seed coat (Phupaichitkun et al., 2006) can reflect the light related to the error in spectrum acquisition (Osborne, 1993).





**Table 12** Calibration and validation results for moisture content of seed by NIRS.

Fruit part	Position	Pre processing	Wavelength (nm)	PLS factor	Calibration set (60%)		Validation set (40%)			RPD
					R <sup>2</sup>	RMSEC(%)	R <sup>2</sup>	RMSEP(%)	Bias(%)	
Seed	P1	MSC	1332.3-1640.9	10	0.9231	3.29	0.9441	2.67	-0.411	4.28
	P2	SNV	1332.3-1640.9 1833.5-2175	6	0.9041	3.61	0.9342	2.90	-0.678	4.01
	P3	First derivative+MSC (17pts.)	1833.5-2356.9	9	0.9250	3.21	0.9551	2.39	-0.497	4.83
	P4	MSC	1063.4-1836.1	10	0.9282	3.14	0.9428	2.72	-0.259	4.20
	P1P2P3P4	First derivative+MSC (17pts.)	1332.3-1640.9 2171.3-2356.9	10	0.9182	3.31	0.9355	2.88	-0.304	3.96
	Average P	First derivative+SNV (17pts.)	1332.3-1640.9	7	0.9336	3.01	0.9577	2.32	-0.37	4.93

Abbreviations: R<sup>2</sup>: coefficients of determination, RMSEC: root mean square error of calibration, RMSEP: root mean square error of prediction, RPD: ratio of standard deviation of reference data in validation set to SEP, MSC: multiplicative scatter correction, SNV: standard normal variate, 17 pts: 17 smoothing points, P1: calyx, P2: bottom, P3 and P4: 2 side of cheek, P1P2P3P4: all positions and Average P: average all positions

The scatter plot for the moisture content of seed model is shown in Figure 29. It can be seen that most points close to the target line that means good prediction of model (Nicolai et al., 2007). Obviously, some points were under the target line that means the average actual value from reference method had higher value than the average NIRS predicted value and correspond to negative bias from the model result (Nicolai et al., 2007).

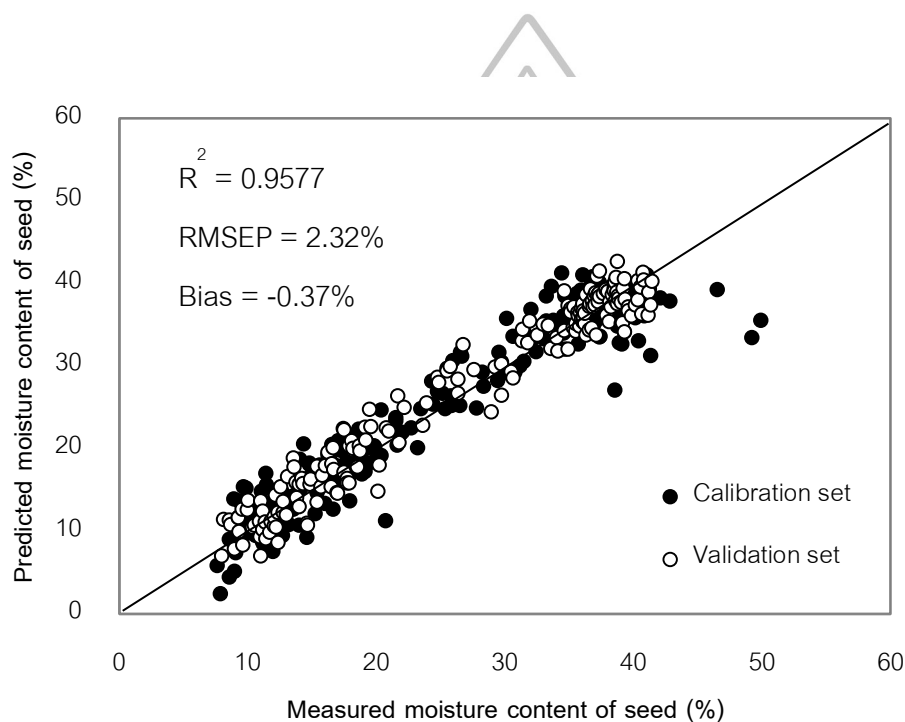


Figure 29 Scatter plot of moisture content of seed of from the model built from averaging spectra.

For flesh and seed part, the calibration and validation results associated with the PLS models are shown in Table 13. The result showed that the optimum models generated from averaging spectra at all positions of measurement were by using 9 PLS factors in the range of 1332.3-1471.4 nm and 1833.5-2064.2 nm that were pre-treated by MSC methods. This model shows  $R^2$ , RMSEP, RPD and a bias of 0.9604, 4.13%, 5.10 and -0.731%, respectively. The result of  $R^2$  showed that this model is usable in most applications, including that of quality assurance (Williams, 2007). RPD values was

larger than 3 corresponds to excellent prediction accuracy (Nicolai et al., 2007). Moreover, the fairly high error also found same as the results of flesh model and seed model in previous table (Table 11 and 12).



**Table 13** Calibration and validation results for moisture content of flesh and seed by NIRS.

Fruit part	Position	Pre processing	Wavelength (nm)	PLS factor	Calibration set (60%)		Validation set (40%)			RPD
					R <sup>2</sup>	RMSEC(%)	R <sup>2</sup>	RMSEP(%)	Bias(%)	
Flesh and seed	P1	SNV	1063.4-1836.1 2171.3-2356.9	7	0.9168	6.17	0.9386	5.19	-1.06	4.12
	P2	Second derivative (17pts.)	1332.3-2356.9	9	0.9102	6.43	0.9295	5.55	-0.292	3.77
	P3	First derivative+SNV (17pts.)	1063.4-1640.9 1833.5-2356.9	10	0.9102	6.38	0.9237	5.82	-0.438	3.63
	P4	First derivative+SNV (17pts.)	1063.4-1640.9 1833.5-2356.9	9	0.9236	5.93	0.9484	4.74	-0.627	4.44
	P1P2P3P4	First derivative+SNV (17pts.)	1063.4-1640.9 1833.5-2175	10	0.8919	6.97	0.9310	5.51	-0.540	3.83
	Average P	MSC	1332.3-1471.4 1833.5-2064.2	9	0.9451	5.03	0.9604	4.13	-0.731	5.10

Abbreviations: R<sup>2</sup>: coefficients of determination, RMSEC: root mean square error of calibration, RMSEP: root mean square error of prediction, RPD: ratio of standard deviation of reference data in validation set to SEP, MSC: multiplicative scatter correction, SNV: standard normal variate, 17 pts: 17 smoothing points, P1: calyx, P2: bottom, P3 and P4: 2 side of cheek, P1P2P3P4: all positions and Average P: average all positions

According to the result from Table 13, the scatter plot for the moisture content of flesh and seed model is shown in Figure 30. Most points close to the target line that means good prediction of model (Nicolai et al., 2007).

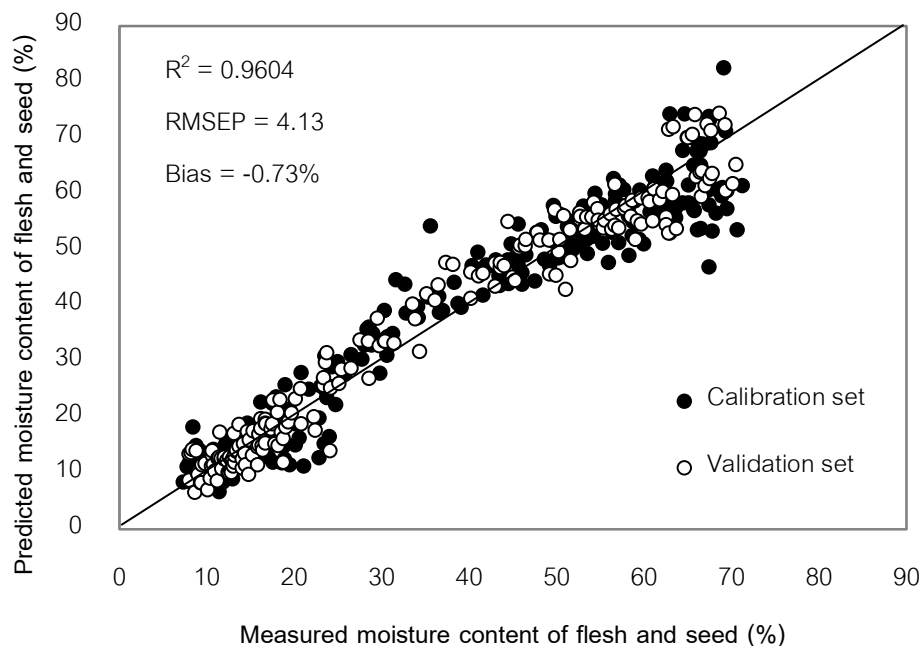


Figure 30 Scatter plot of moisture content of flesh and seed from the model built from averaging spectra.

The calibration and validation results associated with the PLS models for moisture content of the whole fruit by NIRS are shown in Table 14. The result represented that the optimum models for moisture content of whole fruit generated from averaging spectra at all positions of measurement were by using 10 PLS factors in the range of 1289.8-1640.9 nm and 2060.9-2356.9 nm that were pre-treated by the first derivative+SNV methods. This model showed  $R^2$ , RMSEP, RPD and a bias of 0.9673, 3.89%, 5.53 and -0.138%, respectively. According to Williams (2007) and Nicolai et al. (2007),  $R^2$  and RPD of this model can be used in most applications, including that of quality assurance. Moreover, good prediction of moisture content ( $R^2$  was 0.880 and

RMSEP was 1.35%) also found in Morales-Sillero et al. (2011) that applied NIRS for assessing moisture content of table olive.



**Table 14** Calibration and validation results for moisture content of whole fruit by NIRS.

Fruit part	Position	Pre processing	Wavelength (nm)	PLS factor	Calibration set (60%)		Validation set (40%)			RPD
					R <sup>2</sup>	RMSEC(%)	R <sup>2</sup>	RMSEP(%)	Bias(%)	
Whole fruit	P1	MSC	1332.3-1471.4	10	0.9459	5.18	0.9412	5.25	-0.334	4.13
			1833.5-2064.2							
	P2	MSC	1063.4-1333.6	3	0.8933	7.18	0.9586	4.34	-0.355	4.93
			1638.8-2175.0							
	P3	SNV	1638.8-2175.0	9	0.9129	6.56	0.9354	5.46	-0.775	3.97
			2171.3-2356.9							
	P4	First derivative+MSC (17pts.)	1063.4-1640.8	10	0.9280	5.97	0.9626	4.20	-0.24	5.18
			2171.3-2356.9							
P1P2P3P4	SNV	1063.4-1836.1	10	0.9097	6.59	0.9419	5.19	-0.313	4.15	
		2171.3-2356.8								
Average P	First derivative+SNV (17pts.)	1289.8-1640.9	10	0.9535	4.80	0.9673	3.89	-0.138	5.53	
		2060.9-2356.9								

Abbreviations: R<sup>2</sup>: coefficients of determination, RMSEC: root mean square error of calibration, RMSEP: root mean square error of prediction, RPD: ratio of standard deviation of reference data in validation set to SEP, MSC: multiplicative scatter correction, SNV: standard normal variate, 17 pts: 17 smoothing points, P1: calyx, P2: bottom, P3 and P4: 2 side of cheek, P1P2P3P4: all positions and Average P: average all positions

The scatter plot for the moisture content of the whole fruit model is shown in Figure 31. Most points also close to the target line that means good prediction of model (Nicolai et al., 2007). However, the error points also found that related to high RMSEP in the prediction model.

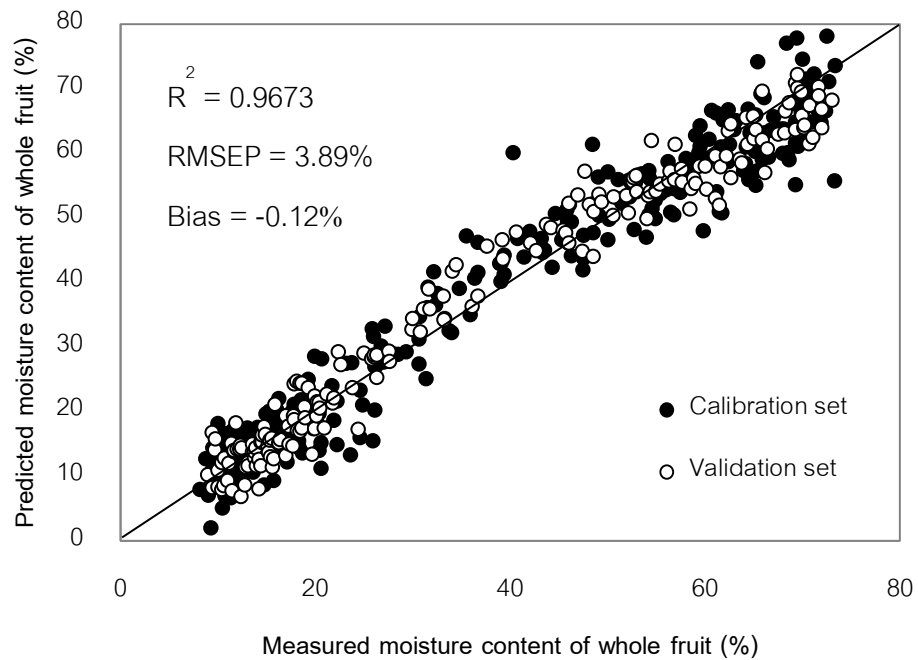


Figure 31 Scatter plot of moisture content of whole fruit from the model built from averaging spectra.

Figure 32 shows the regression coefficient plots for moisture content of flesh from the model built from averaging spectra. The strong effects of the bond vibration on the predictions of moisture content are displayed by the high peaks of the regression coefficient plots. This plot had wavelengths in the range of 1063.4-1640.9 nm and 2171.3-2356.9 nm. As mentioned by Osborne et al. (1993), the apparent peaks, their bond vibration and the structure in the regression coefficient plot are shown in Table 15 which displays the intensity of the peaks in descending order. It was observed that the vibration band of O-H which appeared as high peak (1455 nm) indicated that water had an important influence on the prediction of moisture content of longan (Osborne et al.,



1993; Magwaza et al., 2012; Rungpichayapichet et al., 2016). There were also high absorption peaks owing to the C-H which related to the structure of starch and sugar in sample (1175 nm and 1390 nm) (Rungpichayapichet et al., 2016).

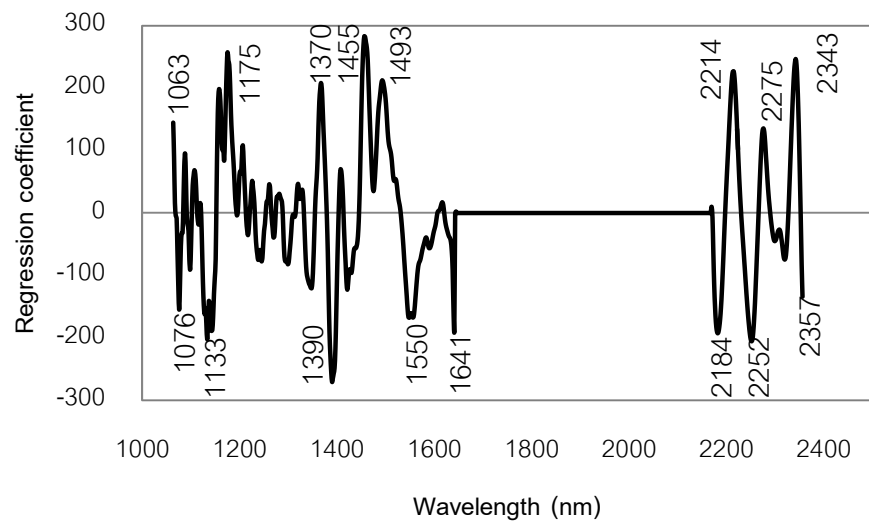


Figure 32 Regression coefficient plot of moisture content of flesh from the model built from averaging spectra.



**Table 15** The absorption bands with high regression coefficients of model for moisture content of flesh of the longan fruits.

Wavelength (nm)	Wavelength (nm) from references	Bond vibration	Structure
1063	1060	N-H str. second overtone	RNH <sub>2</sub>
1076	1080	2×C-H str.+2×C-C str.	benzene
1133	1143	C-H str. second overtone	aromatic
1175	1170	C-H str. second overtone	HC=CH
1370	-	-	-
1390	1395	2×C-H str.+ C-H def.	CH <sub>2</sub>
1455	1450	O-H str. first overtone	starch, H <sub>2</sub> O
1493	1490	O-H str. first overtone (intramol. H-bond)	cellulose
1550	-	-	-
1641	1645	C-H str. first overtone	aromatic
2184	2180	2×amide I + amide III	protein
2214	-	-	-
2252	2252	O-H str. + O-H def.	starch
2275	2276	O-H str. + C-C def.	starch
2343	2347	CH <sub>2</sub> sym. Str. +=CH <sub>2</sub> def.	HC=CHCH <sub>2</sub>
2357	-	-	-

Source: Osborne et al. (1993)

Figure 33 shows the regression coefficient plot of for moisture content of the whole fruit from the model built from averaging spectra. This plot had wavelengths in the range of 1289.8-1640.9 nm and 2060.9-2356.9 nm. The obvious peaks and their bond vibration in the regression coefficient plot are shown in Table 16 which indicates the intensity of the peaks in descending order. It was observed that the vibration of O-H also appeared as high peak (1449 nm), indicating an implicit high influence on the prediction of the moisture content of the whole longan fruit (Osborne et al., 1993; Magwaza et al., 2012; Rungpichayapichet et al., 2016). Moreover, there is also a high peak in the absorption band for cellulose and starch at 1494 nm and 1526 nm, respectively (Onsawai and Sirisomboon, 2015).

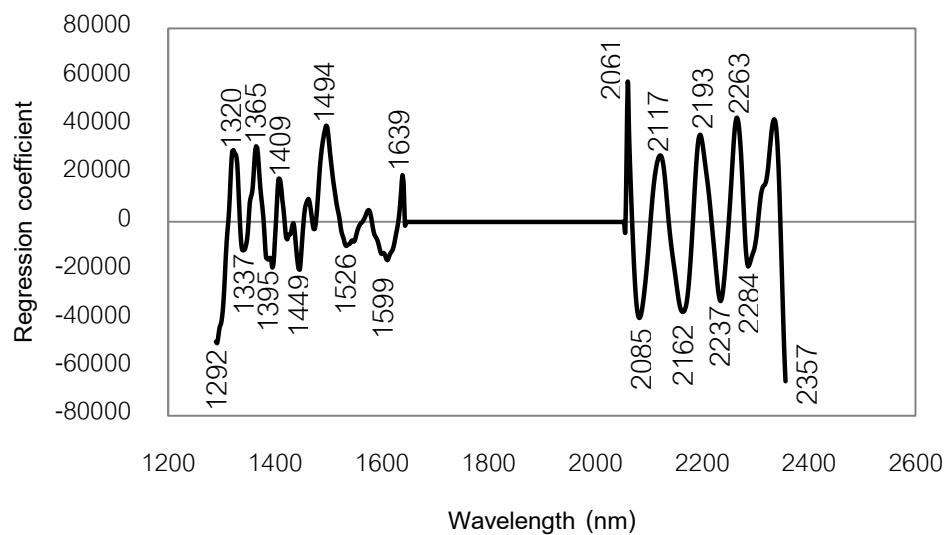


Figure 33 Regression coefficient plot of moisture content of the whole fruit from the model built from averaging spectra.

**Table 16** The absorption bands with high regression coefficients of the PLS model for moisture content of the whole longan fruits.

Wavelength (nm)	Wavelength (nm) from references	Bond vibration	Structure
1292	-	-	-
1320	-	-	-
1337	-	-	-
1365	1360	2×C-H str.+ C-H def.	CH <sub>3</sub>
1395	1395	2×C-H str.+ C-H def.	CH <sub>2</sub>
1409	1410	O-H str. first overtone	ROH
1449	1450	O-H str. first overtone	starch, H <sub>2</sub> O
1494	1490	O-H str. first overtone (intramol. H-bond)	cellulose
1526	1528	O-H str. first overtone (intramol. H-bond)	starch
1578	1580	O-H str. first overtone (intramol. H-bond)	starch, glucose
1599	-	-	-
1639	-	-	-
2016	-	-	-
2080	2080	O-H str.+ O-H def.	ROH, sucrose, starch
2117	2110	N-H sym. Str. + amide III	CONH <sub>2</sub> , CONHR
2162	2160	2×amide I + amide III	CONHR
2193	2190	CH <sub>2</sub> asym. Str. + C=str.	HC=CH
2237	2242	N-H str. + NH <sub>3</sub> <sup>+</sup> def.	amino acid
2284	2280	C-H str. + C-H def.	CH <sub>3</sub>

Wavelength (nm)	Wavelength (nm) from references	Bond vibration	Structure
2357	2352	C-H def. second overtone	cellulose

Source: Osborne et al. (1993)

For checking accuracy of the model, the average spectra of all position of 120 dried whole longan fruits from this study which had moisture content of flesh in the range of 14-24% were predicted by the best fit model for moisture content of flesh. This moisture range could be in the range of the final moisture content of flesh when the drying stopped at the drying manufacturing. Table 17 represents the comparison of measured and predicted moisture content of flesh from 120 dried whole longans by best fit model for moisture content of flesh. To compare the methods between destructive and NIRS measurement, the paired *t* test method was applied. The result showed that the *p*-value was 0.513 which was higher than 0.05 (data not shown). The paired *t* test result demonstrated that the predicted values obtained from the NIR spectroscopy and the measured values from reference method did not show significant difference at 95% confidence interval ( $p > 0.05$ ).

**Table 17** The comparison of measured and predicted moisture content of flesh of 120 dried whole longan fruits from this study by the best fit model.

N	Measured (%)	Prediction (%)	% error	N	Measured (%)	Prediction (%)	% error
1	14.21	17.17	20.86	31	18.42	23.40	27.07
2	14.42	18.32	27.07	32	18.54	16.49	11.06
3	14.50	14.29	1.42	33	18.58	18.72	0.75
4	14.60	13.25	9.27	34	18.69	16.94	9.38
5	14.61	13.13	10.14	35	18.77	14.38	23.38
6	14.66	19.48	32.91	36	18.81	18.19	3.31
7	15.09	13.87	8.08	37	19.24	17.58	8.62
8	15.28	14.32	6.27	38	19.27	24.67	28.06
9	15.62	18.43	18.01	39	19.28	21.74	12.77
10	15.72	19.06	21.28	40	19.50	22.71	16.46
11	15.75	17.06	8.30	41	19.52	20.59	5.51
12	16.05	15.62	2.70	42	19.58	23.81	21.62
13	16.07	19.05	18.56	43	20.04	16.75	16.42
14	16.27	14.60	10.25	44	20.06	18.68	6.86
15	16.48	15.26	7.43	45	20.44	21.87	6.99
16	16.62	17.82	7.25	46	20.68	22.18	7.23
17	16.63	18.43	10.82	47	20.80	23.78	14.34
18	16.79	14.92	11.16	48	21.16	22.58	6.71
19	16.88	16.15	4.33	49	21.16	24.22	14.45
20	17.31	18.11	4.65	50	21.24	19.22	9.52
21	17.32	16.42	5.19	51	21.57	21.74	0.81
22	17.50	17.82	1.83	52	21.62	23.35	7.98
23	17.63	16.52	6.30	53	21.68	22.53	3.92
24	17.64	17.42	1.26	54	21.90	18.93	13.55
25	17.72	15.62	11.87	55	22.01	23.29	5.82
26	17.90	19.79	10.55	56	22.02	21.48	2.47
27	18.04	21.19	17.46	57	22.19	23.04	3.81
28	18.11	19.16	5.83	58	22.32	21.39	4.15
29	18.11	16.50	8.87	59	22.50	15.07	33.03
30	18.11	13.96	22.93	60	22.70	26.18	15.33

**Table 17** The comparison of measured and predicted moisture content of flesh of 120 samples by PLS models (cont.).

N	Measured (%)	Prediction (%)	% error	N	Measured (%)	Prediction (%)	% error
61	22.82	27.86	22.10	91	17.52	18.45	5.32
62	22.85	28.76	25.86	92	17.84	15.68	12.09
63	23.12	21.22	8.21	93	17.84	16.11	9.70
64	23.20	25.66	10.62	94	18.06	18.06	0.01
65	23.23	28.96	24.68	95	18.07	20.63	14.16
66	23.48	22.60	3.74	96	18.15	16.41	9.60
67	23.48	21.03	10.45	97	18.63	22.26	19.48
68	23.50	25.20	7.24	98	18.69	14.26	23.70
69	23.64	15.87	32.88	99	18.83	21.38	13.56
70	23.87	23.80	0.28	100	19.39	23.05	18.87
71	23.92	26.41	10.41	101	19.41	21.48	10.66
72	23.99	19.14	20.22	102	19.61	19.31	1.53
73	24.05	18.75	22.04	103	19.77	18.67	5.55
74	24.07	24.72	2.71	104	20.12	21.49	6.84
75	14.05	13.03	7.29	105	20.24	16.29	19.53
76	14.06	10.28	26.90	106	20.95	17.19	17.94
77	14.60	19.65	34.60	107	20.98	15.54	25.93
78	14.81	11.12	24.90	108	21.41	21.08	1.52
79	15.00	12.63	15.80	109	21.43	22.24	3.77
80	15.45	13.13	15.03	110	21.74	24.50	12.71
81	15.49	19.13	23.50	111	22.56	25.13	11.37
82	15.79	11.22	28.89	112	22.57	25.02	10.87
83	15.92	19.04	19.57	113	22.86	22.18	2.98
84	16.28	15.91	2.24	114	23.11	27.18	17.62
85	16.33	18.36	12.41	115	23.24	24.59	5.81
86	16.65	12.11	27.26	116	23.33	29.88	28.08
87	16.68	18.31	9.74	117	23.57	18.87	19.92
88	16.96	18.30	7.91	118	23.60	21.75	7.82
89	17.10	16.04	6.19	119	23.93	22.22	7.16
90	17.51	17.29	1.26	120	23.95	25.32	5.72
				<b>Average</b>	<b>19.24</b>	<b>19.42</b>	<b>12.41</b>

Moreover, the best fit model was applied to predict moisture content of flesh of 20 unknown dried longan samples from the market. Table 18 shows the comparison of measured and predicted moisture content of flesh of the unknown samples by the best fit model of flesh part. To compare the methods between destructive and NIRS measurement, the paired *t* test method was applied. The result showed that the *p*-value was 0.135 which was higher than 0.05 (data not shown). It can be concluded that the predicted values obtained from the NIR spectroscopy and the measured values from reference method did not show significant difference at 95% confidence interval ( $p > 0.05$ ).





**Table 18** The comparison of measured and predicted moisture content of flesh of 20 unknown samples by the best fit models.

No	Measured (%)	Prediction (%)	% error
1	27.10	24.73	8.76
2	25.93	22.62	12.78
3	28.23	29.17	3.33
4	27.49	27.99	1.80
5	26.62	23.88	10.31
6	27.54	26.71	3.01
7	25.69	22.84	11.11
8	29.26	23.61	19.31
9	28.87	33.21	15.04
10	27.41	28.81	5.09
11	28.14	30.54	8.52
12	26.27	31.57	20.18
13	28.73	34.35	19.58
14	26.76	32.18	20.26
15	26.28	28.43	8.21
16	28.15	34.74	23.44
17	25.68	27.88	8.57
18	25.32	25.09	0.90
19	28.17	28.96	2.78
20	25.79	30.25	17.28
<b>Average</b>	<b>27.17</b>	<b>28.38</b>	<b>11.01</b>

To ensure the accuracy of prediction PLS model of flesh and other parts, bias checking, SEP checking and slope checking methods from International standard ISO 12099 were used. These methods can demonstrate that predicted value obtained from the instrument were not different from actual values significantly at 95% confidence interval. Therefore, the models that pass all tests are usable in any application.

It can be seen in Table 19, the results showed that NIRS moisture content of peel, flesh and the whole fruit models passed bias checking, SEP checking and slope checking method. However, NIRS moisture content of seed and flesh+seed models did not pass bias checking that mean the results show significant difference between NIRS predicted and measured values. The reason might be due to the gloss of black seed coat of the longan fruit which can reflect the light and make some errors in NIRS measurement. The details of verification of each method were illustrated in Appendix D.

**Table 19** Verifying the accuracy by bias checking, SEP checking and slope checking method for NIRS moisture content models.

Model	Bias checking	SEP checking	Slope checking
NIRS moisture content of peel	✓	✓	✓
NIRS moisture content of flesh	✓	✓	✓
NIRS moisture content of seed	✗	✓	✓
NIRS moisture content of flesh and seed	✗	✓	✓
NIRS moisture content of the whole fruit	✓	✓	✓

#### 4.2.3 Calibration models for TSS of flesh by NIRS

A total of 186 spectra were divided into calibration set (60% of all samples) and validation set (40% of all samples) for building the TSS models. Mean, standard deviation (SD), minimum and maximum of TSS of flesh of longan fruit samples are shown in Table 20. The range of TSS in flesh of samples were 13-98 °Brix in calibration set and 18-90 °Brix in validation set.

**Table 20** Mean, standard deviation (SD), minimum and maximum of TSS of flesh in longan fruit samples.

Parameter	Data set	N	Min	Max	Mean	SD
TSS (°Brix)	Calibration (60%)	112	13	98	56.71	24.00
	Validation (40%)	74	18	90	55.64	23.43

N = number of samples

Figure 34 (a) and (b) show the distribution of TSS of flesh in longan samples in calibration set and validation set, respectively. It can be seen that there were more samples at a low TSS (30-40 °Brix) and high TSS (80-90 °Brix) than other values. According to Thai Agricultural Standard (2006), TSS of the flesh must not lower than 80 °Brix for flesh dried longan and 76 °Brix for flesh of dried whole longan for exporting.

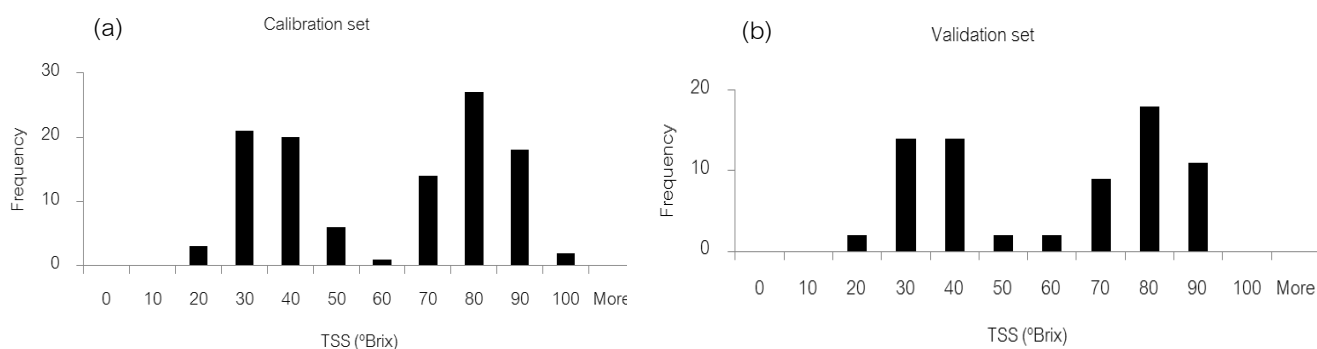


**Figure 34** Histogram of the distribution of TSS of flesh of samples in calibration and validation set.

The calibration and validation results with the PLS models for TSS of flesh in longan fruit samples are shown in Table 21. The best model was obtained by averaging spectra at all positions of measurement which was pretreated by SNV preprocessing technique and using 4 PLS factors in the range of 1833.5-2175.0 nm. This model shows  $R^2$ , RMSEP, RPD and a bias of 0.9219, 6.52 °Brix, 3.59 and -0.454 °Brix, respectively. This model showed the RPD value above 3 which corresponds to excellent prediction accuracy (Nicolai et al., 2007). However, rather high RMSEP in TSS of flesh might be due to the penetration of light which had to pass through the peel and air gap between peel and dried flesh of longan affected to some errors of prediction model as mentioned in previous result about moisture content of flesh part.

Recently, NIRS was also used to assess TSS in Japanese plums, navel oranges and mangoes (Louw and Theron, 2010; Liu et al., 2013; Rungpichayapichet et al., 2016) that reported the good prediction and  $R^2$  were shown above 0.80.

Figure 35 shows the relationship between measured and predicted TSS of flesh from the model built from averaging spectra. It can be seen that the points close to the target line that mean this model had good prediction. Some points were found under the target line that related to negative bias of the model (Nicolai et al., 2007).



**Table 21** Calibration and validation results for TSS in flesh of dried whole longan by NIRS.

Position	Pre processing	Wavelength (nm)	PLS factor	Calibration set (60%)		Validation set (40%)			RPD
				R <sup>2</sup>	RMSEC(°Brix)	R <sup>2</sup>	RMSEP(°Brix)	Bias(°Brix)	
P1	First derivative+SNV (17pts.)	1332.3-1640.9	7	0.9111	7.39	0.8751	8.22	-0.434	2.83
P2	Second derivative (17pts.)	1730.7-1836.1 2171.3-2356.9	6	0.8659	9.04	0.8810	8.03	-0.589	2.91
P3	Second derivative (17pts.)	1833.5-2175.0	2	0.8386	9.73	0.8941	7.55	0.289	3.08
P4	MSC	1332.3-1640.9 2171.3-2356.9	10	0.9142	7.37	0.9131	6.88	-0.724	3.41
P1P2P3P4	MSC	1063.4-1640.9 2171.3-2356.9	10	0.8854	8.11	0.9049	7.29	-0.558	3.25
Average P	SNV	1833.5-2175.0	4	0.8947	7.93	0.9219	6.52	-0.454	3.59

Abbreviations: R<sup>2</sup>: coefficients of determination, RMSEC: root mean square error of calibration, RMSEP: root mean square error of prediction, RPD: ratio of standard deviation of reference data in validation set to SEP, MSC: multiplicative scatter correction, SNV: standard normal variate, 17 pts: 17 smoothing points, P1: calyx, P2: bottom, P3 and P4: 2 side of cheek, P1P2P3P4: all positions and Average P: average all positions

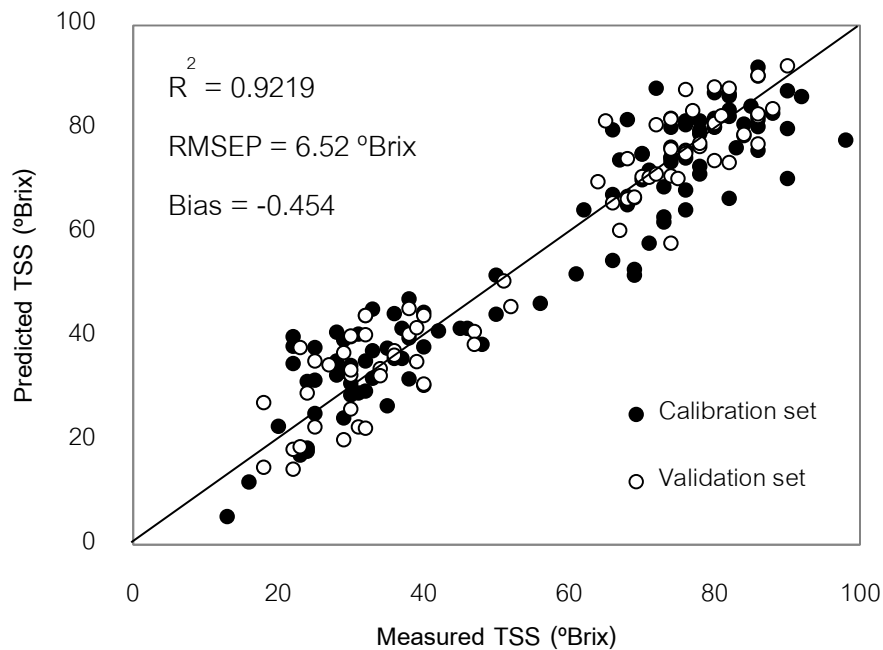
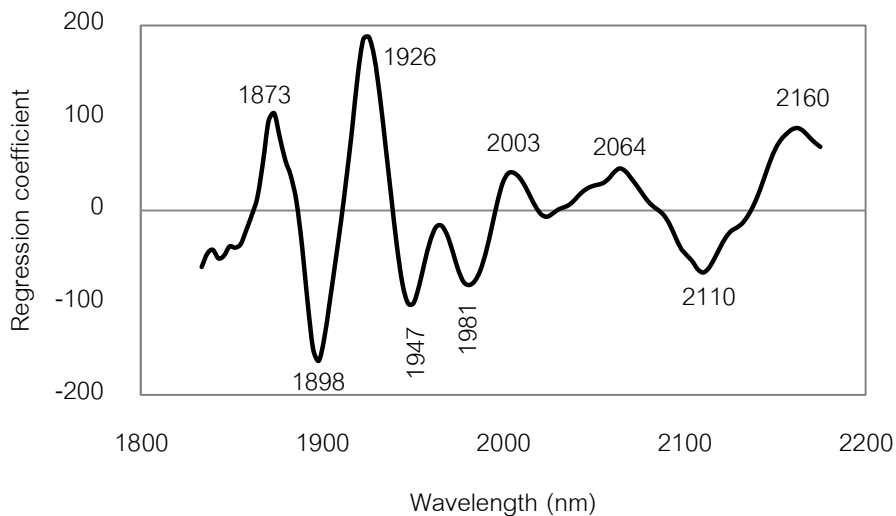


Figure 35 Scatter plot of TSS of flesh from the model built from averaging spectra.

The regression coefficient plot of the best fit TSS model is shown in Figure 36. This plot had wavelengths in the range of 1833.5-2175.0 nm. The important wavelengths for TSS were 1873, 1898, 1926, 1947, 1981, 2003, 2064, 2110 and 2160 nm. These wavelengths represented -H and -OH functional groups which are related to carbohydrates (starches and sugars), water and organic acids (Rungpichayapichet et al., 2016).



**Figure 36** Regression coefficient plot of TSS of flesh from the model built from averaging spectra.

Table 22 shows the verification of the accuracy of TSS model by bias checking, SEP checking and slope checking method. As demonstrated, the model passed all verification methods. NIRS predicted values were not different from actual values from standard method significantly at 95% confidence interval. The details of verification of each method were illustrated in Appendix D.

**Table 22** Verifying the accuracy by bias checking, SEP checking and slope checking method for TSS model

Model	Bias checking	SEP checking	Slope checking
NIRS TSS in flesh	✓	✓	✓

#### 4.2.4 Calibration models for sugar content of flesh by NIRS

A total of 181 spectra were divided into calibration set (60% of all samples) and validation set (40% of all samples) for building the models. Mean, standard deviation (SD), minimum and maximum of sugar content of longan fruit samples are showed in Table 23. The range of sucrose was 12.47-593.92 mg/g fresh weight, the range of glucose was 11.05-148.96 mg/g fresh weight, the range of fructose was 17.84-157.70 mg/g fresh weight and the range of total sugar was 116.94-655.84 mg/g fresh weight. Compared in 3 type of sugar, it can be seen that sucrose had the widest range of sugar content in flesh of longan. During drying, each sugar was increased. For example, fresh longan had the sugar content of 125.51 mg/g fresh weight, 21.46 mg/g fresh weight, 21.23 mg/g fresh weight and 168.20 mg/g fresh weight for sucrose, glucose, fructose and total sugar content, respectively. At the end point of drying, each sugar content were found 388.93 mg/g fresh weight, 76.21 mg/g fresh weight, 91.53 mg/g fresh weight and 556.66 mg/g fresh weight for sucrose, glucose, fructose and total sugar content, respectively. Obviously, sucrose had the highest content in flesh of dried longan while, glucose had the lowest content. The lowest value of glucose might be due to glucose was used as a substrate for generating Maillard reaction in dried longan (Rungtip, 2006).

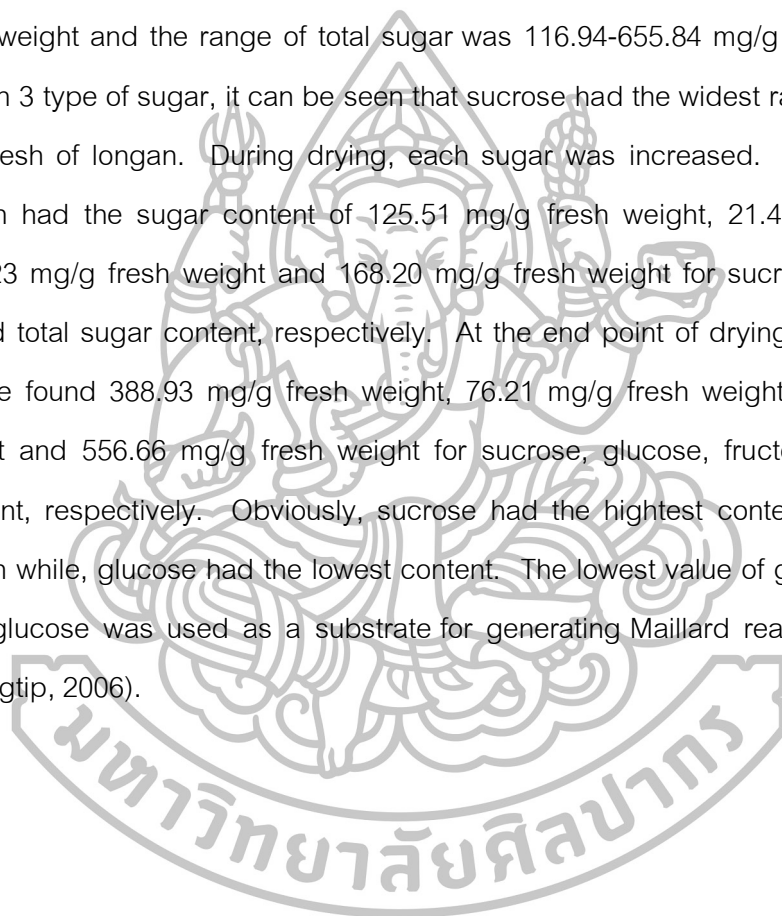




**Table 23** Mean, standard deviation (SD), minimum and maximum of sugar content of flesh in longan fruit samples.

Sugar (mg/g fresh weight )	N.	Calibration set (60%)				N	Validation set (40%)			
		Min	Max	Mean	SD		Min	Max	Mean	SD
Sucrose	109	12.47	593.92	288.78	138.80	72	79.28	543.18	288.32	133.24
Glucose	109	11.05	148.96	58.21	30.13	72	15.65	133.51	57.94	29.43
Fructose	109	17.84	157.70	73.18	35.10	72	19.25	147.45	72.99	34.38
Total sugars	109	116.94	655.84	419.36	172.91	72	145.20	647.75	420.38	171.47

N = number of samples

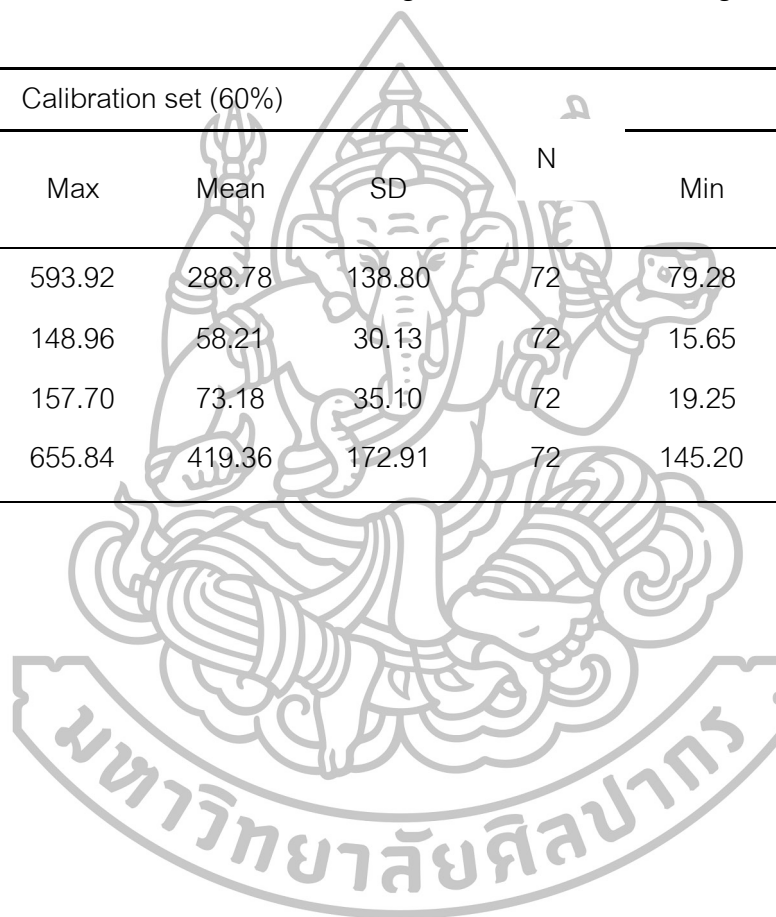
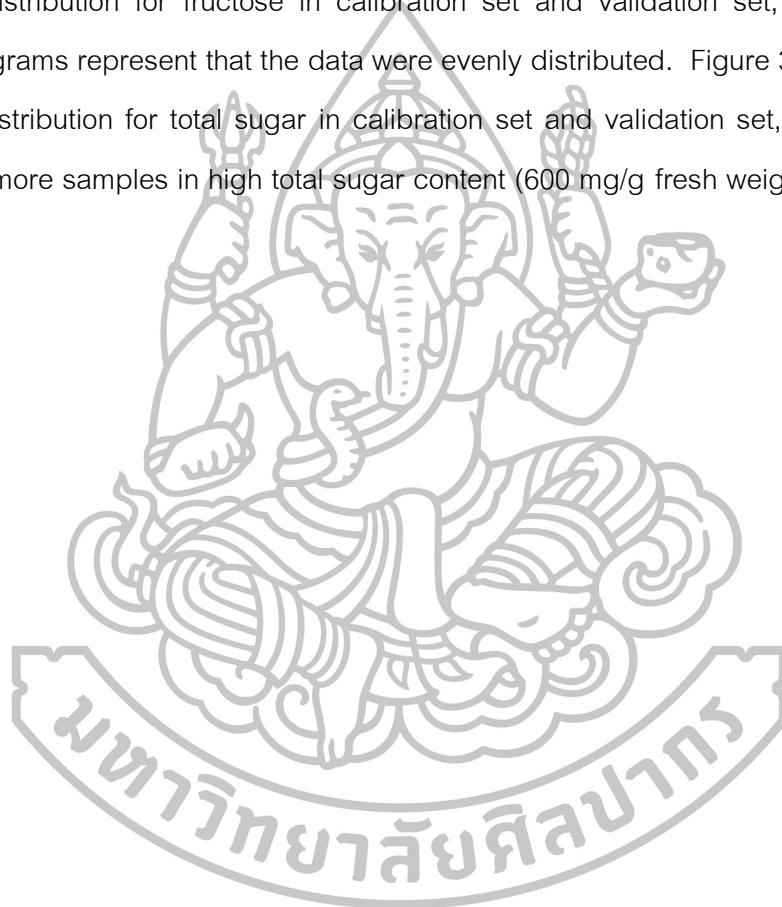
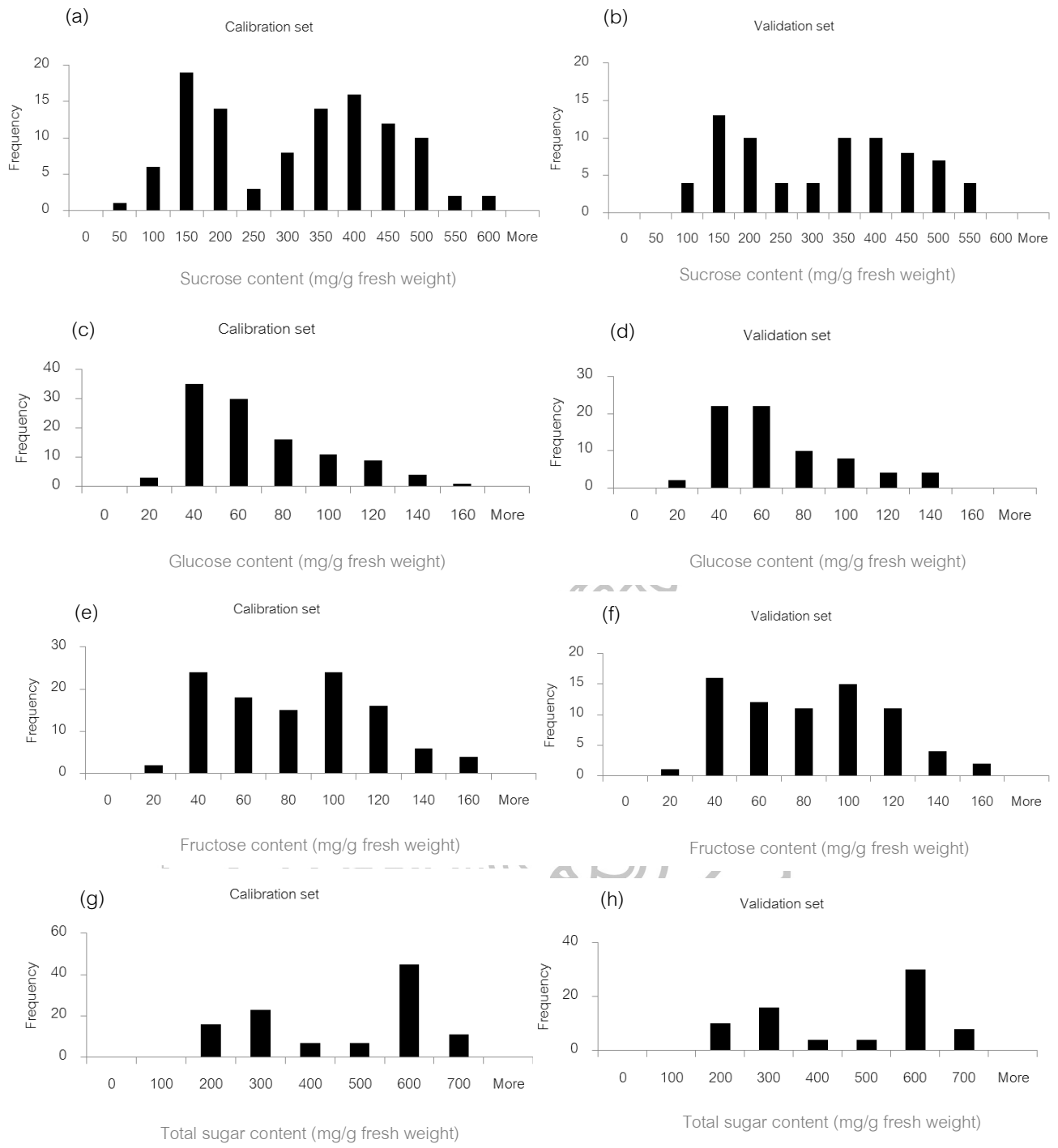


Figure 37 (a) and (b) show the distribution of sucrose content of flesh in longan samples in calibration set and validation set, respectively. Obviously, there were more samples in the range of 150-200 mg/g fresh weight and 350-450 mg/g fresh weight than other values. Figure 37 (c) and (d) show the distribution of glucose content of flesh in calibration set and validation set, respectively. It can be seen that there were more sample at low content (40-60 mg/g fresh weight) than other values. Figure 37 (e) and (f) show the distribution for fructose in calibration set and validation set, respectively. These histograms represent that the data were evenly distributed. Figure 37 (g) and (h) show the distribution for total sugar in calibration set and validation set, respectively. They show more samples in high total sugar content (600 mg/g fresh weight) than other values.





**Figure 37** Histogram of the distribution of sugar content of flesh of samples in calibration and validation set.

#### 4.2.4.1 Sucrose

The calibration and validation results with the PLS models for sucrose content of flesh in longan fruit samples are shown in Table 24. Averaging spectra at all positions of measurement and SNV preprocessing technique by using 6 PLS factors in the range of 1063.4-1836.1 and 2171.3-2356.9 nm were provided the best prediction which gave  $R^2$ , RMSEP, RPD and a bias of 0.8343, 53.8 mg/g fresh weight, 2.48 and -7.26 mg/g fresh weight, respectively. Obviously, the result of the model showed negative bias value which means the average actual value from reference method had higher value than the average NIRS predicted value (Nicolai et al., 2007). It is worth noting that Williams (2007) had demonstrated that  $R^2$  of 0.83-0.90 indicates that a model was usable with caution for most applications, including research and RPD of 2.5 corresponds that the model had good prediction accuracy. In addition, good prediction model was also found in Liu et al. (2006) that applied NIRS for determination of sucrose in apple and R was shown 0.969 and RMSEP of 0.335%.

Figure 38 shows the relationship between measured sucrose content value and predicted sucrose content value from the best model. It clearly showed that the data slightly scattered and some data were under the target line.



**Table 24** Calibration and validation results for sucrose content of flesh by NIRS.

Position	Pre processing	Wavelength (nm)	PLS factor	Calibration set (60%)		Validation set (40%)			
				R <sup>2</sup>	RMSEC (mg/g fresh weight)	R <sup>2</sup>	RMSEP (mg/g fresh weight)	Bias (mg/g fresh weight)	RPD
P1	SNV	1063.4-2175.0	6	0.7247	74.9	0.8281	54.8	-6.24	2.43
P2	First derivative+MSC (17pts.)	2171.3-2356.9	4	0.7118	75.9	0.7708	64.5	-10	2.11
P3	MSC	1063.4-1640.9 1833.5-2175.0	1	0.7035	75.9	0.8049	58.7	-8.52	2.29
P4	MSC	1063.4-1640.9 1833.5-2175.0	1	0.6957	76.9	0.7945	59.9	-10.1	2.24
P1P2P3P4	First derivative+SNV (17pts.)	1063.4-1836.1 2171.3-2262.3	8	0.7514	69.4	0.7946	61.4	-2.66	2.21
Average P	SNV	1063.4-1836.1 2171.3-2356.9	6	0.7969	62.9	0.8343	53.8	-7.26	2.48

Abbreviations: R<sup>2</sup>: coefficients of determination, RMSEC: root mean square error of calibration, RMSEP: root mean square error of prediction, RPD: ratio of standard deviation of reference data in validation set to SEP, MSC: multiplicative scatter correction, SNV: standard normal variate, 17 pts: 17 smoothing points, P1: calyx, P2: bottom, P3 and P4: 2 side of cheek, P1P2P3P4: all positions and Average P: average all positions

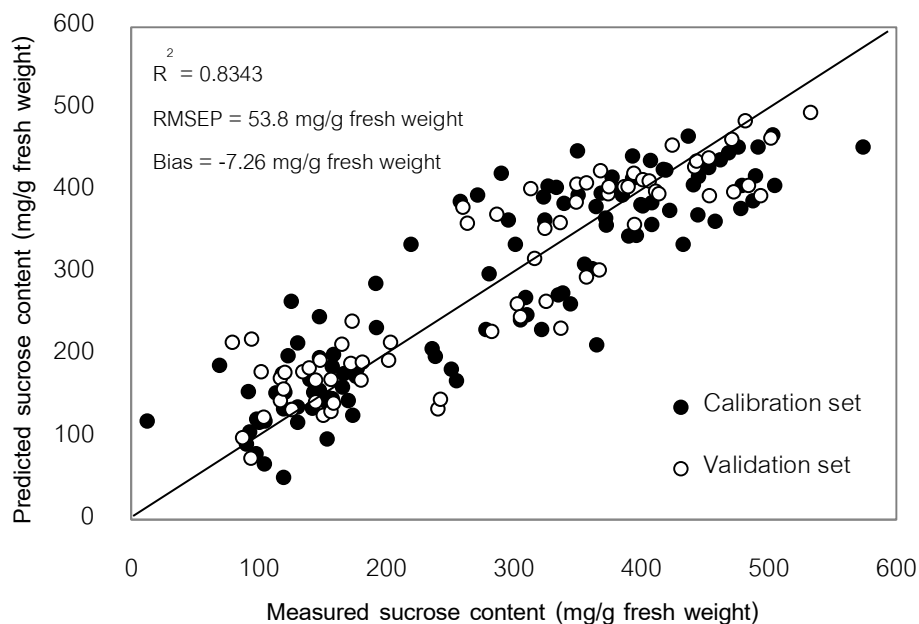


Figure 38 Scatter plot of sucrose of flesh from the model built from averaging spectra.

#### 4.2.4.2. Glucose

The calibration and validation results with the PLS models for glucose content of flesh in longan fruit samples are shown in Table 25. Measurement at average all positions and first derivative+MSC preprocessing technique by using 6 PLS factors in the range of 1332.3-1640.9 and 1833.5-2356.9 nm provided the highest prediction model for glucose content prediction with showed  $R^2$ , RMSEP, RPD and a bias of 0.5146, 17.3 mg/g fresh weight, 1.51 and -5.39 mg/g fresh weight, respectively. As mentioned by Williams (2007),  $R^2$  value of 0.50-0.64 can be used just for rough screening. Nevertheless, RPD from this model was 1.51 which indicates that the model can discriminate low from high values of the response variable but cannot use in research and quality assurance (Nicolai et al., 2007).

Low performance of prediction may be explained by histogram of glucose content in samples (Figure 37) which showed the narrowest and less uniform sugar distribution obtained in longan samples when compared to other sugars. This result also found in Rady and Guyer (2015) that used NIRS for evaluation of sugar content in

potatoes. The prediction result showed low R and RPD (0.73 and 1.44, respectively) because of narrow and less uniform glucose distribution in potato samples.

Figure 39 shows the relationship between measured glucose content value and predicted glucose content value from the best model. This plot clearly showed that the points scattered and almost being under the target line related to negative bias of the model.



**Table 25** Calibration and validation results for glucose content of flesh by NIRS.

Position	Pre processing	Wavelength (nm)	PLS factor	Calibration set (60%)		Validation set (40%)			RPD
				R <sup>2</sup>	RMSEC (mg/g fresh weight)	R <sup>2</sup>	RMSEP (mg/g fresh weight)	Bias (mg/g fresh weight)	
P1	First derivative+MSC (17pts.)	1063.4-2175.0	7	0.4035	24.1	0.4622	19.9	-3.57	1.39
P2	SNV	1063.4-1333.6 1638.8-2175.0	7	0.4408	23.3	0.5386	16.6	-1.07	1.48
P3	First derivative+SNV (17pts.)	1063.4-1640.9 1833.5-2356.9	4	0.4266	23.2	0.3294	23.2	1.18	1.18
P4	SNV	1063.4-1640.9 1833.5-2356.9	3	0.3255	25.1	0.2917	24.6	-4.51	1.21
P1P2P3P4	First derivative+MSC (17pts.)	1063.4-2356.9	9	0.4218	23.1	0.4962	19.7	-1.09	1.41
Average P	First derivative+MSC (17pts.)	1332.3-1640.9 1833.5-2356.9	6	0.5282	21.3	0.5146	17.3	-5.39	1.51

Abbreviations: R<sup>2</sup>: coefficients of determination, RMSEC: root mean square error of calibration, RMSEP: root mean square error of prediction, RPD: ratio of standard deviation of reference data in validation set to SEP, MSC: multiplicative scatter correction, SNV: standard normal variate, 17 pts: 17 smoothing points, P1: calyx, P2: bottom, P3 and P4: 2 side of cheek, P1P2P3P4: all positions and Average P: average all positions



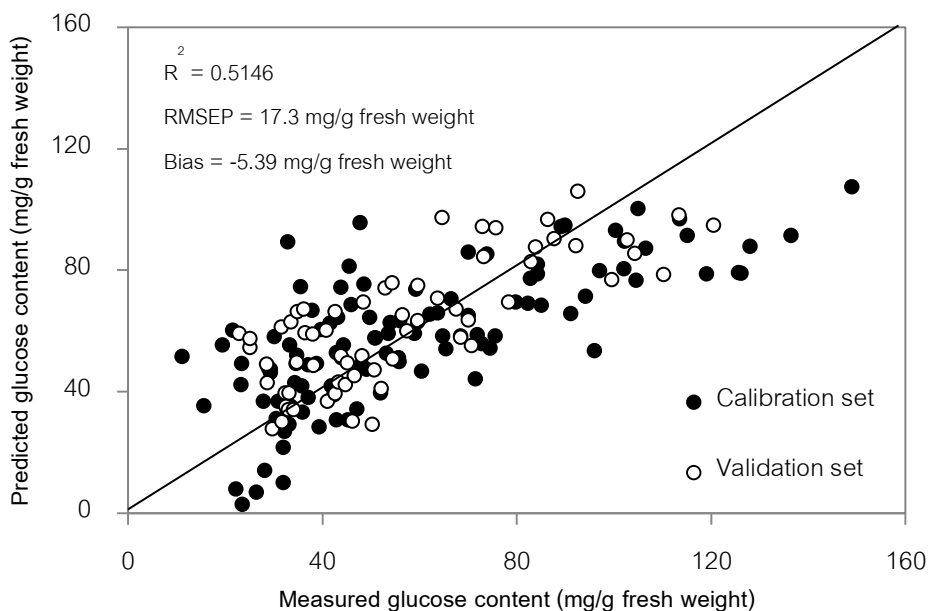


Figure 39 Scatter plot of glucose of flesh from the model built from averaging spectra.

#### 4.2.4.3. Fructose

The calibration and validation results with the PLS models for fructose content of flesh in longan fruit samples are shown in Table 26. The best prediction model for fructose was obtained by averaging spectra at all positions of measurement which was pretreated by combination of first derivative and MSC preprocessing techniques and using 7 PLS factors in the range of 1332.3-1640.9 and 1833.5-2175.0 nm.  $R^2$ , RMSEP, RPD and bias of this model were 0.8158, 13.9 mg/g fresh weight, 2.33 and -0.321 mg/g fresh weight, respectively. The  $R^2$  value of 0.82-0.90 implies that a model was usable with caution for most applications, including research (Williams, 2007) and the RPD of 2-2.5 demonstrates that coarse quantitative predictions are possible (Nicolai et al., 2007). The relationship between measured and prediction results of fructose content are illustrated in Figure 40.

In the case of intact apple fruit, NIRS model for predicting fructose content provided R value of 0.968 and RMSEP value of 0.298%. This result showed that NIRS can be used for sugar content analysis (Liu et al., 2006).

**Table 26** Calibration and validation results for fructose of flesh by NIRS.

Position	Pre processing	Wavelength (nm)	PLS factor	Calibration set (60%)		Validation set (40%)		RPD	
				R <sup>2</sup>	RMSEC (mg/g fresh weight)	R <sup>2</sup>	Bias (mg/g fresh weight)		
P1	Second derivative (17pts.)	2171.3-2356.9	2	0.5456	23.9	0.7140	17.5	1.62	1.88
P2	First derivative+MSC (17pts.)	1063.4-1640.9 1833.5-2356.9	8	0.7507	18.2	0.7696	16.3	0.824	2.09
P3	Second derivative (17pts.)	1332.3-1836.1	1	0.6007	22.0	0.6944	17.7	-1.12	1.88
P4	SNV	1063.4-1333.6 1638.8-1836.1 2171.3-2356.9	8	0.7280	19.0	0.7576	16.4	-3.5	2.08
P1P2P3P4	First derivative+MSC (17pts.)	1063.4-1640.9 1833.5-2356.9	8	0.7017	19.3	0.7411	16.6	-0.926	1.97
Average P	First derivative+MSC (17pts.)	1332.3-1640.9 1833.5-2175.0	7	0.7635	17.7	0.8158	13.9	-0.321	2.33

Abbreviations: R<sup>2</sup>: coefficients of determination, RMSEC: root mean square error of calibration, RMSEP: root mean square error of prediction, RPD: ratio of standard deviation of reference data in validation set to SEP, MSC: multiplicative scatter correction, SNV: standard normal variate, 17 pts: 17 smoothing points, P1: calyx, P2: bottom, P3 and P4: 2 side of cheek, P1P2P3P4: all positions and Average P: average all positions

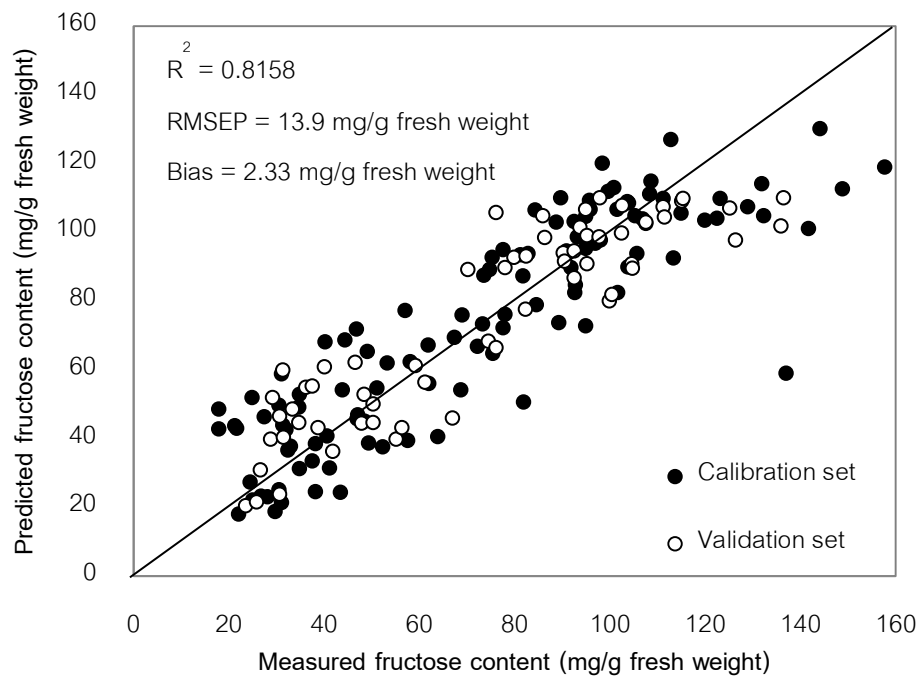


Figure 40 Scatter plot of fructose of flesh from the model built from averaging spectra.

#### 4.2.4.4. Total sugar

The calibration and validation results with the PLS models for total sugar content of flesh in longan fruit samples are shown in Table 27. The best model was achieved by averaging spectra at all positions of measurement which was pretreated by MSC preprocessing technique and using 7 PLS factors in the range of 1332.3-1471.4 nm and 1833.5-2064.2 nm.  $R^2$ , RMSEP, RPD and bias of this model were 0.9082, 51.9 mg/g fresh weight, 3.30 and -1.05 mg/g fresh weight, respectively. According to Williams (2007), An  $R^2$  of 0.83-0.90 indicates that a model was usable with caution for most applications, including research. And RPD of 2.5-3 indicated that the model has excellent prediction accuracy (Nicolai et al., 2007). The scatter plot of measured and prediction result of total sugar is shown in Figure 41.

**Table 27** Calibration and validation results for total sugar of flesh by NIRS.

Position	Pre processing	Wavelength (nm)	PLS factor	Calibration set (60%)		Validation set (40%)			RPD
				R <sup>2</sup>	RMSEC (mg/g fresh weight)	R <sup>2</sup>	RMSEP (mg/g fresh weight)	Bias (mg/g fresh weight)	
P1	SNV	1063.4-1836.1	5	0.8180	75.5	0.8400	68.1	6.51	2.51
P2	MSC	1063.4-1333.6 1638.8-2175.0	8	0.8046	79.4	0.8099	74.2	-5.12	2.30
P3	SNV	1638.8-2175.0	2	0.7757	82.7	0.8358	68.4	-2.02	2.47
P4	SNV	1332.3-2356.9	7	0.8315	73.4	0.8721	60.9	5.85	2.81
P1P2P3P4	First derivative+SNV (17pts.)	1063.4-1836.1 2171.3-2356.9	8	0.8202	73.5	0.8503	66.0	2.39	2.59
Average P	MSC	1332.3-1471.4 1833.5-2064.2	7	0.8590	67.1	0.9082	51.9	-1.05	3.30

Abbreviations: R<sup>2</sup>: coefficients of determination, RMSEC: root mean square error of calibration, RMSEP: root mean square error of prediction, RPD: ratio of standard deviation of reference data in validation set to SEP, MSC: multiplicative scatter correction, SNV: standard normal variate, 17 pts: 17 smoothing points, P1: calyx, P2: bottom, P3 and P4: 2 side of cheek, P1P2P3P4: all positions and Average P: average all position

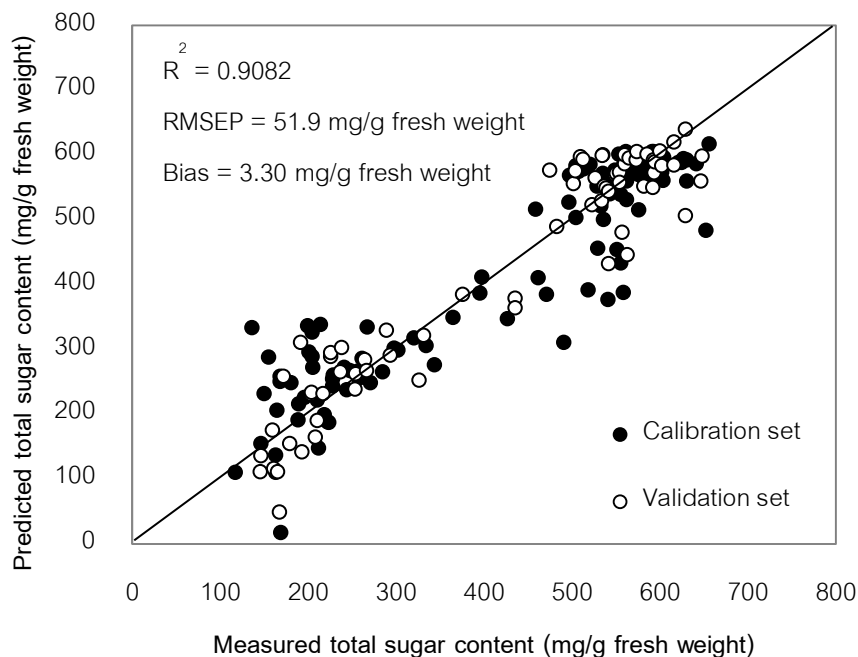
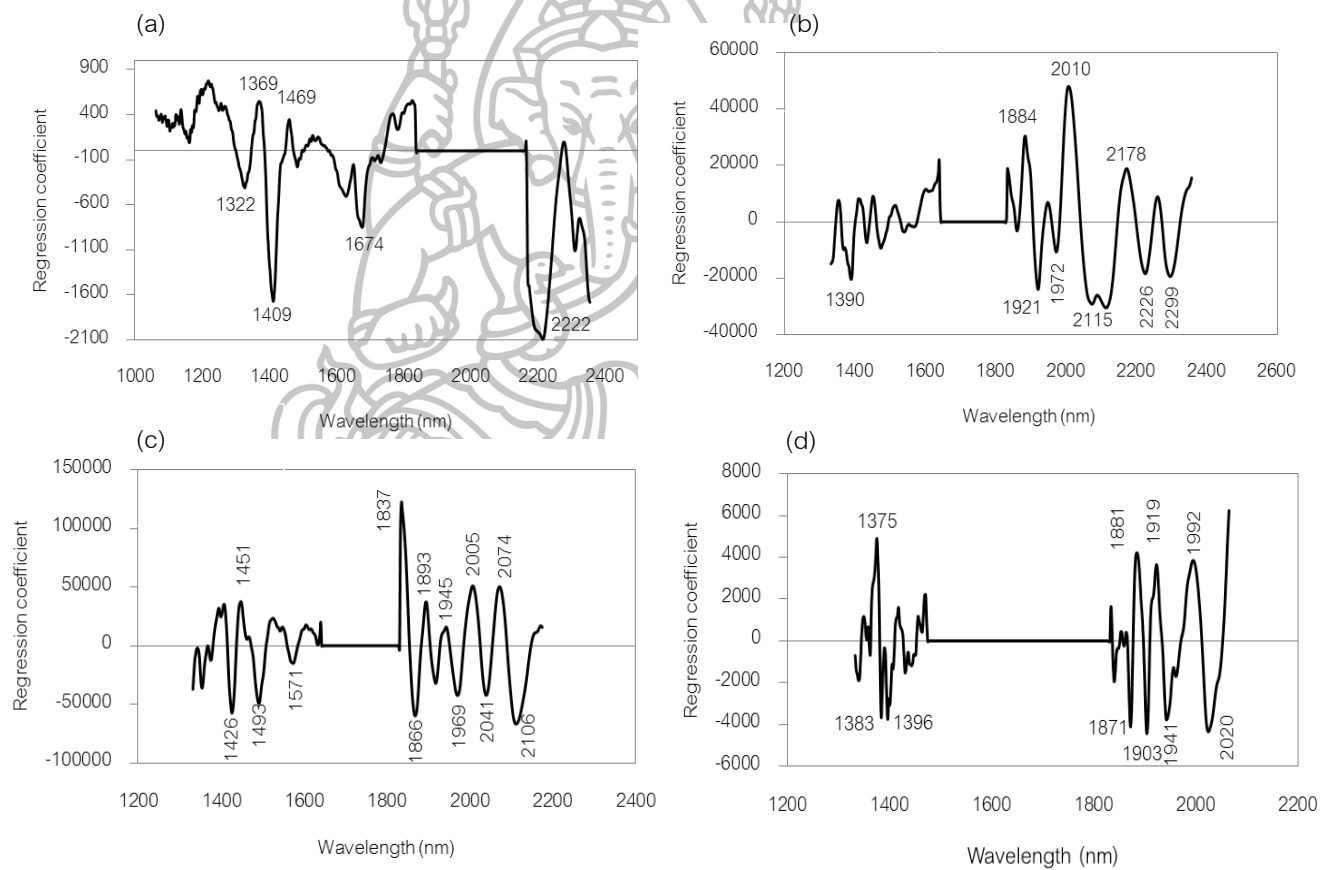


Figure 41 Scatter plot of total sugar of flesh from the model built from averaging spectra.

Figure 42 (a) shows the regression coefficient plot of the best fit of sucrose content model. These wavelengths (1369 nm and 1409 nm) own to  $-H$  and  $-OH$  of carbohydrates (Rungpichayapichet et al., 2016). Figure 42 (b) shows the regression coefficient plot of the best fit of glucose content model. There were high peaks at 1921 nm, 2178 nm and 2294 nm owing to the second overtone of CONH group in amide, combination of protein and combination of amino acid, respectively. Figure 42 (c) show the regression coefficient plot of the best fit of fructose content model. The peaks at 1426, 1451, 1893, 2005 and 2074 nm related to  $-OH$  functional groups of carbohydrates such as sugar and starch (Osborne et al., 1993; Magwaza et al., 2012; Rungpichayapichet et al., 2016). And Figure 42 (d) shows the regression coefficient plot of total sugar. There were high peak at 1396 nm and 1919 nm which represented first overtone of  $CH_2$  and second overtone of  $CO_2H$ , respectively. Moreover, there were high peak at 1903, 1941 and 1992 nm which related to carbohydrates (starches and

sugars), water and organic acids (Osborne et al., 1993; Rungpichayapichet et al., 2016).

The regression coefficient plots of sucrose, fructose and total sugar also found the wavelengths which corresponded to sugar indicated sugar had an important influence on the prediction of sucrose, fructose and total sugar content of longan. However, the wavelengths which related to sugar were not found in the regression plot of glucose affected to poor prediction of glucose model.



**Figure 42** Regression coefficient plot of PLS models validated for sugar content of flesh of the longan fruits: (a) sucrose; (b) glucose; (c) fructose and (d) total sugars.

The models that had RPD value more than 2.0 were tested for verifying the accuracy by bias checking, SEP checking and slope checking method. Table 28 represents that sucrose, fructose and total sugars model passed the verification.

**Table 28** Verifying the accuracy by bias checking, SEP checking and slope checking method for sugar content models.

Model	Bias checking	SEP checking	Slope checking
NIRS sucrose in flesh	✓	✓	✓
NIRS fructose in flesh	✓	✓	✓
NIRS total sugar in flesh	✓	✓	✓



### 4.3 Hyperspectral imaging for determination of moisture content and sugar content in dried whole longan

#### 4.3.1 HSI images and reflectance spectra of fresh and dried whole longans

HSI images acquisition and extracted spectra were obtained from fresh and dried whole longan at 60°C for 40 hours which were are shown in Figure 43. 10 points selected from R program were averaged and represent the spectrum of the fruit. These spectra of fresh and dried whole longan can observe that the spectrum of dried had higher %relative reflectance that the spectrum of fresh. The original HSI spectra of fresh and dried whole longan at different temperatures for 40 hours are shown in Figure 44. From this Figure, there were 2 absorption peaks around 690 and 780 nm related to the presence of chlorophyll pigment (Rajkumar et al., 2012) and O-H third stretching overtone was assigned to moisture content (Wu et al., 2012).

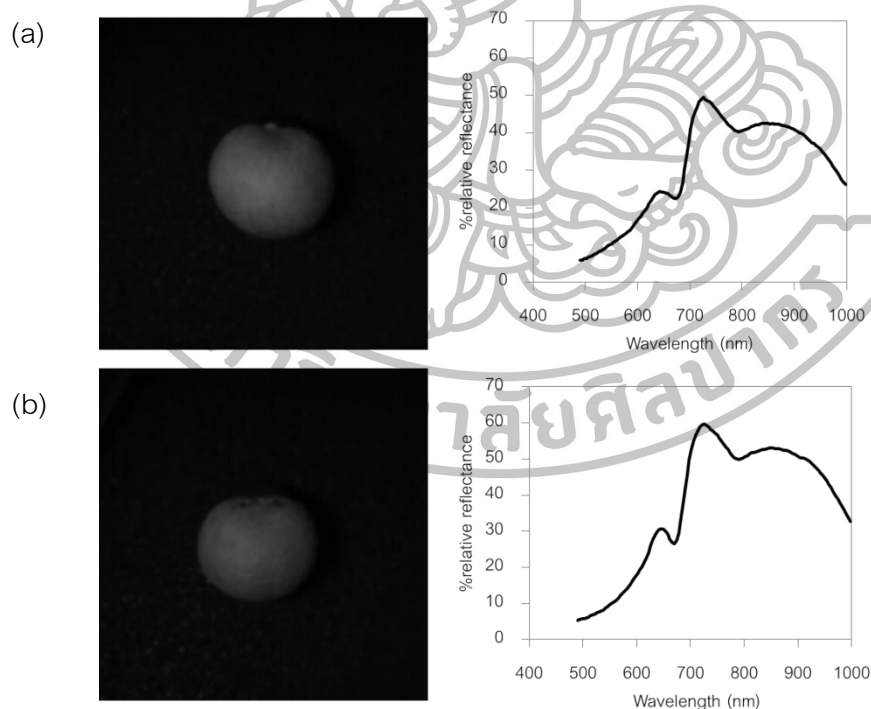


**Figure 43** Example of HSI image and reflectance spectrum of whole longan (a) fresh and (b) dried at 60°C for 40 hours.



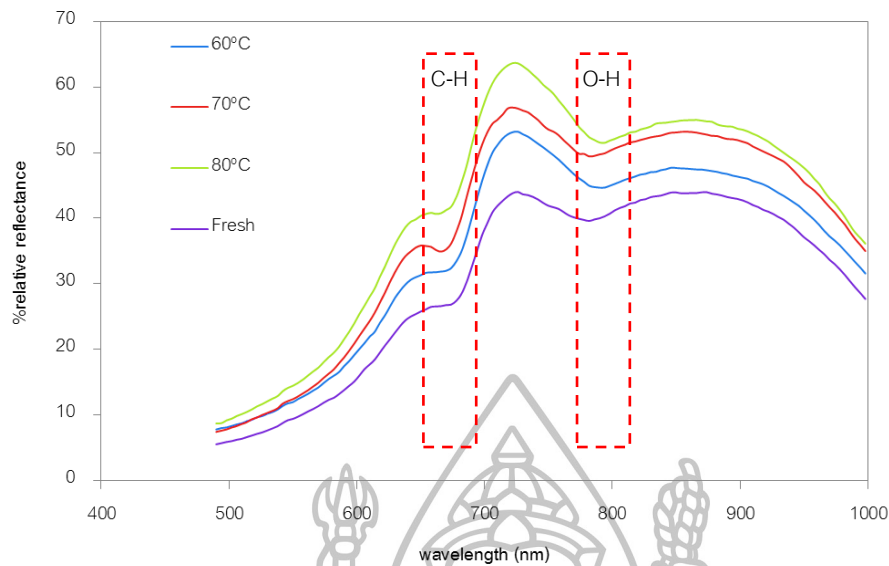


**Figure 44** Example of original spectra of fresh and dried whole longan dried at different temperatures for 40 hour.

However, the broad band and overlap peak of HSI spectra were observed. And same as the NIR spectra, they need preprocessing techniques to remove these problems such as second derivative which performs resolves peak overlapping and removing baseline shifts (Nicolai et al., 2007). Second derivative HSI spectrum of dried whole longan obtained from drying at 60°C for 40 hours is shown in Figure 45. There was a strong absorption peak at around 690 nm which was associated with the presence of chlorophyll (Rajkumar et al., 2012). Moreover, absorption bands at around 780 nm and 980 nm were the results from the absorption behavior of sugar and water corresponding to its stretching third and second overtone, respectively (Osborne et al., 1993).

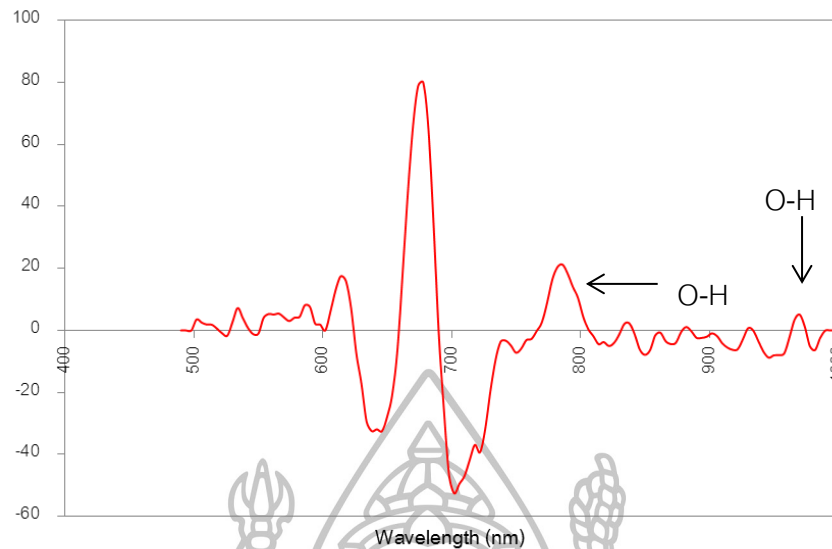


**Figure 45** Example of second derivative HSI spectrum of dried whole longan obtained from drying at 60°C for 40 hours.

#### 4.3.2 Calibration models for moisture content by HSI

A total of 496 spectra were divided into calibration set (52.5% of all samples) and validation set (47.5% of all samples) for building the models. Mean, standard deviation (SD), minimum and maximum of moisture content (%) of longan fruit samples from different fruit parts and the whole fruit showed in Table 29. The results were similar as the statistics of NIRS prediction which had the range of peel between 3.35-51.74%, the range of flesh part was between 9.99-88.62%, the range of seed part was between 7.61-49.90%, the range of whole was between 8.15-73.36% and the range of flesh and seed was between 7.27-71.26%. Same as NIRS, the result showed that the flesh part had the widest range of moisture content.

**Table 29** Mean, standard deviation (SD), minimum and maximum of moisture content (%) for longan fruit samples from different fruit parts and the whole fruit (HSI).

Fruit part	N	Calibration set (52.5%)				N	Validation set (47.5%)			
		Min	Max	Mean	SD		Min	Max	Mean	SD
Peel	261	3.35	51.74	15.75	9.73	235	3.72	45.76	15.45	9.05
Flesh	261	9.99	88.62	44.65	25.47	235	11.04	83.07	44.44	25.17
Seed	261	7.61	49.90	26.45	11.66	235	7.98	46.98	26.33	11.41
Flesh+seed	261	7.27	71.26	34.74	21.23	235	7.92	70.12	34.53	20.98
Whole fruit	261	8.15	73.36	36.99	21.97	235	8.77	72.93	36.79	21.72

N = number of samples

The calibration and validation results associated with the PLS models for moisture content by HSI are shown in Table 39-43 (Appendix F). As a result of one position of imaging, the results were compared the preprocessing method such as smoothing, normalize, MSC, first derivative, second derivative, SNV and combined methods to find the optimum model. Table 30 shows the best models for moisture content from different fruit parts and the whole fruit.

For moisture content of peel, the result found that the optimum model was from raw spectra by using 10 PLS factors. This model showed  $R^2$ , RMSEP, RPD and a bias of 0.6396, 5.43%, 1.69 and 1.01%, respectively. For flesh part, the result showed that the optimum models generated from smoothing (7) method by using 10 PLS factors. This model showed  $R^2$ , RMSEP, RPD and a bias of 0.7071, 13.60%, 1.85 and -0.19%, respectively. For seed part, the result showed that the optimum models generated from MSC+ first derivative method by using 10 PLS factors. This model showed  $R^2$ , RMSEP, RPD and a bias of 0.6663, 6.58%, 1.74 and -0.76%, respectively. For flesh and seed, the result showed that the optimum models generated from second derivative (5) method by using 10 PLS factors. This model showed  $R^2$ , RMSEP, RPD and a bias of 0.7175, 11.1%, 1.88 and 0.61%, respectively. The optimum models for moisture content

of whole fruit generated from smoothing (7) method by using 14 PLS factors. This model showed  $R^2$ , RMSEP, RPD and a bias of 0.7458, 10.93%, 1.98 and 0.31%, respectively.

Obviously, the model of peel and seed showed the lowest performance when compared with other parts. It could be expected that the chemical data of these 2 parts had narrower range than the others. Moreover, low performance of seed model might be due to the presence of seed of longan which is deepest part and the characteristic of seed that has glossy seed coat. As the result of these problems, the light can reflect and make an error in HSI measurement.

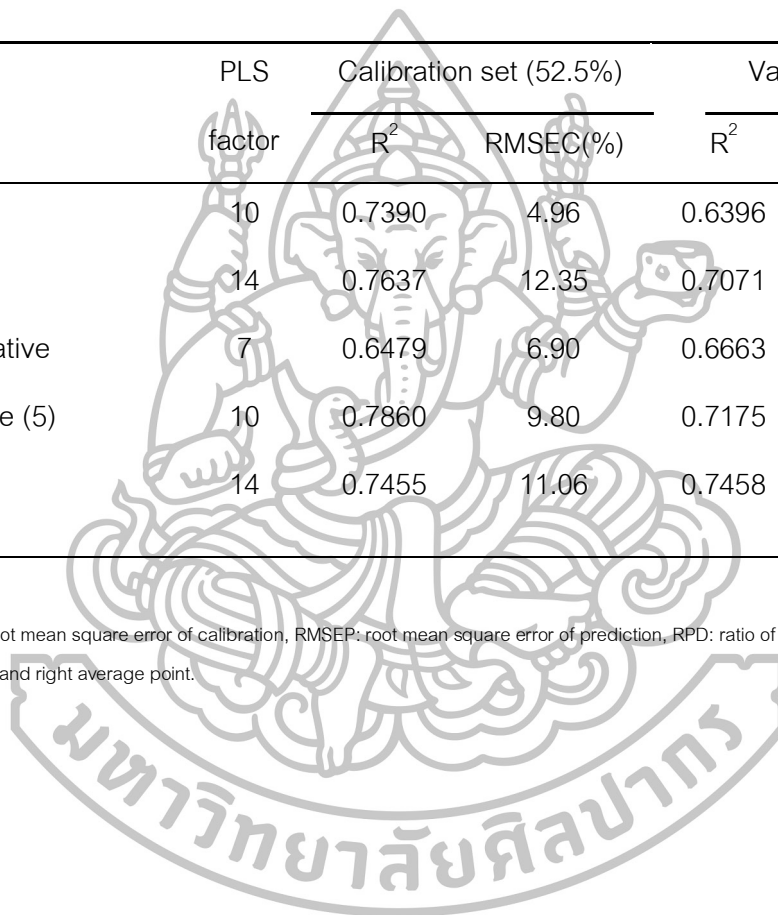
Williams (2007) had indicated that  $R^2$  of 0.50-0.64 implies that a model usable for rough screening and  $R^2$  of 0.66-0.81 implies that a model usable for screening and some other approximate calibrations. For RPD evaluation of these moisture content models, all models had RPD between 1.5 and 2 indicates that the model can discriminate low from high values of the response variable (Nicolai et al., 2007). In case of vegetable soybean (Huang et al., 2014), HSI (400-1000 nm) was applied for prediction of moisture content during drying. The moisture content was in the range of 4.9-67.7% that has narrower range than longan in this study. However, the results showed high R and RPD of 0.971 and 4.3, respectively while low RMSEP (4.7%) was found.

Comparing to NIRS result, the results from HSI were not as good as the result from NIRS technique. The poorer correlation might be due to the difference of the range of wavelength which relate to the difference of the presence of absorption peaks and the conditions of hyperspectral imaging system which might not suitable with small and round shape of sample such as longan. Each point of their surface can reflect the light from light source differently that affect to dark area in the HSI image. Furthermore, the dark image (Figure 41) from HSI technique affect to the uncorrected spectra which relate to poorer correlation when built the models between measured and predicted value (Go´mez-Sanchis et al., 2008).

**Table 30** Calibration and validation results for moisture content from different fruit parts and the whole longan fruit samples by HSI.

Fruit part	Pre processing	PLS factor	Calibration set (52.5%)		Validation set (47.5%)			RPD
			R <sup>2</sup>	RMSEC(%)	R <sup>2</sup>	RMSEP(%)	Bias(%)	
Peel	Raw	10	0.7390	4.96	0.6396	5.43	1.01	1.69
Flesh	Smoothing (7)	14	0.7637	12.35	0.7071	13.60	-0.19	1.85
Seed	MSC+ first derivative	7	0.6479	6.90	0.6663	6.58	-0.76	1.74
Flesh and seed	Second derivative (5)	10	0.7860	9.80	0.7175	11.13	0.61	1.88
Whole fruit	Smoothing (7)	14	0.7455	11.06	0.7458	10.93	0.31	1.98

Abbreviations: R<sup>2</sup>: coefficients of determination, RMSEC: root mean square error of calibration, RMSEP: root mean square error of prediction, RPD: ratio of standard deviation of reference data in validation set to SEP, MSC: multiplicative scatter correction, (5,7): number of left and right average point.



The scatter plots demonstrating the measured value of moisture content (X) and the prediction value (Y) for the peel model, flesh model, seed model, flesh and seed model and the whole fruit model are shown in Figure 46-50. However, the points rather dispersed from the target line that showed low performance of prediction.

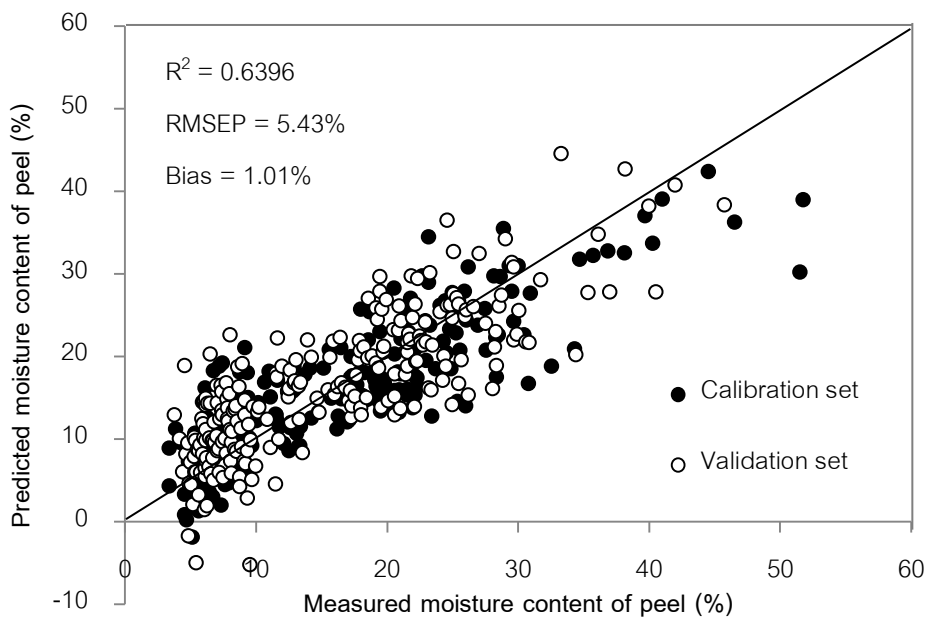


Figure 46 Scatter plot of moisture content of peel by HSI.



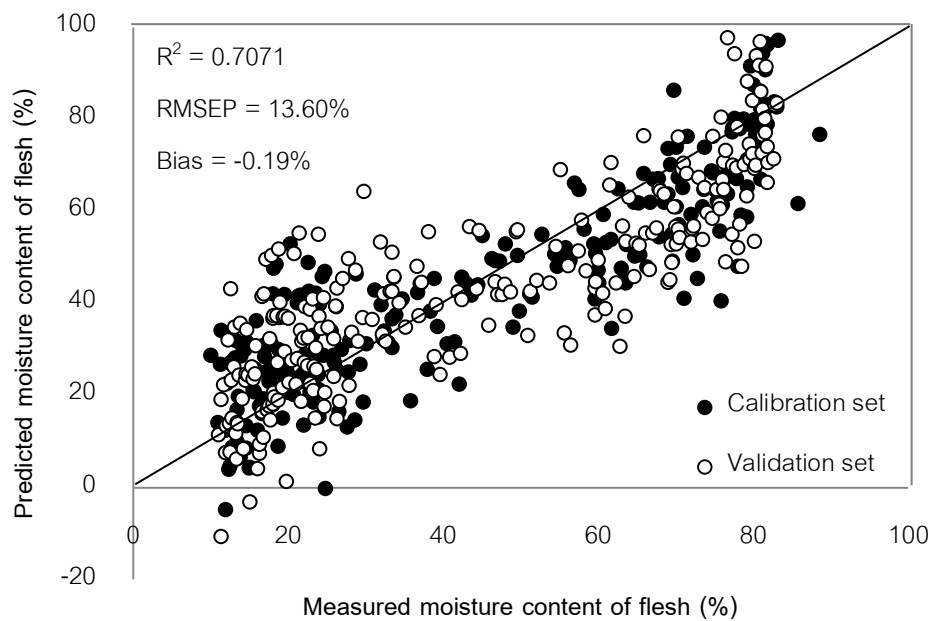


Figure 47 Scatter plot of moisture content of flesh by HSI.

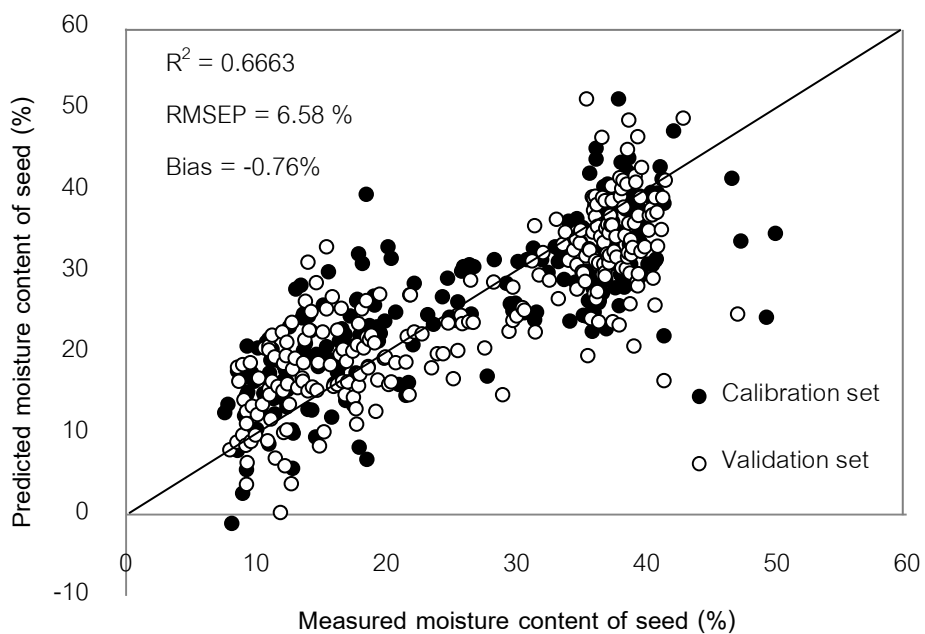


Figure 48 Scatter plot of moisture content of seed by HSI.

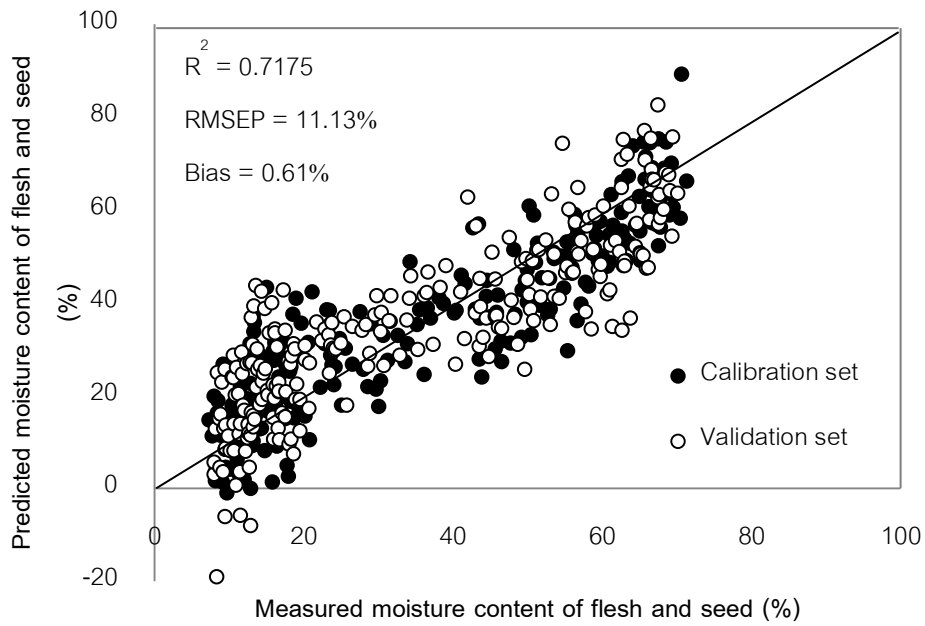


Figure 49 Scatter plot of moisture content of flesh and seed by HSI.

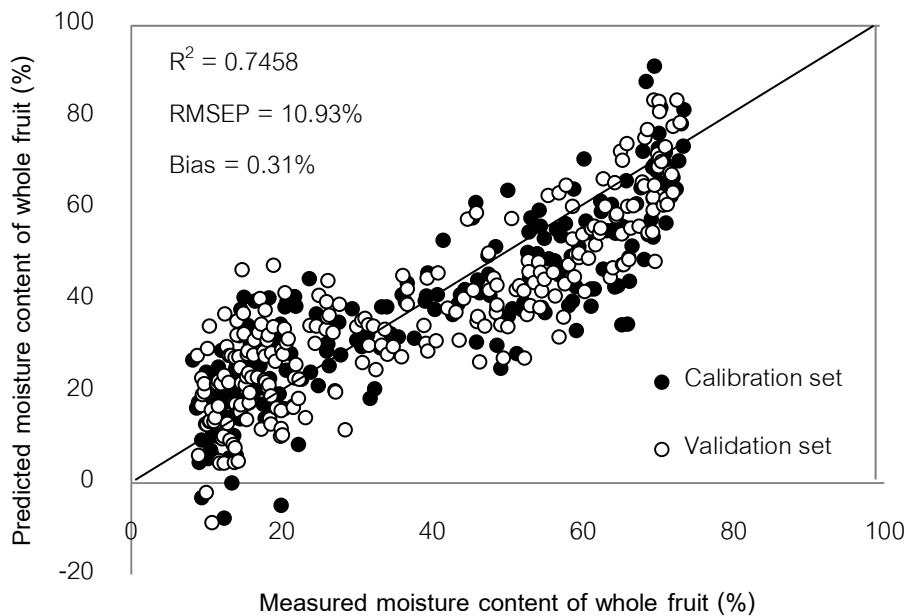
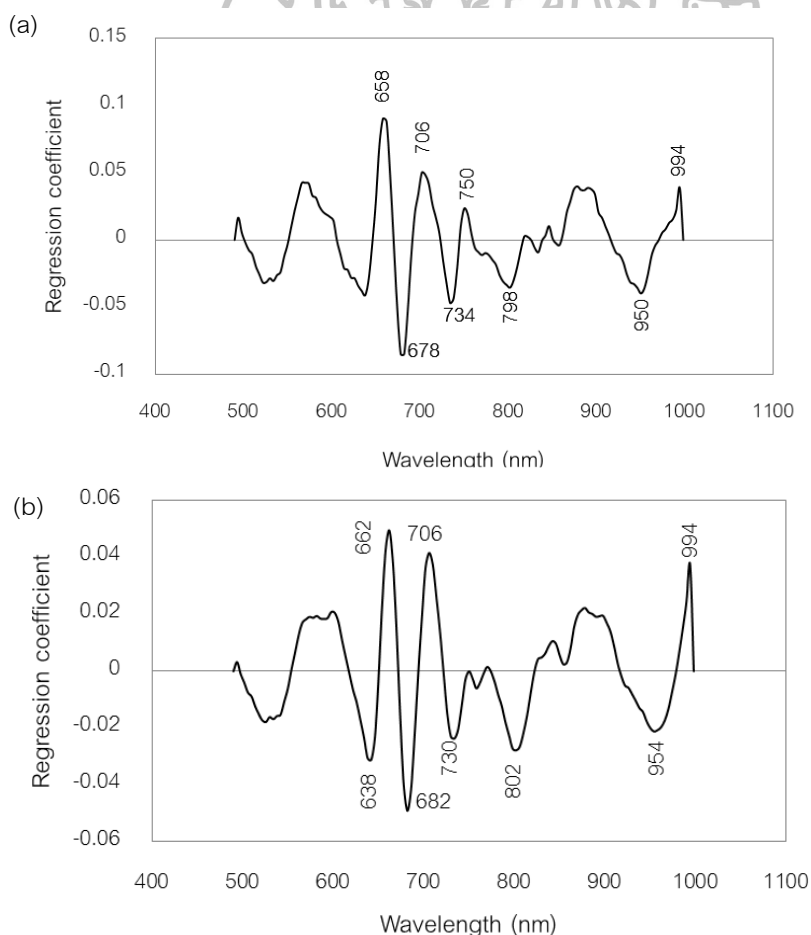


Figure 50 Scatter plot of moisture content of whole fruit by HSI.



Figure 51 (a) shows the regression coefficient plot of moisture content of flesh. There were high peaks at 658, 678, 706, 734, 750, 798, 950 and 994 nm. Wavelengths at 678 nm could be associated with chlorophyll pigment (Rajkumar et al., 2012) and 734 and 750 nm could be associated with the O-H stretching third overtone vibration in ROH and ArOH and the wavelength at 994 nm could be associated with O-H stretching second overtone vibration of starch (Osborne, 1993). Figure 51 (b) shows the regression coefficient plot of moisture content of the whole fruit. The wavelengths at 682, 802 and 994 nm could be associated with the vibration of chlorophyll pigment, amino group and starch, respectively. However, the wavelengths which associated with water (760 and 970 nm) were not found in both regression coefficient plots.



**Figure 51** Regression coefficient plots of (a) moisture content of flesh and (b) moisture content of the whole fruit by HSI.

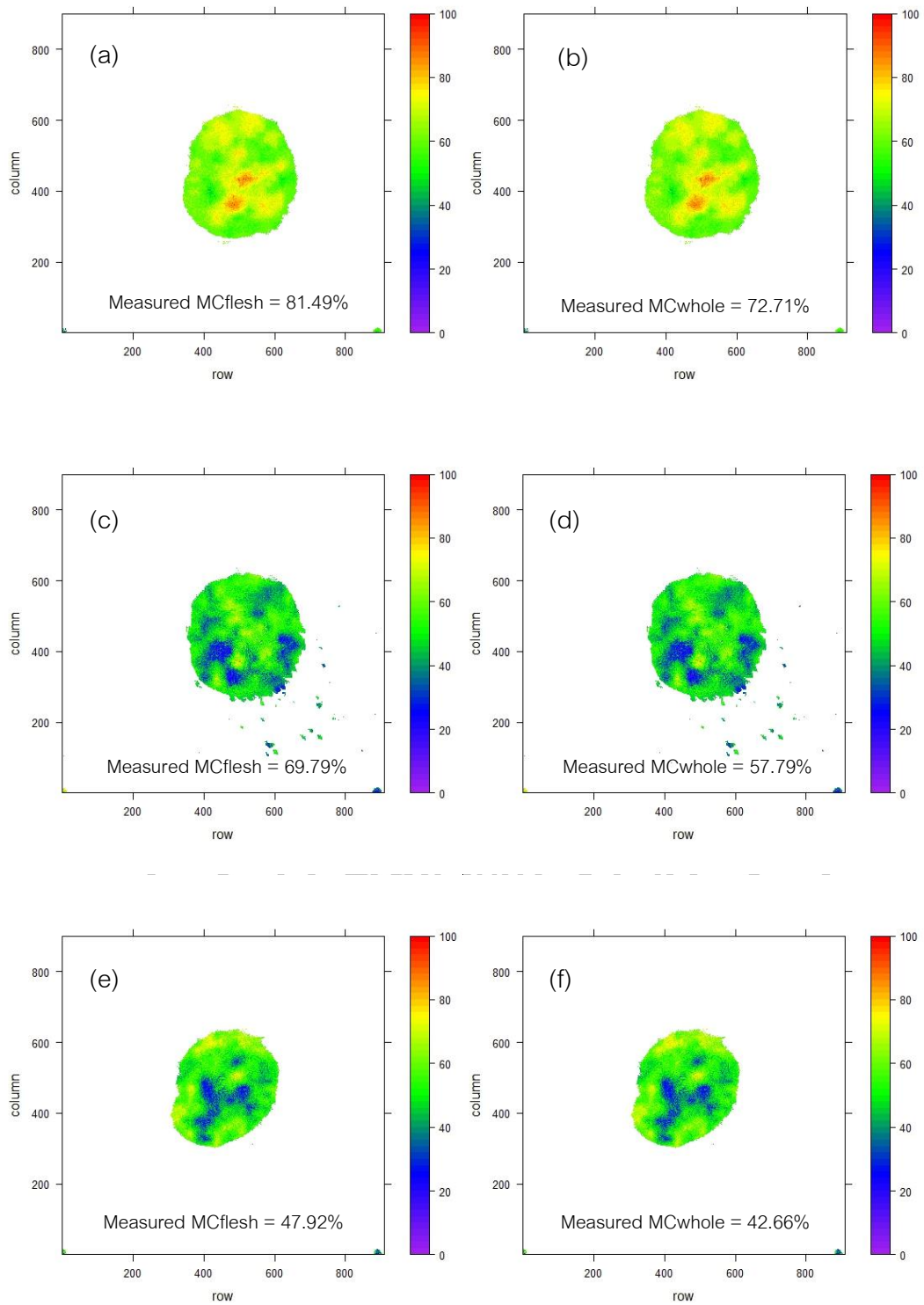
Due to HSI technique can collect the spectra in term of areas. Thus, this technique can provide the chemical properties distribution in fruit. With regard to the distribution of water in dried whole longan is absolutely important determining the quality of dried whole longan products. Beuchat (1981) said that water activity is an important factor for inducing the growth of microorganism especially, pathogenic bacteria in food. Furthermore, high moisture content would influence the high water activity that affected the microorganism growth. Thus, water content affects the quality and shelf life of dried whole longan and the determination of moisture content distribution in dried whole longan by HSI technique is very useful.

In this research, the observed maps was generated based on the PLS models of moisture content of flesh and the whole fruits which build from R program to exhibit the distribution of moisture content within flesh and the whole fruits. The pixels that had homologous spectral characteristics in the distribution map produced the same predicted values of moisture, which were observed in a same color in the acquired image. Figure 52 shows the example of distribution maps of the whole longan fruits with different moisture content of flesh and the whole fruit levels. The changes in moisture content were defined with a linear colour scale which was used to present different moisture concentrations in different area of the whole fruit with different colors (purple, blue, green, yellow and red). Figure 52 (a) and (b) show the fresh whole longan which was opened from the PLS models of moisture content of flesh and the whole fruits, (c) and (d) are dried whole longan at 60°C for 12 hr, (e) and (f) are dried whole longan at 60°C for 30 hr; (g) and (h) are dried whole longan at 60°C for 36 hr. and (i) and (j) are dried whole longan at 60°C for 60 hr.

The color in maps explained the distribution of moisture in the whole longan fruit which could not be distinguished by normal color image. The variation of moisture content in fresh longan is subject to longan species, farming condition, natural variations due to climatic and seasonal factors, harvesting time and storage condition. Whereas, the variation of moisture content in dried whole longan might be depend on the drying condition. The fresh fruit showed a more uniform yellow and red, indicating that their

moisture content of flesh and whole fruit were relatively high (Figure 52 (a) and (b)). While, the dried fruits which contained lower moisture content had the color tended to blue (Figure 52 (c) - (j)). However, the poor correlation from the models gave some errors of prediction in the distribution maps. As can be seen in the figures, the image from PLS models of moisture content of flesh and the whole fruit of each fruit had similar the variation of color while the sample had different moisture content between flesh and the whole fruit. Moreover, the uncorrected colors on distribution map are observed at the low moisture content (Figure 52 (i) and (j))





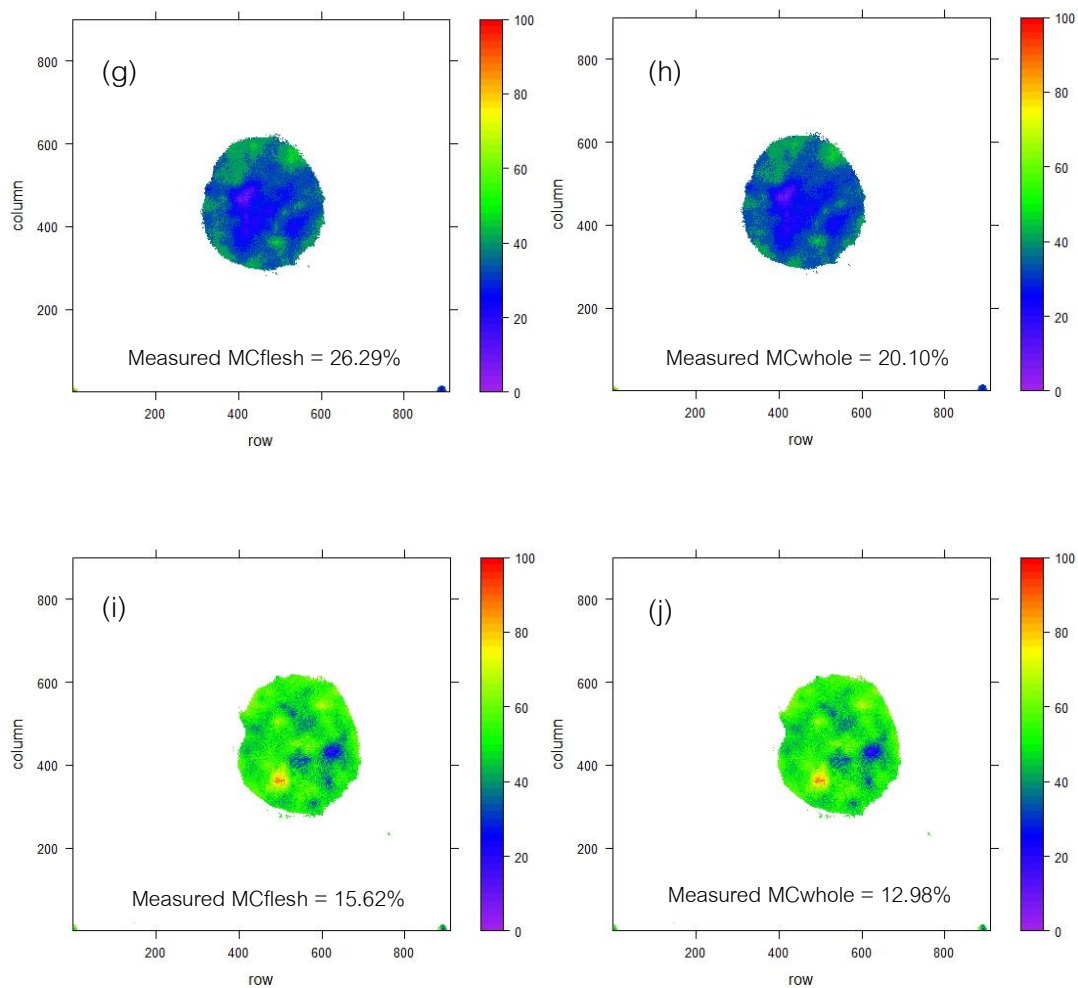


**Figure 52** The example of moisture content distribution maps of whole longan generated by PLS model of moisture content for flesh and the whole fruit (a) and (b) fresh whole longan; (c) and (d) dried whole longan at 60°C for 12 hr; (e) and (f) dried whole longan at 60°C for 30 hr; (g) and (h) dried whole longan at 60°C for 36 hr and (i) and (j) dried whole longan at 60°C for 60 hr.

### 4.3.3 Calibration models for TSS of flesh by HSI

A total of 186 spectra were divided into calibration set (52.5% of all samples) and validation set (47.5% of all samples) for building the models. Mean, standard deviation (SD), minimum and maximum of TSS of flesh are showed in Table 31. The range of TSS between 13-98 °Brix was found same as the statistic of NIRS.

**Table 31** Mean, standard deviation (SD), minimum and maximum of TSS of flesh in longan fruit samples for predicting TSS (HSI).

Parameter	Data set	N	Min	Max	Mean	SD
TSS (°Brix)	Calibration (52.7%)	98	13	98	56.72	24.15
	Validation (47.5%)	88	18	90	56.75	23.30

N = number of samples

The calibration and validation results associated with the PLS models for TSS by HSI are shown in Table 44 (Appendix F). Table 32 shows the best models for moisture content from different fruit parts and the whole fruit. The best model was obtained from MSC+ smoothing preprocessing techniques by using 11 PLS factors. The results showed  $R^2$ , RMSEP, RPD and a bias of 0.6676, 13.36 °Brix, 1.78 and 3.05 °Brix. According to Williams (2007),  $R^2$  of 0.66-0.81 indicates that a model usable for screening and some other approximate calibrations. About RPD of this model, the value was found between 1.5 and 2 indicates that the model can discriminate low from high values of the response variable (Nicolai et al., 2007).

Moreover, there was using HSI (500-1000 nm) for predicting TSS in blueberries (Leiva-Valenzuela et al., 2013) which had fairly a similar shape to longan. Lower correlations ( $R_p = 0.69-0.79$ ) and RPD (1.3-1.6) were found, compared with that reported for large fruits such as apple (Lu, 2004).

**Table 32** Calibration and validation results for TSS in flesh of longan fruit samples by HSI

Pre processing	PLS factor	Calibration set (52.5%)		Validation set (47.5%)			RPD
		R <sup>2</sup>	RMSEC (°Brix)	R <sup>2</sup>	RMSEP (°Brix)	Bias (°Brix)	
MSC+ smoothing	11	0.7729	11.45	0.6676	13.36	3.05	1.78

Abbreviations: R<sup>2</sup>: coefficients of determination, RMSEC: root mean square error of calibration, RMSEP: root mean square error of prediction, RPD: ratio of standard deviation of reference data in validation set to SEP, MSC: multiplicative scatter correction

Figure 53 showed the relationship between measured and predicted TSS from the best calibration model. It can be seen that the points dispersed from the target line that showed low performance of prediction.

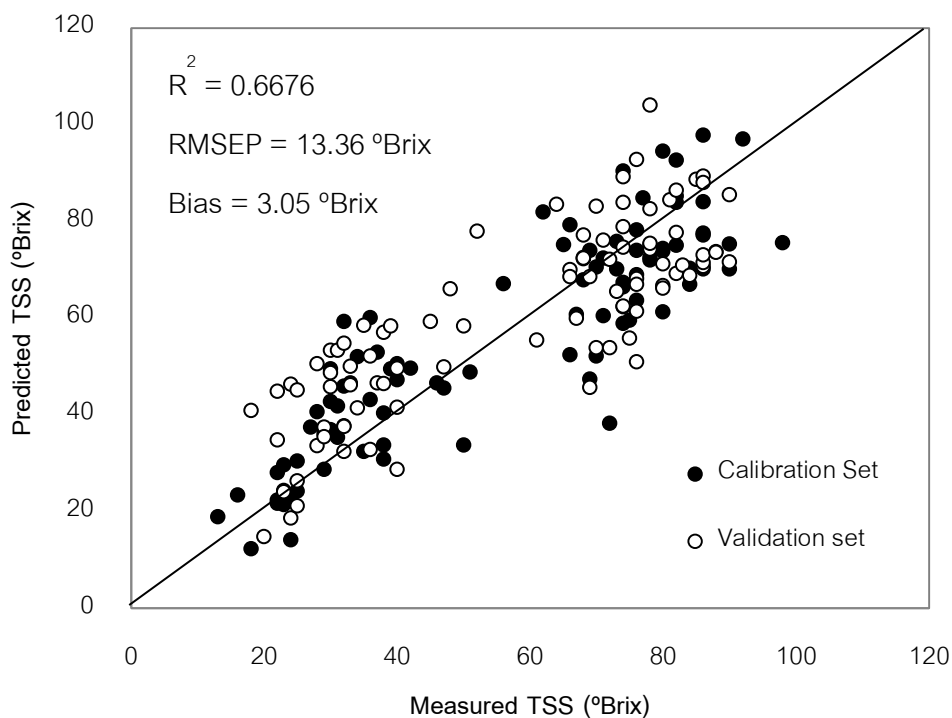


**Figure 53** Scatter plot of TSS of flesh by HSI

Figure 54 shows the regression coefficient plot of the best TSS model. There were high peaks at 538, 586, 614, 638, 658, 678, 708, 722, 746 and 770 nm. Wavelengths at 678 nm could be associated with chlorophyll pigment (Rajkumar et al., 2012) and Wavelengths at 746 nm could be associated with the C-H stretching fourth overtone vibration in  $\text{CH}_2$  (Osborne, 1993).

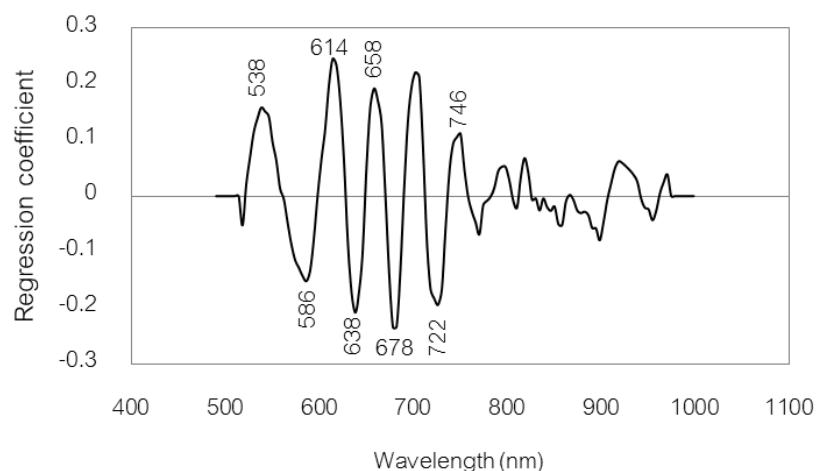


Figure 54 Regression coefficient plots of TSS of flesh by HSI.

#### 4.3.4 Calibration models for sugar content of flesh by HSI

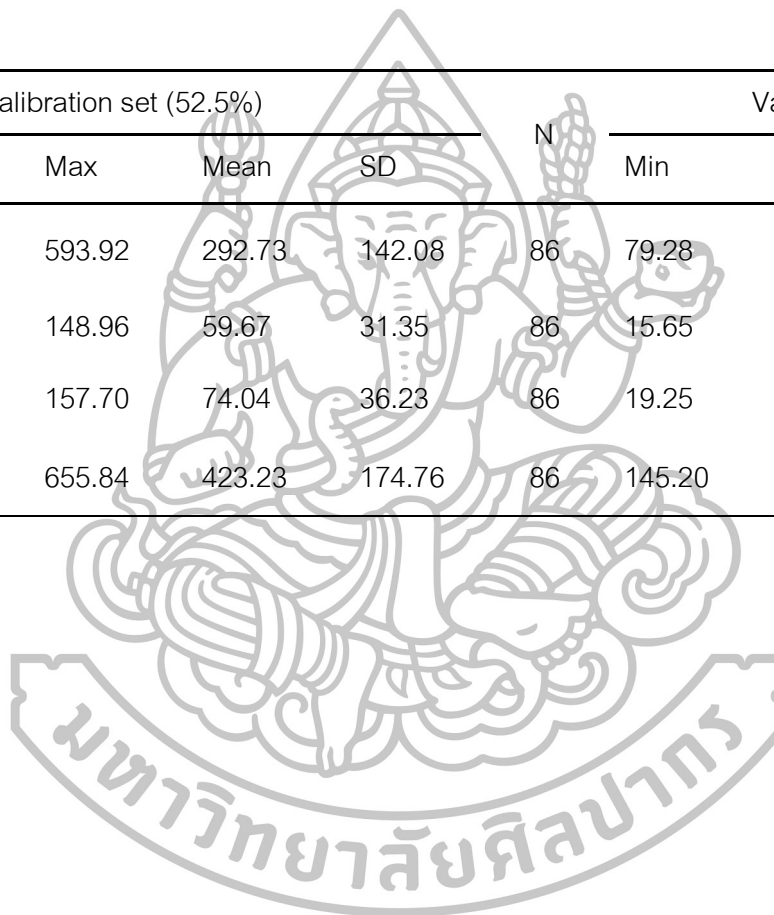
The statistics of HSI prediction for sugar content are shown in Table 33. The results were similar as the statistics of NIRS prediction which had the range of sucrose content between 12.47-593.92 mg/g fresh weight, the range of glucose content between 11.05-148.96 mg/g fresh weight, the range of fructose content between 17.84-157.70 mg/g fresh weight and the range of total sugar content between 116.94-655.84 mg/g fresh weight. Same as NIRS, the result showed that glucose had the lowest value and narrowest range.



**Table 33** Mean, standard deviation (SD), minimum and maximum of sugar content for longan fruit samples (HSI).

Sugar (mg/g fresh weight )	N	Calibration set (52.5%)				N	Validation set (47.5%)			
		Min	Max	Mean	SD		Min	Max	Mean	SD
Sucrose	95	12.47	593.92	292.73	142.08	86	79.28	532.84	289.00	132.60
Glucose	95	11.05	148.96	59.67	31.35	86	15.65	130.06	57.43	28.23
Fructose	95	17.84	157.70	74.04	36.23	86	19.25	144.46	72.67	33.72
Total sugars	95	116.94	655.84	423.23	174.76	86	145.20	646.68	421.83	169.93

N = number of samples



The calibration and validation results associated with the PLS models for sugar content by HSI are shown in Table 45-48 (Appendix F). Table 34 shows the best models for sugar content of flesh. For sucrose, the result found that the optimum model was organized from MSC+ smoothing preprocessing techniques by using 10 PLS factors. This model showed  $R^2$ , RMSEP, RPD and a bias of 0.5247, 5.43 mg/g fresh weight, 1.69 and 1.01 mg/g fresh weight, respectively. For glucose, the optimum model was conducted from SNV+ second derivative preprocessing techniques by using 3 PLS factors.  $R^2$ , RMSEP, RPD and bias of this model were 0.2699, 24.03 mg/g fresh weight, 1.17 and -2.25 mg/g fresh weight, respectively. For fructose, first derivative (4) was given the optimum model by using 6 PLS factors. This model shows  $R^2$ , RMSEP, RPD and a bias of 0.4944, 23.86 mg/g fresh weight, 1.41 and 2.54 mg/g fresh weight. And for total sugar, the optimum model was organized from MSC+smoothing preprocessing techniques by using 7 PLS factors. This model shows  $R^2$ , RMSEP, RPD and a bias of 0.5333, 115.42 mg/g fresh weight, 1.47 and 12.98 mg/g fresh weight.

It is worth noting that prediction model of sucrose and total sugar had  $R^2$  of 0.26-0.49 implies that the models have poor correlation. While prediction model of glucose and fructose had  $R^2$  of 0.50-0.64 implies that the models are OK for rough screening (Williams, 2007). However, the RPD values of all models were found less than 1.5 that means the models are poor and not recommended for research and most applications (Nicolai et al., 2007).

In the case of potatoes (Rady et al., 2014), HSI (400-1000 nm) was used for predicting glucose and sucrose content. Poor correlation models were found with low R of 0.38 and 0.14, and low RPD of 0.93 and 1.02 for glucose and sucrose, respectively.

Same as sugar content results by NIRS, the glucose content model gave the lowest accuracy predicted. One reason might be due to low concentration of glucose in longan.

**Table 34** Calibration and validation results for sugar content in flesh of longan fruit samples by HSI

Sugar	Pre processing	PLS factor	Calibration set (52.5%)		Validation set (47.5%)			
			R <sup>2</sup>	RMSEC (mg/g fresh weight)	R <sup>2</sup>	RMSEP (mg/g fresh weight)	Bias (mg/g fresh weight)	RPD
Sucrose	MSC+ smoothing	10	0.6704	81.12	0.5247	90.93	19.32	1.48
Glucose	SNV+ second derivative	3	0.2221	27.50	0.2699	24.03	-2.25	1.17
Fructose	First derivative (4)	6	0.4796	25.99	0.4944	23.86	2.54	1.41
Total sugars	MSC+ smoothing	7	0.6883	97.03	0.5333	115.42	12.98	1.47

Abbreviations: R<sup>2</sup>: coefficients of determination, RMSEC: root mean square error of calibration, RMSEP: root mean square error of prediction, RPD: ratio of standard deviation of reference data in validation set to SEP, MSC: multiplicative scatter correction, SNV: standard normal variate, (4): number of left and right average point

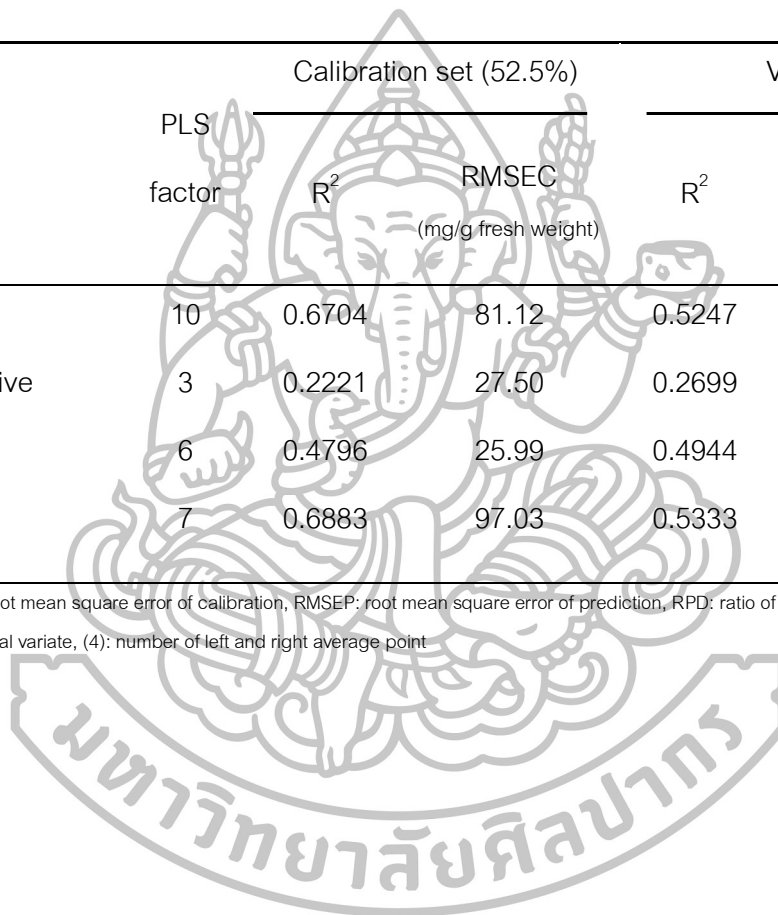


Figure 55-58 show the scatter plots of sucrose, glucose, fructose and total sugar model. According to poor performance of these models, the points scattered out from the target line.

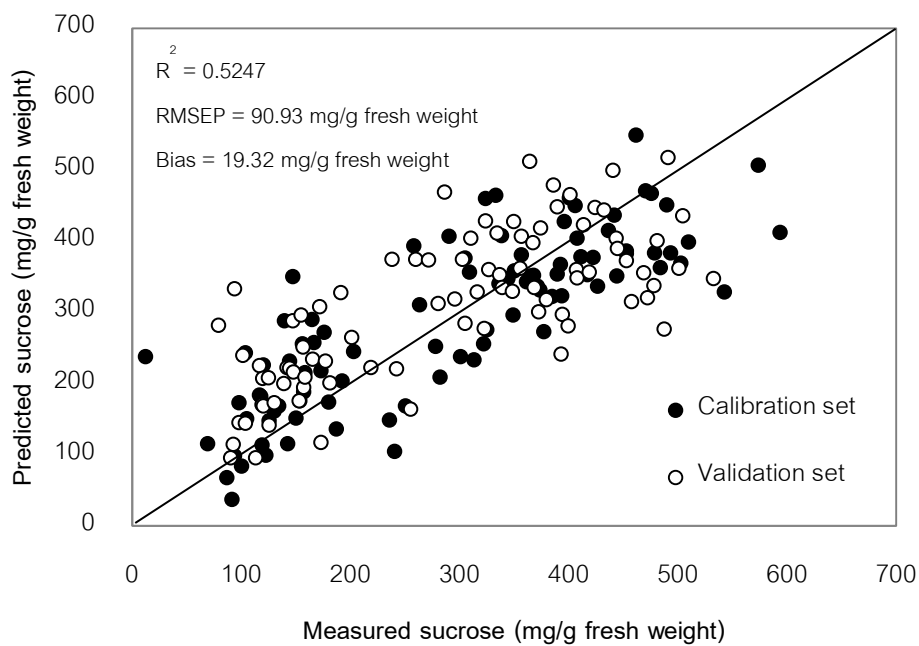


Figure 55 Scatter plot of sucrose of flesh by HSI.



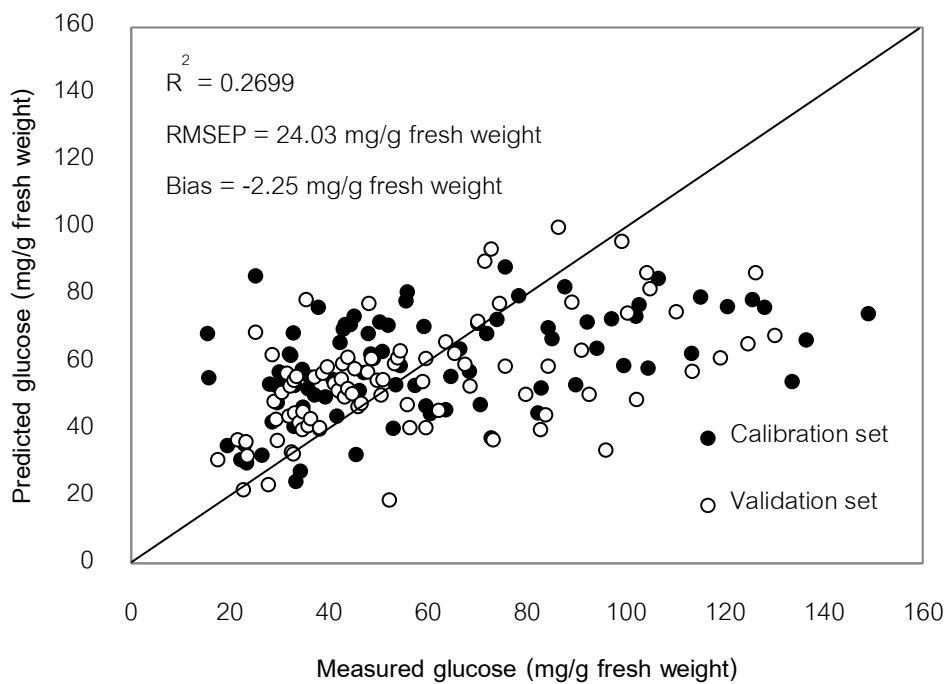


Figure 56 Scatter plot of glucose of flesh by HSI.

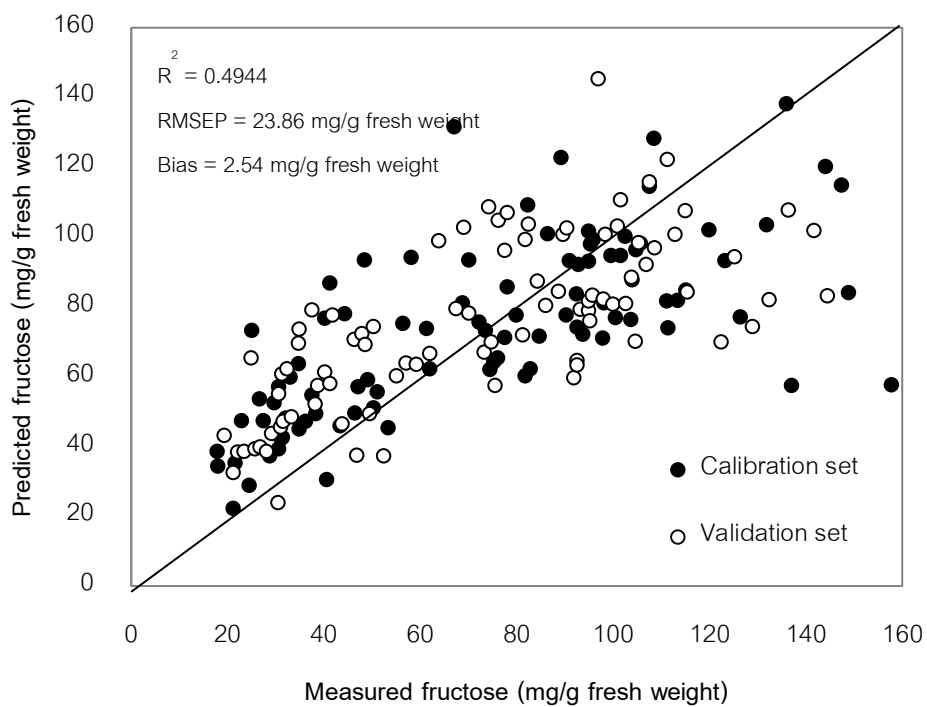


Figure 57 Scatter plot of fructose of flesh by HSI.

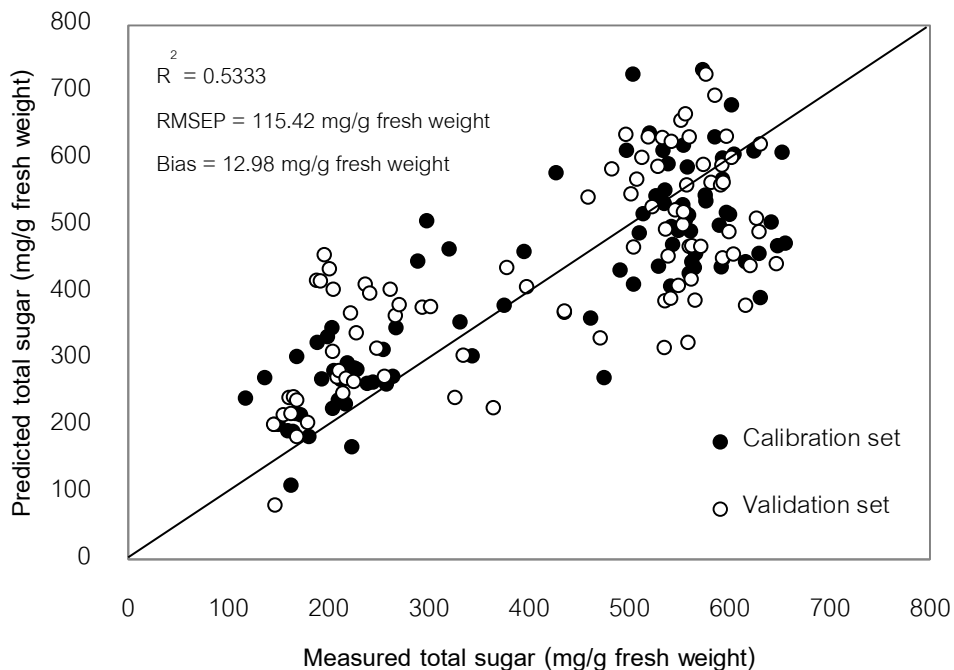


Figure 58 Scatter plot of total sugar of flesh by HSI.

Figure 59 (a) shows the regression coefficient plot of sucrose. The wavelengths at 678, 882, and 938 nm could be associated with chlorophyll pigment, chloroform and methylene compound, respectively (Osborne, 1993; Rajkumar et al., 2012). Figure 57 (b) shows the regression coefficient plot of sucrose. The wavelengths at 690 and 714 nm could be associated with chlorophyll pigment and benzene (Osborne, 1993; Rajkumar et al., 2012). Figure 59 (c) and (b) also show the peaks of chlorophyll in the plots (Rajkumar et al., 2012).

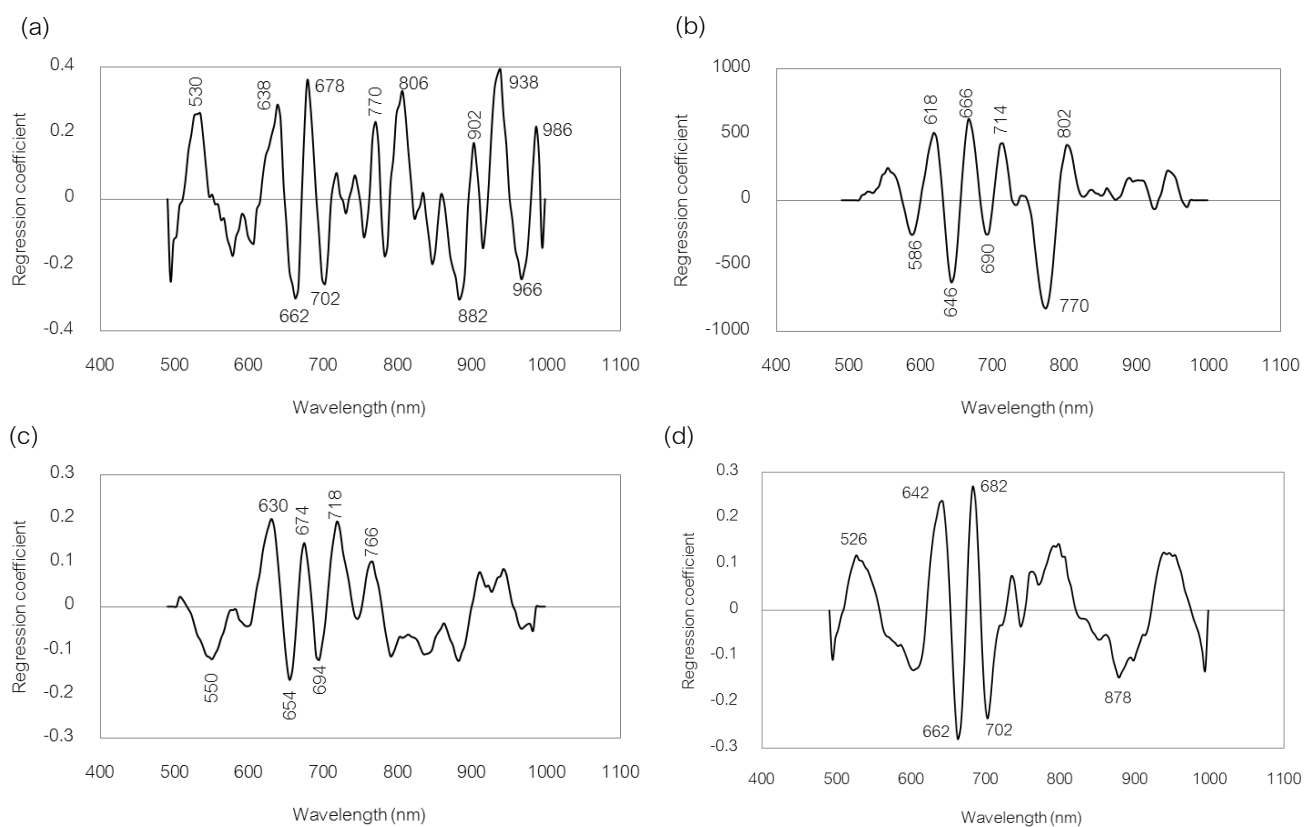
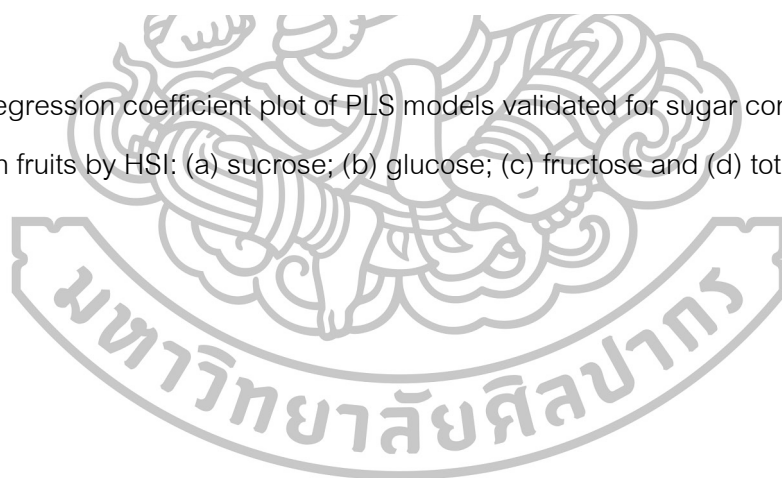


Figure 59 Regression coefficient plot of PLS models validated for sugar content of flesh of the longan fruits by HSI: (a) sucrose; (b) glucose; (c) fructose and (d) total sugars



## CHAPTER 5

### CONCLUSION

The results from this study have been shown that the NIRS technique had better prediction performance than the HSI technique in all parameters (moisture content, TSS, sucrose, glucose, fructose and total sugar). HSI technique showed poor accuracy model for prediction because the small and round shape of longan provided the dark acquired image that affected to the uncorrected spectral acquirement and related to poor correlation when built the prediction models.

High effective of all prediction models were obtained using average spectra of all position from NIRS technique. For moisture content, the best fit model of peel, flesh and the whole fruit showed acceptable prediction accuracy and precision. The prediction statistics recommend that these models are usable in most applications, including quality assurance. In addition, the predictive values for new dried longan samples obtained with developed NIRS model for flesh part did not show significant difference with the reference values.

For TSS and sucrose, fructose and total sugar, the results of best fit model showed high accuracy of prediction while, NIRS could not be predicted glucose in any positions. The reason might be due to low concentration and low distribution of glucose content in flesh of dried whole longan.

Thus, NIRS which is a rapid non-destructive method could be used as an alternative technique to determine quality of whole dried longan especially, moisture content of peel, flesh, whole fruit, TSS, sucrose, fructose and total sugar parameters.



## References

- Ahmad, U., Sutrisno, Purwanto, Y., Budiasta, W., Makino, Y., Oshita, S., Kawagoe, Y., Kuroki, S. and Novita, D. D. (2014). Prediction of hardness development in mangosteen peel using NIR spectroscopy during low temperature storage. *Engineering in Agriculture, Environment and Food*. 7, 86-90.
- Alamar, P. D., Carames, E. T. S., Poppi, R. and Pallone, J. A. L. (2016). Quality evaluation of frozen guava and yellow passion fruit pulps by NIR spectroscopy and chemometrics. *Food Research International*. 85, 209-214.
- Angkasith, P., Nalampang, D. and Apichatpongchai, R., Longan: the important economical crop for industrial development (Chiang Mai: Ming Muang, 1999), 137 (in Thai).
- A.O.A.C. (2000). *Official Methods of Analysis*, 17<sup>th</sup> ed. Association of Official Analytical Chemists. Washington D.C. 376-384.
- Bai, W., Yoshimura, N. and Takayanagi, M. (2014). Quantitative analysis of ingredients of blueberry fruits by near infrared spectroscopy. *Journal of Near Infrared Spectroscopy*. 22, 357-365.
- Baiano, A., Terracone, C., Peri, G. and Romaniello, R. (2012). Application of hyperspectral imaging for prediction of physico-chemical and sensory characteristics of table grapes. *Computers and Electronics in Agriculture*. 87, 142-151.
- Beuchat, L. R. (1981). Microbial stability as affected by water activity. *Cereal Foods World*. 26(7), 345-349.
- de Oliveira, G. A., de Castilhos, F., Catherine, M. G. C. Renard, Bureau, S. (2014). Comparison of NIR and MIR spectroscopic methods for determination of individual sugars, organic acids and carotenoids in passion fruit. *Food Research International*. 60, 154-162.

- EIMasry, G. and Sun, D. *Hyperspectral Imaging for Food Quality Analysis and Control*. (London: Elsevier Inc, 2010), 3.
- Fan, S., Zhang, B., Li, J., Huang, W. and Wang, C. (2016). Effect of spectrum measurement position variation on the robustness of NIR spectroscopy models for soluble solids content of apple. *Biosystems Engineering*. 143, 9-19.
- Fernandes, A. M., Franco, C., Mendes-Ferreira, A., Mendes-Faia, A., da Costa, P. L. and Melo-Pinto, P. (2015). Brix, pH and anthocyanin content determination in whole Port wine grape berries by hyperspectral imaging and neural networks. *Computers and Electronics in Agriculture*. 115, 88-96.
- Go´mez-Sanchis, J., Molto´, E., Camps-Valls, G., Go´mez-Chova, L., Aleixos, N. and Blasco, J. (2008). Automatic correction of the effects of the light source on spherical objects. An application to the analysis of hyperspectral images of citrus fruits. *Journal of Food Engineering*. 85, 191-200.
- He, H., Wu, D. and Sun, D. (2013). Non-destructive and rapid analysis of moisture distribution in farmed Atlantic salmon (*Salmo salar*) fillets using visible and near-infrared hyperspectral imaging. *Innovative Food Science and Emerging Technologies*. 18, 237-245.
- Huang, G., Wang, B., Lin, W., Huang, S., Lee, C., Yen, M. and Huang, M. (2012). Antioxidant and anti-inflammatory properties of longan (*Dimocarpus longan* Lour.) pericarp. Hindawi Publishing Corporation. 10 p.
- Huang, H. B. (1995). Advances in fruit physiology of the arillate fruits of litchi and longan. *Annual Review of Horticultural Science*. 1,107-20.
- Huang, M. and Lu, R. (2010). Apple mealiness detection using hyperspectral scattering technique. *Postharvest Biology and Technology*. 58 (3), 168–175.
- Huang, M., Wang, Q., Zhang, M. and Zhu, Q. (2014). Prediction of color and moisture content for vegetable soybean during drying using hyperspectral imaging technology. *Journal of Food Engineering*. 28, 24-30.
- International standard ISO 12099. (2010). Animal feeding stuffs, cereals and milled cereal products. Guidelines for the application of near infrared spectrometry.

- Iqbal, A., Sun, D., and Allen, P. (2013). Prediction of moisture, color and pH in cooked, pre-sliced turkey hams by NIR hyperspectral imaging system. *Journal of Food Engineering*. 117, 42-51.
- Iqbal, A., Sun, D.W. and Allen, P. (2014). An overview on principle, techniques and application of hyperspectral imaging with special reference to ham quality evaluation and control. *Food Control*. 46, 242-254.
- Jiang, Y., Zhang, Z., Joyce, D.C. and Ketsa, S. (2002). Postharvest biology and handling of longan fruit (*Dimocarpus longan* Lour.). *Postharvest Biology and Technology*. 26, 241-252.
- Janjai, S., Intawee, P., Chaichoet, C., Mahayothee, B., Haewsungcharern, M. and Muller, J. (2006). Improvement of the air flow and temperature distribution in a conventional longan dryer. International symposium towards sustainable livelihoods and ecosystems in mountainous regions, 7-9 March 2006, Chiang Mai, Thailand.
- Kaewsorn, K. and Sirisomboon, P. (2014). Determination of the gamma-aminobutyric acid content of germinated brown rice by near infrared spectroscopy. *Journal of Near Infrared Spectroscopy*. 22, 45-54.
- Kramchote, S., Nakano, K., Kanlayanarat, S., Ohashi, S., Takizawa, K. and Bai, G. (2014). Rapid determination of cabbage quality using visible and near-infrared spectroscopy. *Food Science and Technology*. 59, 695-700.
- Leiva-Valenzuela, G. A., Lu, R. and Aguilera, J. M. (2013). Prediction of firmness and soluble solids content of blueberries using hyperspectral reflectance imaging. *Journal of Food Engineering*. 115, 91-98.
- Li, J. R., Miao, S. X., Jiang, Y. M. (2009). Changes in quality attributes of longan juice during storage in relation to effects of thermal processing. *Journal of Food Quality*. 32, 48-57.
- Liu, F., Fu, S., Bi, X., Chen, F., Liao, X., Hu, X. and Wu, J. (2013). Physico-chemical and antioxidant properties of four mango (*Mangifera indica* L.) cultivars in China. *Food Chemistry*. 138, 396-405.

- Liu, Y., Ying, Y., Yu, H. and Fu, X. (2006). Comparison of the HPLC method and FT-NIR analysis for quantification of glucose, fructose, and sucrose in intact apple fruits. *Journal of Agricultural and Food Chemistry*. 54, 2810-2815.
- Louw, E. and Theron, K. (2010). Robust prediction models for quality parameters in Japanese plums (*Prunus salicina* L.) using NIR spectroscopy. *Postharvest Biology and Technology*. 58(3), 176-184.
- Lu, R. (2004). Multispectral imaging for predicting firmness and soluble solids content of apple fruit. *Postharvest Biology and Technology*. 31, 147–157.
- Magwaza, L. S., Opara, U. L., Nieuwoudt, H., Cronje, P. J. R., Saeys, W. and Nicolaï, B. (2012). NIR Spectroscopy applications for internal and external quality analysis of citrus fruit—a review. *Food Bioprocess Technology*. 5, 425-444
- Maitree Youvarat and Wijit Jeorentong. (2004). Longan processing. *Journal for Rural Development*. 4, 93-99 (in Thai).
- Menzel, C. M. and Waite, G. K. (2005). Litchi and longan. *Botany Production and Uses*. Cromwell Press. Trowbridge. 305 p.
- Morales-Sillero, A., Fernández-Cabanás, V., Casanova, L., Jiménez, M., Suárez, M. and Rallo, P. (2011). Feasibility of NIR spectroscopy for non-destructive characterization of table olive traits. *Journal of Food Engineering*. 107, 99-106.
- Nagle, M., González Azcárraga, C., Mahayothee, B., Haewsungcharern, M., Janjai, S. and Müller, J. (2010). Improved quality and energy performance of a fixed-bed longan dryer by thermodynamic modifications. *Journal of Food Engineering*. 99, 392-399.
- Nicolaï, B. M., Beullens, K., Bobelyn, E., Peirs, A., Saeys, W., Theron, K. I. and Lammertyn J. (2007). Nondestructive measurement of fruit and vegetable quality by means of NIR spectroscopy. *Postharvest Biology and Technology*. 46, 99-118.
- Office of Agricultural Economic, Thailand. (2016). Import and export statistic. Available from: [http://www.oae.go.th/oae\\_report/export\\_import/export\\_result.php](http://www.oae.go.th/oae_report/export_import/export_result.php). Accessed on 1 April 2016.

- Onsawan, P. and Sirisomboon, P. (2015). Determination of dry matter and soluble solids of durian pulp using diffuse reflectance near infrared spectroscopy. *Journal of Near Infrared Spectroscopy*. 23, 167-179.
- Osborne, B. G., Fearn, T. and Hiddle, P. H. , *Practical NIR spectroscopy with application in food and beverage analysis*, 2<sup>nd</sup> ed. (Harlow: Longman Group UK Limited, 1993), 29.
- Pawin Manochai, *Longan*, 2<sup>nd</sup> ed. (Chiang Mai: Sirinat printing, 2000), 115 (in Thai).
- Phupaichitkun, S., Mahayothee, B., Heawsungcharen, M., Janjai, S. and Müller, J. (2005). Single-layer drying behavior of longan (*Dimocarpus longan* Lour.). *Deutscher Tropentag*. Stuttgart-Hohenheim, October 11-13.
- Phupaichitkun, S., Mahayothee, B., Heawsungcharen, M., Janjai, S. and Müller, J. (2006). Drying behavior of Thai unpeeled longan: modeling of shrinkage inside fruit. *15<sup>th</sup> International Drying Symposium*. 388.
- Posom, J., Shrestha, A., Saechua, W and Sirisomboon, P. (2016). Rapid non-destructive evaluation of moisture content and higher heating value of *Leucaena leucocephala* pellets using near infrared spectroscopy. *Energy*. 107, 464-472.
- Prasad, K. N., Hao, J., Shi, J., Liu, T., Li, J., Wei, X., Qiu, S., Xue, S. and Jiang, Y. (2009). Antioxidant and anticancer activities of high pressure-assisted extract of longan (*Dimocarpus longan* Lour.) *Innovative Food Science and Emerging Technologies*. 10, 413-419.
- Pu, Y. and Sun, D. (2016). Vis-NIR hyperspectral imaging in visualizing moisture distribution of mango slices during microwave-vacuum drying. *Food Chemistry*. 188, 271-278.
- Rady, A. M. and Guyer, D. E., Kirk, W. and Donis-Gonzalez, I. R. (2014). The potential use of visible/near infrared spectroscopy and hyperspectral imaging to predict processing-related constituents of potatoes. *Journal of Food Engineering*. 135, 11-25.

- Rady, A. M. and Guyer, D. E. (2015). Evaluation of sugar content in potatoes using NIR reflectance and wavelength selection techniques. *Postharvest Biology and Technology*. 103, 17-26.
- Rajkumar, P., Wang, N., Elmasry, G., Raghavan, G. (2012). Studies on banana fruit quality and maturity stages using hyperspectral imaging. *Journal of Food Engineering*. 108, 194-200.
- Rangkadilok, N., Worasuttayangkurn, L., Bennett, R. N. and Satayavivad, J. (2005). Identification and quantification of polyphenolic compounds in longan (*Euphoria longana Lam.*) fruit. *Journal of Agricultural and Food Chemistry*. 53, 1387-1392.
- Reich, G. (2005). Near-infrared spectroscopy and imaging: Basic principles and pharmaceutical applications. *Advanced Drug Delivery Reviews*. 57, 1109– 1143.
- Ren, G. and Chen, F. (1996). Determination of moisture content of ginseng by near infra-red reflectance spectroscopy. *Food Chemistry*. 60, 433–436.
- Rungpichayapichet, P., Mahayothee, B., Nagle, M., Khuwijitjaru, P. and Müller, J. (2016). Robust NIRS models for non-destructive prediction of postharvest fruit ripeness and quality in mango. *Postharvest Biology and Technology*. 111, 31-40.
- Rungtip Wongtom. "Browning reactions occur during drying the whole longan (*Euphoria longana Lam.*)" Master of Science, Department of Food Technology, Graduate School, Silpakorn University, 2006.
- Sirisomboon, P and Nawayon, J. (2016). Evaluation of total solids of curry soup containing coconut milk by near infrared spectroscopy. *Journal of Near Infrared Spectroscopy*. 24, 191-198.
- Shiroma, C. and Rodriguez-Saona, L. (2009). Application of NIR and MIR spectroscopy in quality control of potato chips. *Journal of Food Composition and Analysis*. 22, 596–605.
- Sun, T., Xu, H. and Ying, Y. (2009). Progress in application of near infrared spectroscopy to nondestructive on-line detection of products/food quality. *Spectrosc Spectr Anal*. 29(1), 122-126.

- Surin, S., Seesuriyachan, P., Thakeow, P. and Phimolsiripol, Y. (2012). Optimization of enzymatic production of fructooligosaccharides from longan syrup. *Journal of Applied Sciences*. 12, 1118-1123.
- Tippayawong, N., Tantakitti, C. and Thavornun, S. (2008). Energy efficiency improvements in longan drying practice. *Energy*. 33, 1137–1143.
- The National Bureau of Agricultural Commodity and Food Standards. 2006. Thai agricultural standard. Available from:  
[http://www.acfs.go.th/standard/dried\\_whole\\_longan\\_fruit](http://www.acfs.go.th/standard/dried_whole_longan_fruit). Accessed on 28 June 2015.
- Tongdee, S.C. Postharvest physiology and storage of tropical and subtropical fruits. (New York: CAB INTERNATIONAL, 1997), 335.
- Williams, P. "Grains and seeds." In *Near-Infrared Spectroscopy in Food Science and Technology*, 165-217. Edited by Ozaki, Y., McClure, W. F. and Christy, A. A. Hoboken: John Wiley & Sons, Inc, 2007.
- Wu, D., Shi, H., Wang, S., He, Y., Bao, Y. and Liu, K. (2012). Rapid prediction of moisture content of dehydrated prawns using online hyperspectral imaging system. *Analytica Chimica Acta*. 726, 57-66.
- Wu, D. and Sun, D. W. (2013). Advanced applications of hyperspectral imaging technology for food quality and safety analysis and assessment: Part I: Fundamentals. *Innovative Food Science and Emerging Technologies*. 19, 1–14.
- Yang, Y., Sun, D. and Wang, N. (2015). Rapid detection of browning levels of lychee pericarp as affected by moisture contents using hyperspectral imaging. *Computers and Electronics in Agriculture*. 113, 203-212.



Appendix A  
Sugars standards



### Standard preparation

Standard solutions of sugars (sucrose, glucose and fructose) were prepared 7 levels by dilution with distilled water. The concentrations of sucrose were 500, 2500, 5000, 10000, 15000, 20000 and 30000 ppm and the concentrations of glucose and fructose were 250, 1250, 2500, 5000, 7500, 10000 and 15000 ppm. The standard solution was filtered with a 0.45  $\mu\text{m}$  membrane filter and keep in light brown bottle.

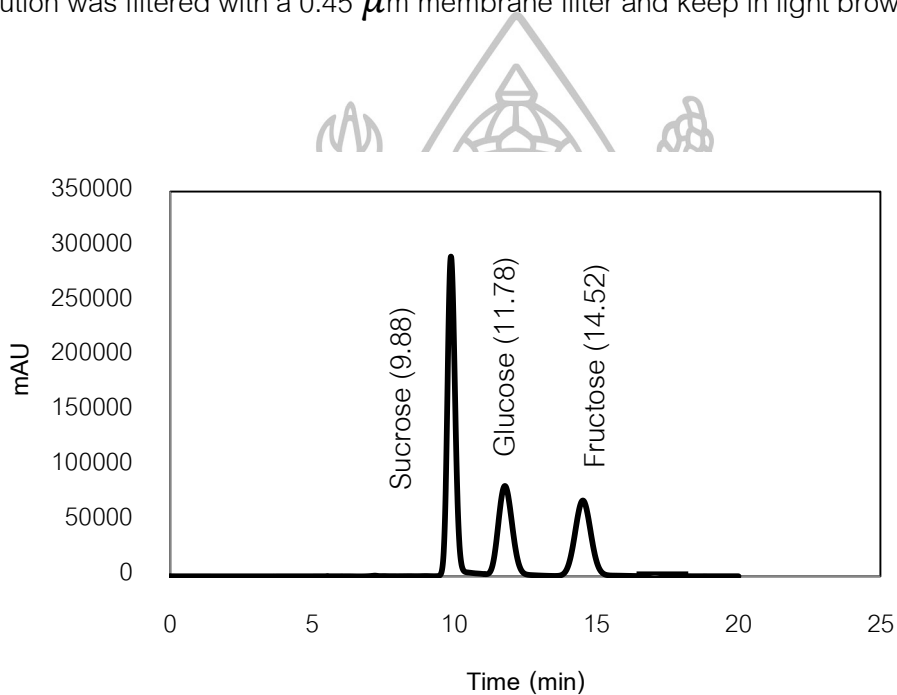


Figure 60 Chromatogram of individual sugars.

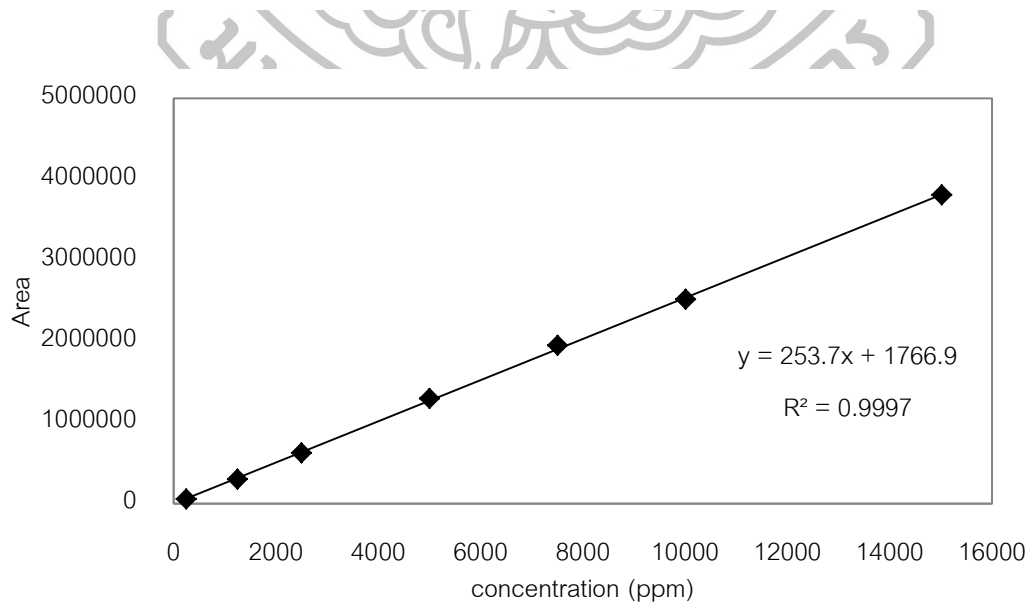
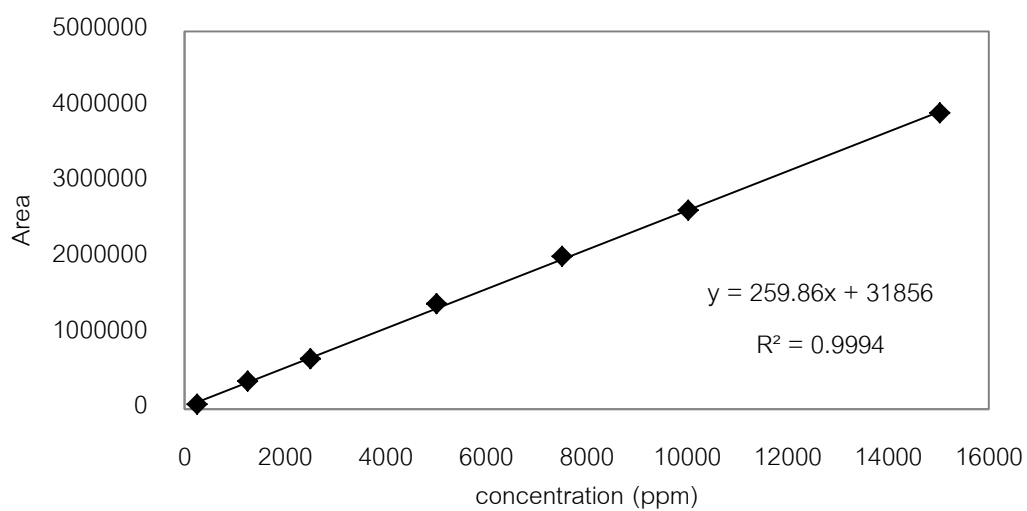
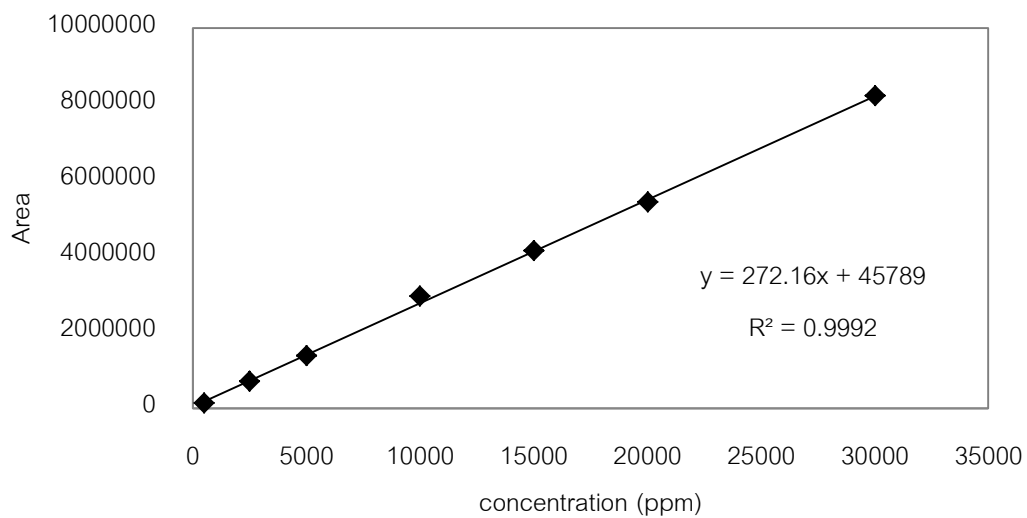


Figure 61 Standard curve for sucrose (a) glucose (b) and fructose (c).



Appendix B  
NIRS

## NIRS

- Coefficient of determination ( $R^2$ )

$$R^2 = \left[ \frac{\sum(Y_{pred} - Y_{mean})^2}{\sum(Y_{cal} - Y_{mean})^2} \right]$$

- Root mean square error of calibration (RMSEC)

$$RMSEC = \sqrt{\frac{\sum(Y_{cal} - Y_{act})^2}{n}}$$

- Root mean squares error of prediction (RMSEP)

$$RMSEP = \sqrt{\frac{\sum(Y_{pred} - Y_{act})^2}{n}}$$

- Bias

$$Bias = \frac{1}{n} \sqrt{\sum(Y_{pred} - Y_{act})^2}$$

- Ratio of standard deviation of reference data in validation set to SEP (RPD)

$$RPD = \frac{SD_{val}}{SEP}$$

Where:

n	The number of spectra
Yact	The actual value
Ymean	The mean value
Ycal	The calculated value
Ypred	The predicted value of the fruit attributes.



Appendix C  
Regression coefficient of NIRS

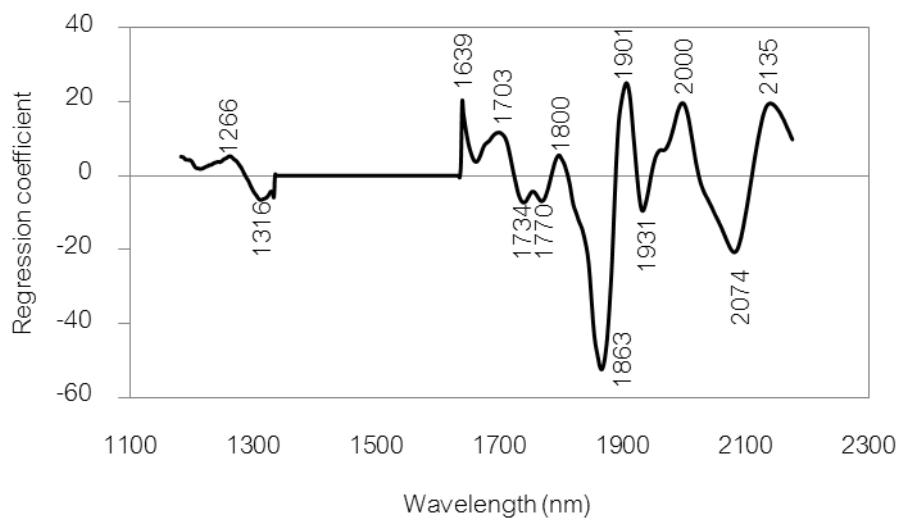


Figure 62 Regression coefficient plot of a PLS model validated for moisture content of peel of the longan fruits.

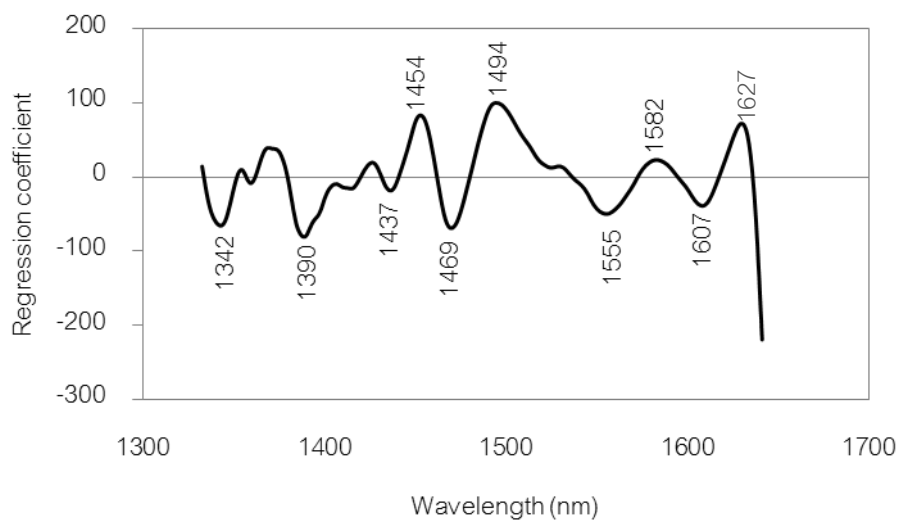


Figure 63 Regression coefficient plot of a PLS model validated for moisture content of seed of the longan fruits.

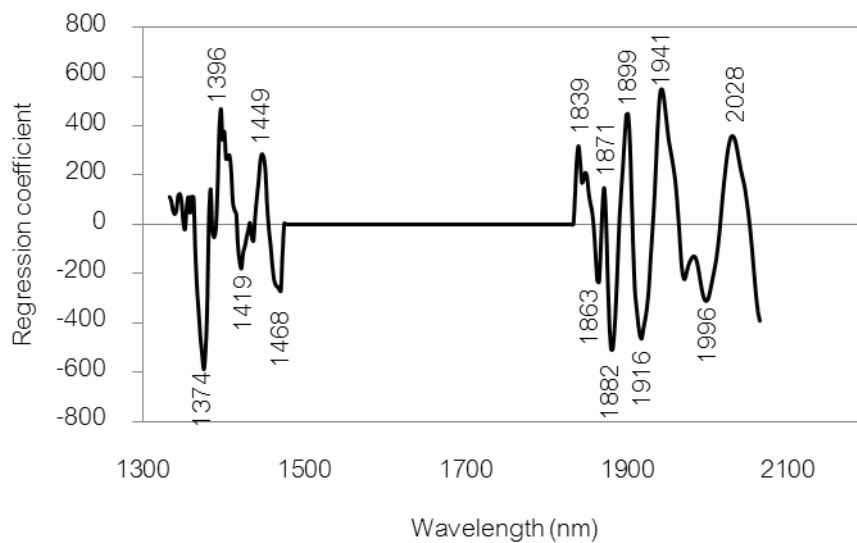


Figure 64 Regression coefficient plot of a PLS model validated for moisture content of flesh and seed of the longan fruits.





Appendix D

Verify accuracy of calibration models



### Verify accuracy of calibration models

The accuracy of prediction models were tested by using bias checking (paired  $t$ -test) method, SEP checking (F-test, ratio of 2 variances) method and slope checking method from International standard ISO 12099. These methods can demonstrate that predicted value obtained from the instrument were not different from actual values significantly at 95% confidence interval. Moreover, the models that pass all tests are usable in any application.

First bias checking, this method is conducted by paired  $t$ -test for calculating the bias confidence limits (BCLs,  $T_b$ ) which is the acceptance or denial limit of efficiency of a predictive model. The bias value from the model must less than  $T_b$  value. It means the bias is accepted (at 95% confidence) and it can conclude that no significant mean difference between NIRS and reference methods. Second SEP checking, this method use F-test for estimating the unexplained error confidence limit (UECLs,  $T_{UE}$ ). The SEP value from the model must less than  $T_{UE}$  value. It means SEP is accepted (at 95% confidence). And slope checking,  $t$ -test can be calculated to check the hypothesis that slope of scatter plot between actual and NIRS predicted value = 1. This method has to calculate observed  $t$ -value ( $t_{obs}$ ) and  $t_{obs}$  value must less than  $t$ -value for a probability of  $\alpha = 0.05$  ( $t(1-\alpha/2)$ ). It means the slope is not significantly difference from 1.

- Bias checking (paired  $t$ -test)

$$T_b = \pm \frac{t_{(1-\alpha/2)} \times SEP}{\sqrt{n}}$$

$$SEP = \sqrt{\frac{\sum(e_i - \bar{e})^2}{n-1}}$$

$T_b$  is bias confidence limits

$n$  = no. of samples in validation set

Bias <  $T_b$ ; Bias is accepted (at 95% confidence)

- SEP checking (F-test, ratio of 2 variances)

$$T_{UE} = SEC \sqrt{F(\alpha; v, M)}$$

$$SEC = \sqrt{\frac{\sum e_i^2}{n_c - p - 1}}$$

$T_{UE}$  = The unexplained error confidence limit (UECLs)

$\alpha$  = probability of making a type I error, 5%

$V$  =  $n-1$  (degree of freedom associated with SEP)

$M$  =  $n_c - p - 1$  (degree of freedom associated with SEC)

$n_c$  = no. of samples in calibration set

$p$  = no. of terms (wavelengths or factors)

$SEP < T_{UE}$ ; SEP is accepted (at 95% confidence)

- Slope checking

$$T_{obs} = |b - 1| \sqrt{\frac{s_y^2(n-1)}{s_{res}^2}}$$

$$s_{res} = \sqrt{\frac{\sum (y_i - a - b\hat{y}_i)^2}{n-2}}$$

$n$  = number of independent samples

$s_y^2$  = variance of the  $n$  predicted values

$s_{res}$  = residual standard deviation

$a$  = intercept

$b$  = slope

$y_i$  = the reference value

$\hat{y}_i$  = the predicted value

$t_{obs} \geq t_{(1-\alpha/2)}$ , slope  $b$  is different from 1

**Table 35** Verifying the accuracy by bias checking, SEP checking and slope checking method.

Model	Bias checking	SEP checking	Slope checking	Usable in any application
NIRS moisture content of peel	✓	✓	✓	✓
NIRS moisture content of flesh	✓	✓	✓	✓
NIRS moisture content of seed	✗	✓	✓	✗
NIRS moisture content of whole fruit	✓	✓	✓	✓
NIRS moisture content of flesh and seed	✗	✓	✓	✗
NIRS TSS in flesh	✓	✓	✓	✓
NIRS sucrose in flesh	✓	✓	✓	✓
NIRS fructose in flesh	✓	✓	✓	✓
NIRS total sugar in flesh	✓	✓	✓	✓

Table 36 Bias checking

Model	t-value	$T_b$	Bias	Result	Bias checking
NIRS moisture content of peel	1.97	$\pm 0.16$	-0.128	bias < $T_b$	✓
NIRS moisture content of flesh	1.97	$\pm 0.78$	0.085	bias < $T_b$	✓
NIRS moisture content of seed	1.97	$\pm 0.31$	-0.37	bias > $T_b$	✗
NIRS moisture content of whole fruit	1.97	$\pm 0.54$	-0.138	bias < $T_b$	✓
NIRS moisture content of flesh and seed	1.97	$\pm 0.60$	-0.731	bias > $T_b$	✗
NIRS TSS in flesh	1.99	$\pm 1.54$	-0.454	bias < $T_b$	✓
NIRS sucrose in flesh	1.99	$\pm 13.17$	-7.26	bias < $T_b$	✓
NIRS fructose in flesh	2.00	$\pm 3.53$	2.33	bias < $T_b$	✓
NIRS total sugar in flesh	2.00	$\pm 12.47$	-1.05	bias < $T_b$	✓

Table 37 SEP checking

Model	F value	$T_{UE}$	SEP	Result	SEP checking
NIRS moisture content of peel	1.24	2.04	1.09	SEP < $T_{UE}$	✓
NIRS moisture content of flesh	1.24	5.77	5.54	SEP < $T_{UE}$	✓
NIRS moisture content of seed	1.24	3.35	2.19	SEP < $T_{UE}$	✓
NIRS moisture content of whole fruit	1.24	5.35	3.77	SEP < $T_{UE}$	✓
NIRS moisture content of flesh and seed	1.24	4.23	4.20	SEP < $T_{UE}$	✓
NIRS TSS in flesh	1.42	8.85	6.44	SEP < $T_{UE}$	✓
NIRS sucrose in flesh	1.43	72.67	55.22	SEP < $T_{UE}$	✓
NIRS fructose in flesh	1.44	20.14	14.01	SEP < $T_{UE}$	✓
NIRS total sugar in flesh	1.43	77.26	51.93	SEP < $T_{UE}$	✓

Table 38 Slope checking

Model	$t_{obs}$	$t$ -value	Result	Slope checking
NIRS moisture content of peel	0.0137	1.97	$t_{obs} < t$ -value	✓
NIRS moisture content of flesh	0.1248	1.97	$t_{obs} < t$ -value	✓
NIRS moisture content of seed	0.1073	1.97	$t_{obs} < t$ -value	✓
NIRS moisture content of whole fruit	0.1960	1.97	$t_{obs} < t$ -value	✓
NIRS moisture content of flesh and seed	0.0840	1.97	$t_{obs} < t$ -value	✓
NIRS TSS in flesh	0.0626	1.99	$t_{obs} < t$ -value	✓
NIRS sucrose in flesh	0.3127	1.99	$t_{obs} < t$ -value	✓
NIRS fructose in flesh	0.2754	2.00	$t_{obs} < t$ -value	✓
NIRS total sugar in flesh	0.0441	2.00	$t_{obs} < t$ -value	✓



## ROI identification

Warning messages:

```

1: package 'hyperSpec' was built under R version 3.1.2
2: package 'mvtnorm' was built under R version 3.1.2
> source("G:\\Yean master degree\\longanselect.r")
> fresh<-select("LFB160W001000.cue")
.read.ENVI.header: Guessing header file name (./LFB160W001000.hdr)
num [1:10, 1:128] 457 585 478 452 844 ...
- attr(*, "dimnames")=List of 2
..$ : chr [1:10] "spec1" "spec2" "spec3" "spec4" ...
..$ : NULL
> save(fresh,file="fresh.Rdata")
> fresh.dataframe<-data.frame(fresh)
> str(fresh)
num [1:10, 1:128] 457 585 478 452 844 ...
- attr(*, "dimnames")=List of 2
..$ : chr [1:10] "spec1" "spec2" "spec3" "spec4" ...
..$ : NULL
> write.csv(fresh.dataframe,file="fresh.csv")
> save.image("D:\\projectปตท\ไปรเจคคำเีย\เล่ม thesis\\freshhhh")

```



### PLS distribution map

```

load("D:\\projectปอโท\\โปรเจคลำไย\\data MC\\HSI result\\distribution map\\mixR.Rdata")
load("D:\\projectปอโท\\โปรเจคลำไย\\data MC\\HSI result\\distribution map\\mixS.Rdata")
local({pkg <- select.list(sort(.packages(all.available = TRUE)),graphics=TRUE)
if(nchar(pkg)) library(pkg, character.only=TRUE)})
mixS.SG<-savitzkyGolay(mixS,p=2,w=15,m=0)
str(mixS.SG)
MCflesh<-data.frame(mixR,mixS.SG)
str(MCflesh)
local({pkg <- select.list(sort(.packages(all.available = TRUE)),graphics=TRUE)
if(nchar(pkg)) library(pkg, character.only=TRUE)})
MCflesh.pls<-pls(V1~.,data=MCflesh,validation="LOO",ncomp=30)
summary(MCflesh.pls)
R2(MCflesh.pls)
plot(MCflesh.pls,"prediction",ncomp=29,asp=1,line=TRUE)
source("G:\\Yean master degree\\longanselect.r")
dried6060<-bgremove("LDB160W170000.cue")
predict<-predict(MCflesh.pls,ncomp=29,newdata=dried6060)
nr<-910
nc<-900
nw<-128
wavelength<-seq(490,998,4)
predict.mean<-matrix(rowMeans(predict),nr,nc)
colpal<-colorRampPalette(c("blue","green","yellow","red"))
levelplot(predict.mean,colorkey=list(at=seq(0,100,by=5)),col.regions=colpal(20))
dried6060<-bgremove("LDB160W168000.cue")
predict<-predict(MCflesh.pls,ncomp=29,newdata=dried6060)
levelplot(predict.mean,colorkey=list(at=seq(0,100,by=5)),col.regions=colpal(20))

```

```
dried<-bgremove("LDB160W165000.cue")  
predict<-predict(MCflesh.pls,ncomp=29,newdata=dried)  
nr<-910  
nc<-900  
nw<-128  
wavelength<-seq(490,998,4)  
predict.mean<-matrix(rowMeans(predict),nr,nc)  
colpal<-colorRampPalette(c("blue","green","yellow","red"))  
levelplot(predict.mean,colorkey=list(at=seq(0,100,by=5)),col.regions=colpal(20))  
q()
```





Appendix F  
HSI results

**Table 39** Calibration and validation results for moisture content of peel of whole longan fruit samples by HSI.

Pre processing	PLS factor	Calibration set		Validation set			RPD
		R <sup>2</sup>	RMSEC(%)	R <sup>2</sup>	RMSEP(%)	bias	
Raw	10	0.7390	4.96	0.6396	5.43	1.01	1.69
Smoothing	10	0.7383	4.97	0.6360	5.45	0.96	1.68
Normalize	9	0.7129	5.20	0.6205	5.57	1.12	1.66
MSC	7	0.6920	5.39	0.6110	5.64	1.09	1.63
First derivative (2)	7	0.7237	5.10	0.6203	5.57	1.23	1.66
Second derivative (9)	10	0.7519	4.84	0.6068	5.67	1.04	1.62
SNV	7	0.7013	5.31	0.6175	5.59	0.96	1.64
SNV+ smoothing	7	0.6974	5.34	0.6159	5.34	0.97	1.63
SNV+ first derivative	5	0.6722	5.56	0.6100	5.64	1.14	1.63
SNV+ second derivative	7	0.7066	5.26	0.5811	5.85	1.26	1.58
MSC+ smoothing	9	0.7281	5.06	0.6236	5.55	1.07	1.66
MSC+ first derivative	8	0.7695	4.66	0.6388	5.43	1.02	1.69
MSC+ second derivative	7	0.7101	5.23	0.5877	5.80	1.19	1.59

Abbreviations: R<sup>2</sup>: coefficients of determination, RMSEC: root mean square error of calibration, RMSEP: root mean square error of prediction, RPD: ratio of standard deviation of reference data in validation set to SEP, MSC: multiplicative scatter correction, SNV: standard normal variate, (2 and 9): number of left and right average point

**Table 40** Calibration and validation results for moisture content of flesh of whole longan fruit samples by HSI.

Pre processing	PLS factor	Calibration set		Validation set			RPD
		R <sup>2</sup>	RMSEC(%)	R <sup>2</sup>	RMSEP(%)	bias	
Raw	9	0.7400	13.00	0.7026	13.70	-0.30	1.83
Smoothing (7)	14	0.7637	12.35	0.7071	13.60	-0.19	1.85
Normalize	9	0.7314	13.17	0.6756	14.31	-1.07	1.76
MSC	7	0.6856	14.25	0.6655	14.53	-1.33	1.74
First derivative (4)	8	0.7311	13.18	0.6951	13.87	0.22	1.81
Second derivative (7)	8	0.7752	12.05	0.7004	13.75	0.01	1.83
SNV	8	0.7024	13.86	0.6595	14.66	-1.31	1.72
SNV+ smoothing	12	0.7428	12.90	0.6849	14.10	-0.75	1.78
SNV+ first derivative	7	0.7167	13.53	0.6687	14.46	-0.68	1.74
SNV+ second derivative	9	0.7780	11.97	0.6845	14.11	-0.75	1.78
MSC+ smoothing	11	0.7360	13.06	0.6794	14.22	-0.80	1.77
MSC+ first derivative	7	0.7153	13.56	0.6668	14.50	0.70	1.73
MSC+ second derivative	9	0.7771	12.00	0.6835	14.13	-0.81	1.78

Abbreviations: R<sup>2</sup>: coefficients of determination, RMSEC: root mean square error of calibration, RMSEP: root mean square error of prediction, RPD: ratio of standard deviation of reference data in validation set to SEP, MSC: multiplicative scatter correction, SNV: standard normal variate, (4 and 7): number of left and right average point

**Table 41** Calibration and validation results for moisture content of seed of whole longan fruit samples by HSI.

Pre processing	PLS factor	Calibration set		Validation set			RPD
		R <sup>2</sup>	RMSEC(%)	R <sup>2</sup>	RMSEP(%)	bias	
Raw	10	0.6276	7.10	0.6486	6.75	-0.73	1.70
Smoothing (7)	13	0.6221	7.15	0.6559	6.68	-0.50	1.71
Normalize	9	0.5956	7.40	0.6528	6.71	-0.70	1.71
MSC	9	0.6027	7.33	0.6496	6.74	-0.74	1.70
First derivative (1)	8	0.6809	6.57	0.6599	6.64	-0.71	1.72
Second derivative (7)	7	0.6178	7.19	0.6450	6.79	-0.74	1.69
SNV	10	0.6154	7.21	0.6474	6.76	-0.56	1.69
SNV+ smoothing	12	0.5942	7.41	0.6434	6.80	-0.23	1.68
SNV+ first derivative	7	0.6491	6.89	0.6654	6.59	-0.71	1.74
SNV+ second derivative	7	0.6093	7.27	0.6370	6.86	-0.86	1.67
MSC+ smoothing	11	0.5846	7.50	0.6443	6.79	-0.76	1.68
MSC+ first derivative	7	0.6479	6.90	0.6663	6.58	-0.76	1.74
MSC+ second derivative	8	0.6154	7.21	0.6454	6.78	-0.96	1.70

Abbreviations: R<sup>2</sup>: coefficients of determination, RMSEC: root mean square error of calibration, RMSEP: root mean square error of prediction, RPD: ratio of standard deviation of reference data in validation set to SEP, MSC: multiplicative scatter correction, SNV: standard normal variate, (1 and 7): number of left and right average point

**Table 42** Calibration and validation results for moisture content of whole longan fruit samples by HSI.

Pre processing	PLS factor	Calibration set		Validation set			RPD
		R <sup>2</sup>	RMSEC(%)	R <sup>2</sup>	RMSEP(%)	bias	
Raw	10	0.7183	11.64	0.7396	11.06	0.10	1.96
Smoothing (7)	14	0.7455	11.06	0.7458	10.93	0.31	1.98
Normalize	9	0.7011	11.99	0.7279	11.31	0.19	1.92
MSC	9	0.7093	11.82	0.7255	11.36	0.20	1.91
First derivative (4)	10	0.7409	11.16	0.7400	11.06	0.60	1.96
Second derivative (7)	8	0.7420	11.14	0.7368	11.12	1.01	1.96
SNV	10	0.7193	11.62	0.7262	11.34	0.25	1.91
SNV+ smoothing	13	0.7215	11.57	0.7315	11.23	0.42	1.93
SNV+ first derivative	10	0.7193	11.62	0.7262	11.34	0.25	1.91
SNV+ second derivative	7	0.7154	11.70	0.7176	11.52	0.97	1.89
MSC+ smoothing	12	0.7187	11.63	0.7294	11.27	0.36	1.92
MSC+ first derivative	7	0.6758	12.48	0.7076	11.72	0.36	1.85
MSC+ second derivative	7	0.7139	11.73	0.7177	11.52	0.98	1.89

Abbreviations: R<sup>2</sup>: coefficients of determination, RMSEC: root mean square error of calibration, RMSEP: root mean square error of prediction, RPD: ratio of standard deviation of reference data in validation set to SEP, MSC: multiplicative scatter correction, SNV: standard normal variate, (4 and 7): number of left and right average point



**Table 43** Calibration and validation results for moisture content of flesh and seed of whole longan fruit samples by HSI.

Pre processing	PLS factor	Calibration set		Validation set			RPD
		R <sup>2</sup>	RMSEC(%)	R <sup>2</sup>	RMSEP(%)	bias	
Raw	10	0.7509	10.57	0.6961	11.54	0.03	1.81
Smoothing (4)	14	0.7698	10.16	0.7065	11.34	0.15	1.85
Normalize	9	0.7302	11.00	0.6834	11.78	0.31	1.78
MSC	10	0.7596	10.39	0.6967	11.53	-0.02	1.82
First derivative (1)	10	0.8191	9.01	0.7113	11.25	0.64	1.86
Second derivative (5)	10	0.7860	9.80	0.7175	11.13	0.61	1.88
SNV	11	0.7659	10.25	0.7198	11.49	0.22	1.82
SNV+ smoothing	12	0.7430	10.74	0.6911	11.64	0.12	1.80
SNV+ first derivative	9	0.7933	9.63	0.7124	11.23	0.89	1.87
SNV+ second derivative	9	0.7629	10.32	0.7157	11.16	0.69	1.88
MSC+ smoothing	11	0.7420	10.76	0.6910	11.64	0.07	1.80
MSC+ first derivative	9	0.7947	9.60	0.7167	11.15	0.74	1.88
MSC+ second derivative	9	0.7624	10.33	0.7166	11.15	0.61	1.88

Abbreviations: R<sup>2</sup>: coefficients of determination, RMSEC: root mean square error of calibration, RMSEP: root mean square error of prediction, RPD: ratio of standard deviation of reference data in validation set to SEP, MSC: multiplicative scatter correction, SNV: standard normal variate, (1 and 4): number of left and right average point



**Table 44** Calibration and validation results for TSS in flesh of dried whole longan fruit samples by HSI.

Pre processing	PLS factor	Calibration set		Validation set		RPD	
		R <sup>2</sup>	RMSEC (°Brix)	R <sup>2</sup>	RMSEP (°Brix)		bias
Raw	8	0.7308	12.46	0.6209	14.27	2.17	1.64
Smoothing (7)	13	0.7968	10.83	0.6170	14.34	3.93	1.68
Normalize	11	0.8200	10.19	0.6328	14.04	3.27	1.70
MSC	7	0.7109	12.91	0.6156	14.36	1.64	1.62
First derivative (1)	6	0.7724	11.46	0.6053	14.56	3.29	1.63
Second derivative (9)	6	0.7355	12.35	0.5754	15.10	3.52	1.58
SNV	7	0.7288	12.51	0.6285	14.12	2.06	1.66
SNV+ smoothing	9	0.7580	11.81	0.6162	14.35	3.00	1.65
SNV+ first derivative	5	0.7536	11.92	0.6117	14.44	2.13	1.62
SNV+ second derivative	7	0.7702	11.51	0.6134	14.41	3.20	1.65
MSC+ smoothing	11	0.7729	11.45	0.6676	13.36	3.05	1.78
MSC+ first derivative	5	0.7533	11.93	0.6114	14.44	2.06	1.62
MSC+ second derivative	7	0.7720	11.47	0.6188	14.31	3.13	1.66

Abbreviations: R<sup>2</sup>: coefficients of determination, RMSEC: root mean square error of calibration, RMSEP: root mean square error of prediction, RPD: ratio of standard deviation of reference data in validation set to SEP, MSC: multiplicative scatter correction, SNV: standard normal variate, (1,7 and 9): number of left and right average point

**Table 45** Calibration and validation results for sucrose in flesh of dried whole longan fruit samples by HSI.

Pre processing	PLS factor	Calibration set		Validation set			RPD
		R <sup>2</sup>	RMSEC (mg/g)	R <sup>2</sup>	RMSEP (mg/g)	bias	
Raw	8	0.5957	89.84	0.5260	90.80	3.63	1.45
Smoothing (1)	8	0.5859	90.93	0.5280	90.61	3.58	1.43
Normalize	7	0.5798	91.60	0.4988	93.37	8.01	1.42
MSC	9	0.6619	82.15	0.5072	92.59	18.01	1.45
First derivative (4)	5	0.5491	94.88	0.5147	91.87	0.53	1.43
Second derivative (3)	2	0.3800	111.25	0.3717	104.54	11.12	1.27
SNV	9	0.6068	82.03	0.4817	94.95	20.32	1.42
SNV+ smoothing	11	0.6821	79.66	0.5108	92.25	20.43	1.47
SNV+ first derivative	5	0.5802	91.55	0.4913	94.06	3.21	1.40
SNV+ second derivative	1	0.3309	115.58	0.3468	106.59	10.51	1.24
MSC+ smoothing	10	0.6704	81.12	0.5247	90.93	19.32	1.48
MSC+ first derivative	5	0.5800	91.57	0.5000	93.30	2.95	1.41
MSC+ second derivative	1	0.3271	115.91	0.3482	106.48	10.51	1.24

Abbreviations: R<sup>2</sup>: coefficients of determination, RMSEC: root mean square error of calibration, RMSEP: root mean square error of prediction, RPD: ratio of standard deviation of reference data in validation set to SEP, MSC: multiplicative scatter correction, SNV: standard normal variate, (1,3 and 4): number of left and right average point

**Table 46** Calibration and validation results for glucose in flesh of dried whole longan fruit samples by HSI.

Pre processing	PLS factor	Calibration set		Validation set			RPD
		R <sup>2</sup>	RMSEC (mg/g)	R <sup>2</sup>	RMSEP (mg/g)	bias	
Raw	6	0.2268	27.41	0.1938	25.25	-1.17	1.11
Smoothing (4)	10	0.3110	25.88	0.2042	25.08	-0.59	1.12
Normalize	5	0.2455	27.08	0.1833	25.41	-1.84	1.11
MSC	5	0.2732	26.58	0.2190	24.85	-0.87	1.13
First derivative (5)	5	0.2574	26.87	0.2369	24.56	-0.27	1.14
Second derivative (7)	3	0.2199	27.54	0.2868	23.75	-1.42	1.18
SNV	5	0.2143	27.64	0.1781	25.49	0.83	1.10
SNV+ smoothing	8	0.3069	25.96	0.2513	24.33	-1.88	1.16
SNV+ first derivative	4	0.2790	26.47	0.2252	24.75	-1.31	1.14
SNV+ second derivative	3	0.2221	27.50	0.2699	24.03	-2.25	1.17
MSC+ smoothing	9	0.3177	25.75	0.2408	24.50	-1.82	1.15
MSC+ first derivative	4	0.2797	26.46	0.2225	24.80	-1.32	1.13
MSC+ second derivative	3	0.2217	27.51	0.2698	24.03	-2.26	1.17

Abbreviations: R<sup>2</sup>: coefficients of determination, RMSEC: root mean square error of calibration, RMSEP: root mean square error of prediction, RPD: ratio of standard deviation of reference data in validation set to SEP, MSC: multiplicative scatter correction, SNV: standard normal variate, (4, 5 and 7): number of left and right average point

**Table 47** Calibration and validation results for fructose in flesh of dried whole longan fruit samples by HSI.

Pre processing	PLS factor	Calibration set		Validation set			RPD
		R <sup>2</sup>	RMSEC (mg/g)	R <sup>2</sup>	RMSEP (mg/g)	bias	
Raw	8	0.5036	25.39	0.4684	24.46	0.98	1.37
Smoothing (1)	8	0.4966	25.56	0.4676	24.48	1.04	1.37
Normalize	6	0.4467	26.80	0.4540	24.79	2.08	1.36
MSC	7	0.4791	26.01	0.4824	24.14	2.48	1.40
First derivative (4)	6	0.4796	25.99	0.4944	23.86	2.54	1.41
Second derivative (4)	2	0.3355	29.37	0.4022	25.94	3.02	1.30
SNV	7	0.4959	25.58	0.4580	24.70	1.17	1.36
SNV+ smoothing	7	0.4854	25.85	0.4603	24.65	1.08	1.36
SNV+ first derivative	6	0.4911	25.70	0.4785	24.23	3.10	1.40
SNV+ second derivative	1	0.3231	29.64	0.3947	26.10	3.37	1.30
MSC+ smoothing	7	0.4688	26.26	0.4832	24.12	2.36	1.40
MSC+ first derivative	5	0.4747	26.12	0.4841	24.10	3.11	1.40
MSC+ second derivative	1	0.3190	29.73	0.3956	26.09	3.43	1.30

Abbreviations: R<sup>2</sup>: coefficients of determination, RMSEC: root mean square error of calibration, RMSEP: root mean square error of prediction, RPD: ratio of standard deviation of reference data in validation set to SEP, MSC: multiplicative scatter correction, SNV: standard normal variate, (1 and 4): number of left and right average point

**Table 48** Calibration and validation results for total sugars in flesh of dried whole longan fruit samples by HSI.

Pre processing	PLS factor	Calibration set		Validation set			RPD
		R <sup>2</sup>	RMSEC (mg/g)	R <sup>2</sup>	RMSEP (mg/g)	bias	
Raw	7	0.6459	103.41	0.5226	116.73	12.65	1.46
Smoothing (1)	7	0.6442	103.68	0.5204	117.00	12.58	1.45
Normalize	7	0.6822	97.98	0.5093	118.36	9.68	1.43
MSC	7	0.6981	95.49	0.5289	115.96	13.25	1.47
First derivative (5)	8	0.6985	95.42	0.5264	116.27	7.74	1.46
Second derivative (7)	6	0.6824	97.94	0.5135	117.84	3.92	1.43
SNV	7	0.7113	93.38	0.5129	117.92	14.22	1.44
SNV+ smoothing	7	0.7078	95.07	0.5075	118.57	13.39	1.43
SNV+ first derivative	8	0.7419	88.30	0.5227	116.73	10.47	1.45
SNV+ second derivative	4	0.5912	111.12	0.4491	125.40	9.16	1.35
MSC+ smoothing	7	0.6883	97.03	0.5333	115.42	12.98	1.47
MSC+ first derivative	8	0.7324	89.91	0.5286	116.00	9.42	1.46
MSC+ second derivative	4	0.5901	111.28	0.4630	123.81	9.31	1.37

Abbreviations: R<sup>2</sup>: coefficients of determination, RMSEC: root mean square error of calibration, RMSEP: root mean square error of prediction, RPD: ratio of standard deviation of reference data in validation set to SEP, MSC: multiplicative scatter correction, SNV: standard normal variate, (1, 5 and 7): number of left and right average point



Appendix G

Calculation of moisture content for the whole fruit and flesh and seed part

### Calculation of moisture content (MC) for the whole fruit

1. Calculate %weight of each part

$$\text{- \% Weight of peel} = \frac{\text{Fresh weight of peel}}{\text{Fresh weight of peel+flesh+seed}} \times 100$$

$$\text{- \% Weight of flesh} = \frac{\text{Fresh weight of flesh}}{\text{Fresh weight of peel+flesh+seed}} \times 100$$

$$\text{- \% Weight of seed} = \frac{\text{Fresh weight of seed}}{\text{Fresh weight of peel+flesh+seed}} \times 100$$

2. Calculate %MC of the whole fruit by %weight

$$\text{- \% MC peel by \%weight} = \frac{\% \text{weight of peel} \times \% \text{MC peel (calculate from Eq.1)}}{100}$$

$$\text{- \% MC flesh by \%weight} = \frac{\% \text{weight of flesh} \times \% \text{MC flesh (calculate from Eq.1)}}{100}$$

$$\text{- \% MC seed by \%weight} = \frac{\% \text{weight of seed} \times \% \text{MC seed (calculate from Eq.1)}}{100}$$

$$\therefore \% \text{MC of the whole fruit} = \% \text{MC peel by \%weight} + \% \text{MC flesh by \%weight} + \% \text{MC seed by \%weight}$$

### Calculation of moisture content (MC) for flesh and seed part

1. Calculate %weight of each part

$$\text{- \% Weight of flesh} = \frac{\text{Fresh weight of flesh}}{\text{Fresh weight of peel+flesh+seed}} \times 100$$

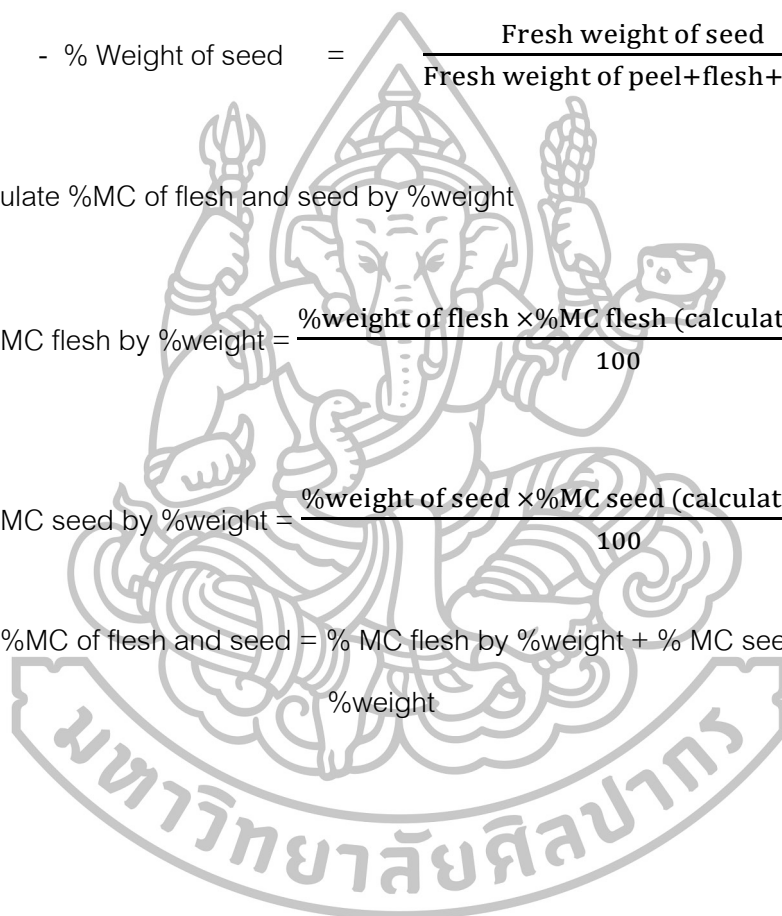
$$\text{- \% Weight of seed} = \frac{\text{Fresh weight of seed}}{\text{Fresh weight of peel+flesh+seed}} \times 100$$

2. Calculate %MC of flesh and seed by %weight

$$\text{- \% MC flesh by \%weight} = \frac{\% \text{weight of flesh} \times \% \text{MC flesh (calculate from Eq.1)}}{100}$$

$$\text{- \% MC seed by \%weight} = \frac{\% \text{weight of seed} \times \% \text{MC seed (calculate from Eq.1)}}{100}$$

$$\therefore \% \text{MC of flesh and seed} = \% \text{MC flesh by \%weight} + \% \text{MC seed by \%weight}$$



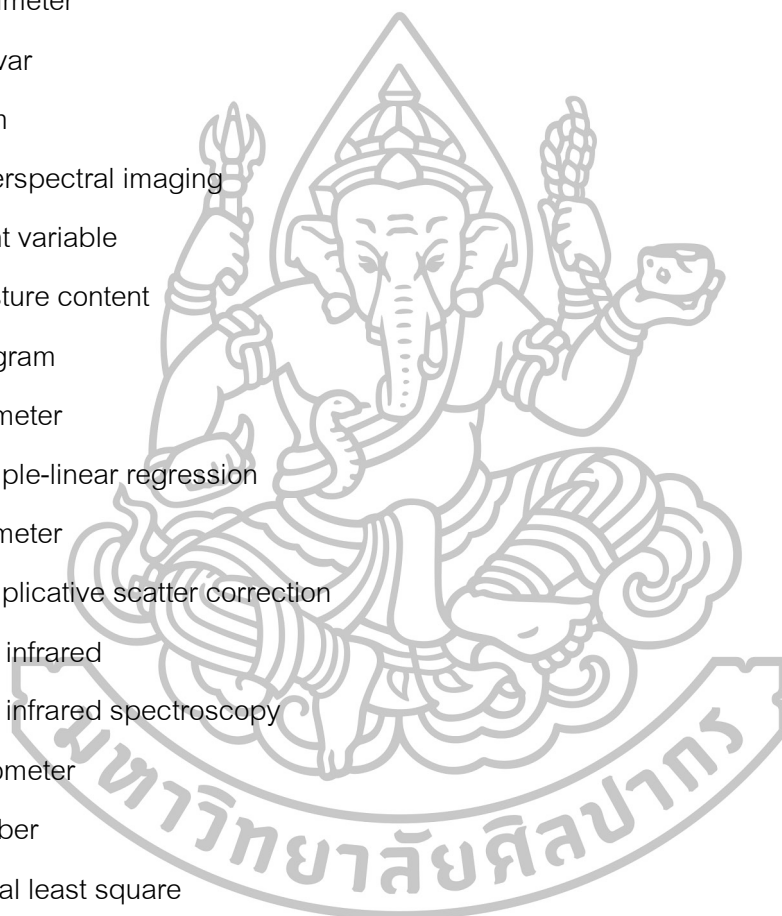




Appendix H  
Nomenclature

## Nomenclature

1, 7	number of left and right averaging point
°Brix	degree brix
°C	degree Celsius
CCD	charge-couple device
cm	centimeter
cv.	cultivar
g	gram
HSI	hyperspectral imaging
LV	latent variable
MC	moisture content
mg	milligram
ml	millimeter
MLR	multiple-linear regression
mm	millimeter
MSC	multiplicative scatter correction
NIR	near infrared
NIRS	near infrared spectroscopy
nm	nanometer
No.	number
PLS	partial least square
R	correlation coefficient
$R^2$	coefficient of determination
RMSEP	root mean square error of prediction
ROI	region of interest
RPD	ratio of standard deviation of reference data in validation set to SEP
SNV	standard normal variate
TSS	total soluble solids



W width

$\mu\text{m}$  micrometer



## Curriculum Vitae

**Researcher** Aleeya Lerdkuson

**Address** 114 Chamadevi road, Wiangnuer, meuang, Lampang 52000

**Education** 2009-2013 Highest education: Bachelor degree  
 Institute: Silpakorn University  
 Major: Bachelor of Science (B.Sc.)  
 Branch: Food Technology

2013-present Studying in Master Degree  
 Institute: Silpakorn University  
 Major: Master of Science (M. Sc.)  
 Branch: Food Technology

### Conference

Aleeya Lerdkuson, Wikarnda suwannaporn, Sarawut Phupaichitkun and Busarakorn Mahayothee. 2013. Applying Hyperspectral Imaging to Detect Chemical Properties in Pineapple. In the Engineering and Technology Conference during 2-3 Dec 2013 at faculty of Engineering and Industrial Technology, Silpakorn University, Nakhon Pathom, Thailand. (Poster presentation)

Aleeya Lerdkuson, Pontalate Duangsuwan, Nilobon Komonsing, Pramote Khuwijitjaru, Busarakorn Mahayothee. 2015. Development of a Rapid Method for Chlorpyrifos Residue Determination in Yard Long Bean using Near Infrared Spectroscopy. In the 13<sup>th</sup> National Postharvest Technology Conference during 18 -19 June 2015 at Greenery Resort, Khoa Yai, Nakorn Ratchasima, Thailand. (Poster presentation)

Aleeya Lerdkuson, Pramote Khuwijitjaru, Eakaphan Keowmaneechai and Busarakorn Mahayothee. 2016. Determination of Moisture Content and Phenolic Compounds in Seed of Dried Whole Longan Using Near-infrared Spectroscopic Technique. In the 9th Silpakorn University International Conference during 11-21 Feb

2016 at Sanam Chandra Art Gallery, Silpakorn University, Nakhon Pathom, Thailand.

(Oral presentation)

